

GAS COMBUSTION RETORTING PERFORMANCE
IN A LARGE DEMONSTRATION RETORT

J. E. Lawson¹, R. L. Clampitt², K. I. Jagel³, and J. W. Hasz⁴

ABSTRACT

The performance of the Gas Combustion oil shale retorting process has been tested in a large demonstration retort (60 sq. ft. cross section) at rates up to 360 tons per day. Satisfactory operations were demonstrated on two shale sizes -- 1 to 2-1/2 inch and 1/4 to 2-1/2 inch -- at shale rates up to 500 lbs/hr/ft². Yields obtained were those which would have been predicted from operation of small pilot units. Conversion of organic values into oil and gas totals about 85% of that in raw shale; however, a substantial quantity of this is utilized in the internal combustion contributing to a loss in useful products. A number of operating limitations were found with the process so that commercial application would have to be restricted to rather narrow limits. The configuration of retort internals also influences process operability, which makes demonstration of proposed modifications in large scale prototype equipment desirable prior to commercial application.

- 1) Atlantic Richfield Co., P. O. Box 2819, Dallas, Texas 75221
- 2) Phillips Petroleum Co., Bartlesville, Oklahoma 74003
- 3) Mobil Research & Development Corp., Research Dept., Paulsboro, N. J. 08066
- 4) Continental Oil Co., P. O. Drawer 1267, Ponca City, Oklahoma 74602

RETORTING UNGRADED OIL SHALE AS RELATED TO IN SITU PROCESSING, II

L. Dockter, A. Long, Jr., and A. E. Harak

Laramie Energy Research Center, Bureau of Mines
U. S. Department of the Interior, Laramie, Wyoming

INTRODUCTION

For many years the Bureau of Mines has engaged in research to provide technology for the development of methods for producing oil from oil shale. The world's known reserves of oil shale in deposits 10 feet or more in thickness and with an assay of 10 or more gallons of oil per ton are estimated to represent 3.1 trillion barrels of oil (1).^{1/} The bulk of the world's known oil shale reserves are in the United States in the Green River Formation which underlies parts of Colorado, Utah, and Wyoming. The known oil shale deposits in this formation are estimated to represent 600 billion barrels of oil in deposits assaying 25 or more gallons of oil per ton. If the shales assaying from 10 to 25 gallons per ton are included, the total known shale oil potential of this formation is about 2 trillion barrels. To put the importance of this shale oil potential in its proper light, note that the proved crude oil reserves in the United States at the end of 1969 were 29.6 billion barrels (not including the recent discoveries on Alaska's North Slope which have not been evaluated), and that 3.2 billion barrels of crude oil were produced in the United States in 1969 (2).

Many different ways to produce the oil from oil shale have been proposed and tried. One method which may have economic and environmental advantages over the others, should it prove technically feasible, is retorting the shale in the formation where it occurs. This process is commonly called in situ retorting. Basically, this method consists of fracturing the nearly impermeable oil shale in place, heating the fractured oil shale by some method to retort it, and recovering the oil produced via wells or other suitable recovery systems.

Under current plans, the fracturing required for in situ retorting will probably be accomplished by the use of either conventional or nuclear explosives. Either method could produce a large mass of broken shale with pieces varying in size from dust to several feet in diameter and varying in assay value from nil to as much as 50 or more gallons of oil per ton.

The present study was conducted to determine the retorting characteristics of oil shale ungraded in size and varying in richness, simulating to some degree the physical conditions of in situ retorting. In general, the oil shale charge has been mine-run material with pieces as large as 20 inches in two dimensions. The third dimension was as large as 36 inches. Grade of the charge, as determined by Fischer assay, ranged from 20.4 to 48.0 gallons of oil per ton. Air rates that have been investigated ranged from 0.58 to 3.74 standard cubic feet per minute per square foot of retort cross section. Yields of oil as high as 80 percent of Fischer assay have been obtained.

Multiple linear regression analysis was used to generate equations predicting the oil yield for given sets of retorting conditions. Using only controlled operating variables, an equation was developed that accounts for 83 percent of the variability in oil yield. Including ambient conditions in the regression improves the percentage to 93.

EXPERIMENTAL EQUIPMENT AND PROCEDURE

Construction of a small, 10-ton batch-type retort was completed at the Bureau of Mines

^{1/} Underlined numbers in parentheses refer to items in the list of references at the end of this report.

Center in Laramie, Wyo., in late 1965 (4). A schematic diagram of the retort and its auxiliary equipment is presented in figure 1.

The retort consists of a cylindrical steel shell 6 feet in outside diameter by 12 feet tall surrounding a tapered refractory lining 6 inches thick at the bottom and 8 inches thick at the top. A hinged grate is made of 1-inch steel plate perforated with 3/8-inch holes. A natural gas burner in the top of the retort is used to ignite the shale. The gas inlet to the retort is designed to permit injection of either air, recycle gas, steam, or any combination of the three. The oil recovery system includes three separation tanks, or demisters, to remove the oil from the gaseous products.

The retorting system is instrumented to obtain process temperatures and flow rates. Sets of four thermocouples are evenly spaced from the center to the outside edge of the bed at 18-inch vertical intervals to obtain bed temperatures during retorting. Gas samples taken downstream from the recycle gas blower are analyzed by a multiple stream process chromatograph.

For all experiments, a 3- to 4-inch layer of crushed and sized granite was placed on top of the grate to prevent oil shale fines from falling through the grate to protect the grate from excessive temperatures during the retorting of the bottom portion of the oil shale bed. When the crushed rock layer was in place, the oil shale charge was loaded into the retort, taking care to limit size degradation or segregation. After the oil shale was loaded, the retort was closed and the retorting operation was started.

In most experiments performed during this study, the oil shale bed was ignited at the top using the natural gas burner. Combustion was maintained by injecting air and recycle gas, if used, into the top of the retort. The combustion zone traveled down through the bed, retorting the oil shale ahead of it. Retorting was assumed to be completed when the bottom set of thermocouples in the bed indicated an average temperature of about 900°F. For two experiments, steam was used as the heat transfer medium.

Oil shale charges for most of the experiments performed in the 10-ton retort were prepared from mine-run shale obtained from the Bureau of Mines Anvil Points mine near Rifle, Colo. Four experiments (experiments 27 through 30) were made with oil shale from an area near Rock Springs, Wyo.

To prepare a sample for analysis for each charge, the smaller pieces of the mine-run shale were sampled by cone and quarter methods. Larger pieces, over 12 inches and limited to 20 inches, were broken perpendicular to the bedding planes, and approximately one-fourth of each piece was added to the sample. This total sample was crushed to about 1 inch. Samples for analysis were prepared from the 1-inch material, and the unused remainder was returned to the retort charge.

For all of the experiments performed on Colorado oil shale in this and a previous study, the potential oil content of the shale as determined by Fischer assay ranged from 20.4 to 48.0 gallons per ton. Table 1 shows the oil content of the charges used in the current study, including four charges of Wyoming oil shale ranging from 23.5 to 27.3 gallons of oil per ton.

Determination of particle size distribution for these retort charges, ranging in particle size from sand-grain size to pieces as large as 20 inches, was difficult. Screening equipment of sufficient capacity was not available; thus, it was necessary to determine the size distribution of each charge by separating the particles into size categories by actual measurement. Average particle sizes for the charges used in this study are shown in table 1. These average sizes range from 4.2 inches to 12.4 inches. When the previous work (4) is included, the range is extended from 4.2 inches to 14.1 inches.

TABLE 1. - Summary of operations of the 10-ton retort

Experiment number ^{1/}	22	23	19	282/ ^{2/}	18	24	26	292/ ^{2/}	32
Oil yield, vol pct of Fischer assay	9.4	38.6	42.0	45.3	47.0	47.0	50.8	51.2	53.0
Run time, days	10.77	2.87	4.19	4.75	2.91	5.79	6.62	7.3	8.0
Fischer assay of charge, gal/ton	23.4	20.4	21.7	23.7	36.8	23.4	24.7	26.3	23.7
Air rate, scf/min/ft ² of bed	Steam	-	1.16	1.29	1.86	0.70	1.03	0.75	0.89
Recycle gas-to-air ratio	do.	-	0	1.28	0	1.46	1.00	0.90	0.88
Total air, scf/ton	do.	-	17,897	19,257	20,328	14,100	13,962	16,561	21,755
Total recycle gas, scf/ton	do.	-	0	24,583	0	20,595	26,017	14,916	19,082
Maximum bed temp., °F	1,125	1,380	1,260	1,240	1,600	1,340	1,140	1,320	-
Average particle size, inches	4.2	7.5	4.6	11.5	9.9	9.9	8.6	9.9	10.2
Selected oil properties:									
Specific gravity, 60°/60°F	0.919	0.921	0.908	0.909	0.914	0.909	0.914	0.915	0.910
Pour point, °F	65	75	10	35	65	65	65	45	40
Viscosity, SUS at 100°F	184	157	72	84	91	82	87	85	71
Nitrogen, wt pct	1.56	1.74	1.54	1.25	1.85	1.56	1.65	1.20	1.21
Sulfur, wt pct	0.70	0.72	1.16	0.48	1.10	0.76	0.64	0.63	1.21
Naphtha, vol pct of crude	5.2	1.3	6.9	6.1	8.5	5.8	5.1	5.0	6.3
Light distillate, vol pct of crude	8.6	17.2	24.1	24.0	20.9	29.8	27.4	26.3	27.6
Heavy distillate, vol pct of crude	45.1	51.6	42.8	47.2	43.4	43.5	35.6	49.0	44.5
Residuum, vol pct of crude	42.1	30.6	25.0	23.7	28.2	21.1	33.3	20.4	21.1
Stack gas composition, vol pct:									
Nitrogen	<u>3/</u>	73.3	76.6	77.5	69.4	78.4	74.9	75.4	76.8
Oxygen	<u>3/</u>	9.4	11.0	8.5	4.9	6.9	4.8	5.7	8.4
Carbon dioxide	<u>3/</u>	15.6	10.8	12.5	20.9	13.5	18.6	16.5	13.4
Carbon monoxide	<u>3/</u>	0.4	0.5	0.8	0.8	0.8	1.0	0.9	0.6
Methane	<u>3/</u>	0.6	0.8	0.5	1.5	0.3	0.5	0.7	0.5
Higher hydrocarbons	<u>3/</u>	0.7	0.3	0.2	1.4	0.1	0.2	0.8	0.3

^{1/} Experiment number:
^{2/} Wyoming oil shale.
^{3/} Not determined.

- 18 - Made with air and steam injected for 12.5 percent of run.
- 19 - Air, no recycle gas.
- 22 - Made with superheated steam only.
- 23 - Made with superheated steam and air. No air rate available.
- 24 - Made with heated air and recycle gas.
- 26 - Heated air and recycle gas used during 58 percent of run. Recycle gas to air ratio, 1.00.
- 28, 29, 32 - Made with air and recycle gas.

TABLE 1. - Summary of operations of the 10-ton retort (con.)

Experiment number ^{1/}	21	31	302/	16	20	17	25	272/
Oil yield, vol pct of Fischer assay	56.0	57.5	61.9	66.8	70.0	72.0	73.7	76.3
Run time, days	2.62	7.96	7.59	2.16	4.0	13.33	4.2	4.75
Fischer assay of charge, gal/ton	24.8	28.3	23.5	32.3	26.2	36.7	23.9	27.3
Air rate, scf/min/ft ² of bed	1.67	0.74	0.74	3.74	1.46	1.47	1.00	1.00
Recycle gas to air ratio	0.29	0.99	1.02	0	0.32	0.53	1.04	1.00
Total air, scf/ton	14,597	20,748	16,971	29,898	18,584	76,126	10,251	14,580
Total recycle gas, scf/ton	777	20,475	17,373	0	5,050	40,351	15,377	14,665
Maximum bed temp., °F	1,550	1,400	1,250	1,475	1,380	1,200	1,300	1,330
Average particle size, inches	6.2	7.9	11.5	12.4	8.7	12.1	9.4	7.7
Selected oil properties:								
Specific gravity, 60°/60°F	0.914	0.914	0.919	0.932	0.918	0.900	0.912	0.916
Pour point, °F	75	50	40	70	65	60	70	55
Viscosity, SUS at 100°F	100	83	101	184	105	77	88	98
Nitrogen, wt pct	1.86	1.09	1.22	2.21	1.81	1.67	1.66	1.38
Sulfur, wt pct	0.99	0.54	0.67	1.05	0.89	0.76	0.80	0.42
Naphtha, vol pct of crude	7.0	4.8	7.3	4.5	6.1	5.3	2.8	8.6
Light distillate, vol pct of crude	21.2	28.3	21.1	16.9	22.3	22.4	25.9	21.7
Heavy distillate, vol pct of crude	39.1	49.3	48.3	40.4	42.3	47.2	31.7	38.3
Residuum, vol pct of crude	32.9	19.9	24.9	38.9	30.9	26.6	41.1	33.1
Stack gas composition, vol pct:								
Nitrogen	69.9	75.9	75.8	70.8	72.0	79.3	73.1	73.6
Oxygen	5.8	8.5	5.9	6.8	4.9	3.0	4.7	4.2
Carbon dioxide	21.3	14.2	16.2	18.2	18.4	13.1	20.4	20.6
Carbon monoxide	1.8	0.7	0.9	3.1	1.9	1.8	1.0	0.8
Methane	1.0	0.5	0.2	0.6	1.5	2.4	0.5	0.6
Higher hydrocarbons	0.2	0.2	1.0	0.5	1.3	0.4	0.3	0.2

^{1/} Experiment number:

- 16 - Made with air, no recycle gas.
- 17 - Made with gas burner operating 94 percent of run.
- 20 - Recycle gas used 84 percent of run. Recycle gas to air ratio during this time, 0.32.
- 21 - Recycle gas used 18 percent of run. Recycle gas to air ratio during this time, 0.29.
- 25 - Started with heated recycle gas at a rate of 1.6 scf/min/ft² for 22 hr. Recycle rate then reduced and heated air injected at recycle gas to air ratio of 1.04.
- 27, 30, 31 - Made with air and recycle gas.

^{2/}

Wyoming oil shale.

RESULTS AND DISCUSSION

A summary of the experiments performed in the 10-ton retort since the last report to the American Chemical Society (4) is presented in table 1. The experiments are arranged in increasing order of oil yield. The oil recovery for this series of experiments ranged from 9.4 percent of Fischer assay for experiment 22 in which steam was used for retorting, to 76.3 percent for experiment 27 on Wyoming shale in which air and recycle gas were used for retorting.

Various methods involving the use of supplementary energy were used in attempts to improve the oil yield during this series of experiments. Additional heat was supplied by the following: In experiment 17 the natural gas burner was operated; in experiments 24 through 26 air and recycle gas were externally heated; in experiment 18 steam was used instead of recycle gas. Experiments 22 and 23 used superheated steam and a mixture of superheated steam and heated air, respectively, to retort charges of unignited oil shale.

Experiment 17, which had additional heat supplied by the natural gas burner, yielded 72 percent oil, while experiment 20 with similar operating conditions yielded 70 percent oil without additional heat. Of the three experiments using heated air and recycle gas (24, 25, and 26), two had yields of about 50 percent, and one had a yield of 74 percent. The high-yield experiment (25) had operating conditions almost identical to those of experiment 27 which yielded 76 percent oil without heated air or recycle gas. Superheated steam proved to be of little value as oil yields from experiments 18, 22, and 23 were low. Based on these results, the addition of supplementary energy appears to be of doubtful benefit. This study indicates that the highest oil yields were obtained with a recycle gas-to-air ratio of about 1:1 while injecting 1 cubic foot of air per minute per square foot of retort cross section. Some of the major factors which may contribute to low oil yields are:

- (1) Incomplete retorting caused by channeling or excessive retorting rates.
- (2) Burning of the oil as it is formed during retorting.
- (3) Loss of oil as a stable mist which was not separated from the stack gas.

Losses from these causes may be minimized by adequate control of air and recycle gas rates and an improved recovery system.

Properties of the crude shale oils produced during this investigation are shown in table 1. These oils are similar to oils produced by other internally heated retorts, in that they are dark and viscous and have a characteristic odor. They also contain material concentrations of sulfur and nitrogen compounds. However, as shown in table 2, the oils produced during the current series of experiments have higher API gravities, lower pour points, and a higher percentage of naphtha and light distillates than oils produced from other internally heated retorts previously studied by the Bureau.

The four experiments (27 through 30) made with Wyoming oil shale produced oil with properties similar to those of the Colorado shale. The nitrogen and sulfur concentrations were slightly lower in the oil produced from Wyoming shale.

REGRESSION ANALYSIS OF RETORTING VARIABLES

In a study of the effects of retorting variables, a convenient measurement of the results of these effects is oil yield. Oil yield, in this study, is expressed as volume percent of Fischer assay; that is, the percent of the total potentially available oil actually recovered during the retorting process.

From a theoretical standpoint the yield should be a function of shale assay, shale particle size, shale mineral matter composition, retorting gas flow rate and oxygen

TABLE 2. - Selected properties of shale oils

Retort	Gravity API	Sulfur, wt pct	Nitrogen, wt pct	Pour point, °F	Volume percent			
					Naphtha distillate	Light distillate	Heavy distillate Residuum	
N-T-U ¹ /	19.8	0.74	1.78	90	2.7	15.7	34.4	45.8
Gas combustion ¹ /	18.6	0.69	2.13	85	4.4	14.6	31.3	49.7
10-ton, Colorado shale ² /	23.2	0.89	1.49	60	6.1	24.9	43.8	26.2
10-ton, Wyoming shale ³ /	23.2	0.55	1.26	45	6.5	23.3	45.7	25.5

¹/ Reference (3).

²/ Average from experiments 20, 21, 31, 32.

³/ Average from experiments 27, 28, 29, 30.

content, and the rate of heat loss from the retort. The retorting-gas flow rate (space velocity) and its oxygen content are functions of the air and recycle gas rates. Of these variables, only air rate, recycle rate, and to a certain extent, shale size can be controlled when retorting oil shale from a given oil shale deposit. Heat losses from the retort can be reduced, but not controlled except by an elaborate and expensive heat shield.

Using the data available from all of the experiments made in the 10-ton retort, from this study, and the preceding work (4), a series of statistical regression analyses were performed in an effort to generate an equation that would predict yield as a function of the retorting variables.

A first order equation for predicting oil yield using all of the data, with the exception of the data from experiments 22 and 23 in which steam was used, proved unsatisfactory. The regression analysis was then upgraded by eliminating data from the experiments on Wyoming oil shales (27 through 30) and data from all experiments in which operating conditions were changed during the course of the experiment (1, 5, 6, 12, 13, 17, 18, 24-26, 31, 32). The results from regression analyses on the remaining 14 experiments (2-4, 7-11, 14-16, 19-21) with Colorado oil shales are presented in table 3.

The first two equations in table 3 are first order linear equations generated by computerized multiple linear regression and are of the form

$$Y = B_0 + B_1X_1 + B_2X_2 + \dots$$

Equation 1 predicts oil yield using Fischer assay, shale size, and retorting-gas space velocity and retorting-gas oxygen content as variables. This equation accounts for only 33 percent of the variation in the data, and the F-test indicates a 50-percent chance that no correlation exists. Because this equation provided such poor correlation, the average wind velocity and ambient temperature prevailing during each run were added to the data in an attempt to include an approximate heat loss function in the correlation. Equation 2, generated using these additional variables, showed essentially no improvement in correlation over equation 1. If anything, the accuracy of the predicted yield was decreased. These regression analyses show that the variability in the data is such that the yield cannot be predicted using a first order equation.

To determine whether second order effects might be important, equations of the form:

$$Y = B_0 + B_1X_1 + B_2X_1X_2 + B_3X_2 + B_4X_1^2 + B_5X_2^2 + \dots$$

were investigated. Equations 3, 4, and 5 of table 3 are of this form and were generated using a computerized stepwise regression analysis program. This program generates a sequence of multiple linear regression equations by adding or removing one variable to or from the equation at each step. The variable added or removed at each step is the one which causes the greatest reduction in the error sum of squares term for the equation.

Using this stepwise regression program, equations 3 and 4 were generated from a selection of 35 terms including seven variables, their cross products, and their squares. The original variables for equation 3 were shale assay and size, retorting gas space velocity and oxygen content, ambient temperature, wind velocity, and average bed temperature.^{2/} For equation 4 the space velocity and oxygen content were replaced by

^{2/} Average bed temperature was calculated by adding all temperatures at 5-hour intervals and dividing by the total number of temperatures used.

TABLE 3. - Summary of regression analyses

Equation ^{1/}	Number of independent variables in equation	Standard error of estimated yield	Index of determination, R ²	F-statistic	Significance level of F test
1	4	11.4	0.33	1.1	0.50
2	6	12.8	0.34	0.59	> 0.50
3	7	6.1	0.87	5.8	0.025
4	7	4.4	0.93	12.0	0.005
5	7	7.0	0.83	4.1	0.10

^{1/} Equations generated:

- $Y = 106.45 - 1.68 (OXY) - .804 (ASY) + 1.82 (SIZ) - 2.57 (SPV)$
- $Y = 110.20 - 1.82 (OXY) - .775 (ASY) + 1.54 (SIZ) - 3.03 (SPV) + .405 (WND) - .0591 (TEM)$
- $Y = 39.26 - .105 (TEM) (OXY) + 1.66 (TEM) + 1.57 (SPV) (OXY) + .0737 (BTM) - .412 (ASY) (SPV) - 1.03 (WND) (SPV) - .00053 (TEM) (BTM)$
- $Y = 93.48 - .239 (TEM) (WND) + .681 (AIR) (TEM) + .795 (REC) (TEM) - 2.82 (REC) (SIZ) + .245 (WND) (WND) + .00004 (BTM) (BTM) - 3.94 (AIR) (AIR)$
- $Y = 18.74 + 107 (REC) + 1.77 (ASY) (AIR) - 1.99 (ASY) (REC) - 11.0 (AIR) (AIR) - 8.42 (REC) (REC) - 13.8 (AIR) (REC) - 0.0122 (ASY) (ASY)$

where:

- Y = oil yield, volume percent of Fischer assay,
- ASY = oil content of shale by Fischer assay, gal/ton,
- AIR = air rate, scfm/ft² of bed,
- BTM = average temperature of bed during run, °F,
- OXY = oxygen content of retorting gas, pct,
- REC = recycle gas rate, scfm/ft² of bed,
- SPV = retorting gas space velocity, scfm/ft² of bed,
- SIZ = average shale particle size, inches,
- TEM = average ambient temperature during run, °F,
- WND = average wind velocity during run, mph.

the air and recycle rates. Equations 3 and 4 account for 87 and 93 percent of the total variation in the data, respectively, and there is only a 2.5- and 0.5-percent chance, respectively, that no correlation exists.

Equations 3 and 4 include several uncontrolled variables--wind velocity, ambient temperature, and average bed temperature--and are useful for evaluating the results of experiments performed under different ambient conditions. Direct comparisons of the effects of the controlled operating variables on oil yield can be made because the effects of changes in ambient conditions on yield can be accounted for by these equations. Equation 5 was generated using only controlled variables--Fischer assay, size, air rates, and recycle rates--to predict the oil yield under a proposed set of retorting conditions. This equation accounts for 83 percent of the total variation in the data and has a 10-percent chance that no correlation exists.

In all five equations the terms are presented in decreasing order of the average effect on the yield by the variables involved. From this the importance of heat loss to the surroundings during retorting can be observed, in that the first two terms of both equations 3 and 4 include the ambient temperature. The size of the retorted shale seems to have little effect on the yield as it was not included in equations 3 and 5 and was included only as a cross-product in equation 4.

The size terms used in the regression analyses of the 14 experiments with Colorado oil shale were average particle sizes ranging from 4.6 to 13.4 inches. Over this rather limited range, the variability in oil yield as a result of changes in size is small. Previous studies by the Bureau of Mines (3) show that, although oil yields are not affected appreciably by changes in size of the largest particles in the shale feed, there is a fairly well defined trend for the oil yield to decrease with increased size. In the present study using mine-run shale with a maximum particle size of 20 inches, a somewhat lower oil yield would be expected than was obtained with the gas-combustion retort (3) operating on relatively narrow particle size range charges.

SUMMARY

This paper further substantiates data presented earlier (4) indicating that retorting oil shale ungraded as to size or oil content is technically feasible. During this series of experiments on mine-run shale having pieces up to 20 inches in two dimensions, yields of up to 76 percent of Fischer assay were attained.

The shale oils produced during this series of retorting operations are similar in appearance to oils produced by other internally heated retorts; however, the oils produced in the 10-ton retort had a higher API gravity, a lower pour point, and higher percentage of distillables than oils produced in other retorts. These differences all make the oil produced in the 10-ton retort more desirable for transporting and further processing. The Wyoming oil shale produced an oil containing less sulfur and nitrogen, but this advantage requires further investigation before concluding that it is typical.

Heating the air and recycle gas before injection into the retort proved to be of doubtful value as a method to increase oil yields. Use of superheated steam as a retorting medium also proved unsatisfactory.

Several equations for predicting oil yield from operating variables were developed by regression analysis. Using only controlled operating variables, an equation was developed that accounts for 83 percent of the variability in oil yield; by including ambient conditions in the equation this percentage was increased to 93.

ACKNOWLEDGMENT

The work upon which this report is based was done under a cooperative agreement between the Bureau of Mines, U. S. Department of the Interior, and the University of Wyoming.

REFERENCES

1. Duncan, Donald C., and Vernon E. Swanson. "Organic-Rich Shale of the United States and World Land Areas." Geol. Surv. Circ. 523, 1965, pp. 10-13.
2. American Gas Assn., Inc., American Petroleum Institute, and Canadian Petroleum Assn. Reserves of Crude Oil, Natural Gas Liquids, and Natural Gas in the United States and Canada and United States Productive Capacity as of December 31, 1969, v. 24, May 1970, p. 11.
3. Matzick, Arthur, R. O. Dannenberg, J. R. Ruark, J. E. Phillips, J. D. Lankford, and B. Guthrie. Development of the Bureau of Mines Gas-Combustion Oil-Shale Retorting Process. BuMines Bull. 635, 1966, 199 pp.
4. Carpenter, H. C., S. S. Tihen, and H. W. Sohns. Retorting Ungraded Oil Shale as Related to In Situ Processing. Div. of Petrol., ACS Preprints, v. 13, No. 2, April 1968, pp. F50-F57.

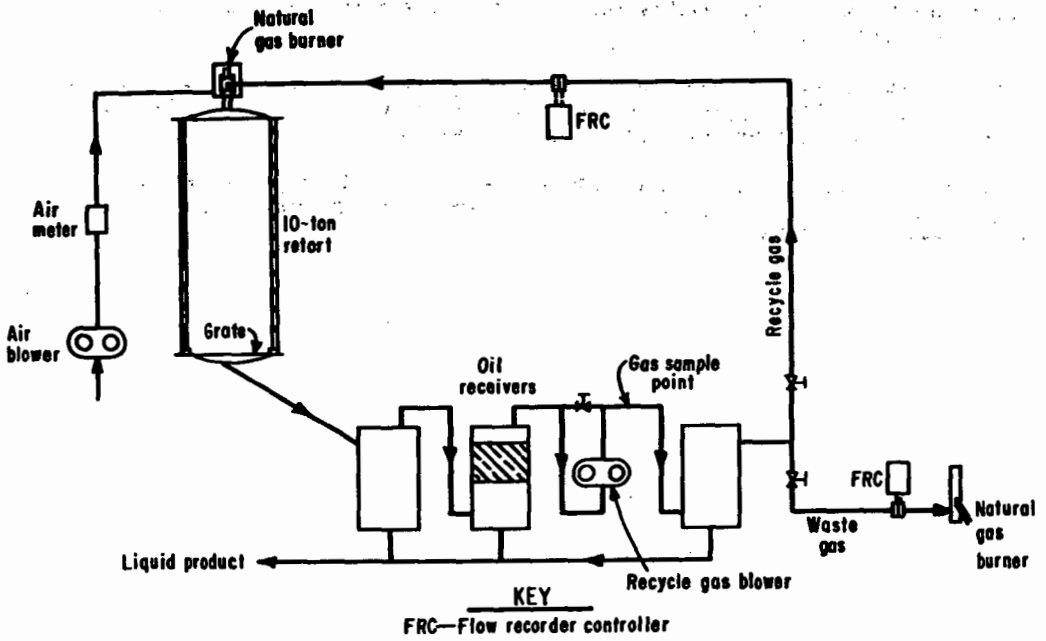


FIGURE 1. - Schematic diagram of experimental 10-ton retort.

WATER POLLUTION POTENTIAL OF SPENT OIL SHALE RESIDUES
FROM ABOVE-GROUND RETORTING

J. C. Ward, G. A. Margheim, G. O. G. Löf

Colorado State University, Fort Collins, Colorado

Oil shale resources in the United States cover more than 11 million acres of Colorado, Utah, and Wyoming, and the known petroleum reserve from this source is more than sixty times the proven reserve of crude oil in the United States. If present trends for needs in petroleum in the United States continue, the use of shale oil to supplement crude oil resources becomes likely as a major future development.

In the event the industrial development of oil shale becomes economically feasible, a considerable quantity of retorted shale residue will require disposal. The disposition of spent shale in a way to prevent water pollution will become a problem for industry. Because a good oil shale yields only 25 to 30 gallons of oil per ton of rock, from 85 to 90% of the weight of the original rock appears as spent shale. Some of the precipitation falling on exposed spent oil shale residue piles will run off and will contain dissolved material leached from these piles. Depending on both the concentration and composition of this runoff water, surface streams and possibly some ground waters may be polluted to some extent. The purpose of this project was to determine the water pollution potential of these exposed oil shale residue piles.

The spent oil shale residues investigated were the waste products from 3 pilot plant processes. The processes were: (1) the U.S. Bureau of Mines Gas Combustion Retorting Process, (2) the Union Oil Company Retorting Process, and (3) the TOSCO retorting process which will henceforth be abbreviated respectively USBM, UOC, and TOSCO. The oil shale from all 3 pilot plants came from the Piceance Basin near Rifle, Colorado.

The investigations included the determination of the physical properties of the oil shale retorting residues, and chemical (concentration and composition of dissolved inorganic solids) parameters after blending, shaking, percolation, and simulated precipitation-runoff experiments.

Following are the physical properties of the various oil shale residues:

oil shale residue	USBM	TOSCO	UOC	Raw
geometric mean size, cm	0.205	0.0070		
geometric standard deviation	8.05	3.27		
particle shape factor	0.0526	0.097		
bulk density, g/cc	1.44	1.30	1.80	
solids density, g/cc	2.46	2.49	2.71	2.34
porosity	0.41	0.47	0.33	
permeability, cm ²	3.46x10 ⁻⁹	2.5x10 ⁻¹⁰		
maximum size, cm	<3.81	<0.476	90	
minimum size, cm	>0.00077	>0.00077	30	

The relationship between geometric mean size, geometric standard deviation of the particle size distribution, particle shape factor, porosity, and permeability is given by equation 107 of reference (1).

With regard to permeability, experiments were run on the TOSCO shale to determine the relationship between saturation and relative permeability. For the solution of this problem, it is more convenient to express relative permeability as a function of capillary pressure, and then using certain approximations, obtain the relationship between relative permeability and capillary pressure (2). For the TOSCO shale the relationship obtained was

$$K_{rw} = S^{3.34} \quad (1)$$

where

K_{rw} = relative permeability, dimensionless
 S^{rw} = fractional saturation, dimensionless.

The saturation moisture content of the TOSCO oil shale residue is 38% by weight ($S = 1$ and $K_{rw} = 1$ when the moisture content is 38%). The value of the exponent in equation (1) indicates that the pore size distribution is quite uniform (A value of 3 is indicative of a completely uniform pore size distribution).

To determine the kind and maximum quantity of dissolved solids leachable, 3 experiments were devised. The first experiment was the blender experiment and consisted of taking a 100 gram sample of the shale which passed the No. 40 sieve, and mixing it with 250 ml of distilled water in a blender. The mixture was then removed from the blender and 750 ml of distilled water added. The mixture was then filtered using a vacuum system with a Büchner funnel and No. 40 Whatman filter paper. The filtrate was then refiltered and the resulting solution placed in a plastic bottle for storage until a chemical analysis could be completed.

The second experiment was the shaker experiment and consisted of taking a 100 gram sample of the shale which passed the No. 40 sieve and placing it in a one gallon container to which 1 liter of distilled water was added. The container was then shaken manually for 5 minutes. The resulting mixture was then filtered using a vacuum system and a Büchner funnel and No. 40 Whatman filter paper. The filtrate was then refiltered and the resulting solution placed in a plastic bottle for storage until a chemical analysis could be completed.

The conductance of each solution was obtained, and a chemical analysis completed on the TOSCO samples. These results are given in Table 1.

Table 1 - Blender and Shaker Experimental Results

Sample	Conductance		Concentration (mg/l)								Test
	(µmhos / cm @ 25°C)		Na ⁺	K ⁺	Ca ⁺⁺	Mg ⁺⁺	HCO ₃ ⁻	NO ₃ ⁻	SO ₄ ⁼	Cl ⁻	
	Blender	Shaker									
Raw	310	300	-	-	-	-	-	-	-	-	-
USBM	1,000	920	-	-	-	-	-	-	-	-	-
TOSCO	1,770	1,640	165	32	114	27.3	20.2	5.6	730	7.6	Blender
Total mg/l	1,102	1,154	206	10	102	30.9	19.5	5.1	775	5.8	Shaker

Considering differences in composition (due to sampling), the blender and shaker experiments yield a filtrate of approximately the same concentration and composition.

To determine the quantities of dissolved solids leachable by percolation, a percolation experiment was conducted on the TOSCO shale. The apparatus for the experiment consisted of a plastic column 120 cm in length and 10 cm in diameter. The column was filled with 12,500 grams of the TOSCO spent shale, and a constant head of

2 cm maintained on the top of the column. A small outlet, 0.5 cm in diameter, was located at the bottom of the column to provide a means of collecting any leachate.

The first leachate was observed 14 days after the water was originally applied. For the following 28 days, volumes of leachate were collected at various time intervals until a total of 4.6 liters had been percolated and collected.

The volume and conductance of each leachate sample collected was determined. The first 8 samples were analyzed for Ca^{++} , Mg^{++} , Na^+ , SO_4^- and Cl^- . These results are given in Table 2.

Table 2 - Experimental Results of the Percolation Experiment on TOSCO Shale

Volume of leachate sample (cc)	Total Volume of leachate (cc)	Conductance of sample ($\mu\text{mhos/cm @ } 25^\circ\text{C}$)	Concentration (mg/l) of sample				
			Na^+	Ca^{++}	Mg^{++}	SO_4^-	Cl^-
254	254	78,100	35,200	3,150	4,720	90,000	3,080
340	594	61,600	26,700	2,145	3,725	70,000	1,900
316	910	43,800	14,900	1,560	2,650	42,500	913
150	1,060	25,100	6,900	900	1,450	21,500	370
260	1,320	13,550	2,530	560	500	8,200	205
125	1,445	9,200	1,210	569	579	5,900	138
155	1,600	7,350	735	585	468	4,520	138
250	1,850	6,825	502	609	536	4,450	80
650	2,500	5,700	-	-	-	-	-
650	3,150	4,800	-	-	-	-	-
650	3,800	4,250	-	-	-	-	-
760	4,560	3,850	-	-	-	-	-

The results of the column experiment indicate that

- (1) the dissolved solids are quite readily leached from the column, and
- (2) the concentrations of the various ionic species are quite high, but when the amount of dissolved solids leached from the column per 100 grams of shale is compared to that of the blender and shaker experiments, the results are quite similar. This is indicated in Table 3.

Table 3 - Mass of Various Ions in mg Leached per 100 Grams of TOSCO Shale

Ion	Test		
	Shaker	Blender	Percolation
Ca^{++}	102	114	64
Mg^{++}	31	27	40
Na^+	206	165	258
SO_4^-	775	728	675
Cl^-	5	8	18
Total	1,119	1,042	1,055

A computer program has been developed which gives "order of magnitude" results for predicting the concentrations of the effluent from the column. The program is set up to consider a three-phase system. The phases are (1) an exchange phase, (2) a solution phase, and (3) a crystalline salt phase. The program uses relationships developed by Gapon, and considers CaSO_4 as the moderately soluble salt.

The procedure is as follows (3). A volume of initial solution equal to the volume of solution contained in each soil segment is brought into equilibrium with the first segment. By alternately holding the shale phase and the crystalline salt phase (CaSO_4) constant, and by making successive approximations on the Gapon equations, the equilibrium solution for the segment may be calculated. The resulting solution is then equilibrated with a second soil segment, and the procedure repeated until the equilibrium solutions have been equilibrated with all soil segments. The concentration of the solution ions is then printed out.

A second volume of the initial solution is now brought into equilibrium with the first soil segment and the procedure continues until the desired amount of solution is percolated through the soil profile.

Pilot studies using TOSCO unweathered spent oil shale residue were carried out on Colorado State University's Rainfall-Runoff Experimental Facility. The model used for this study had the following characteristics. There were approximately 68 tons of the TOSCO unweathered spent shale placed in a pile 80 feet long, 8 feet wide at the maximum depth of 2 feet and 12 feet wide at the surface. This shale was placed on a 0.75% slope. For the first series of experiments, the surface (top 3 in.) had an in-place density of 83 lb/ft³. The density of the shale below the surface was only 54 lb/ft³. A 4-inch layer of sand was placed below the shale to collect any percolation water. An impermeable plastic barrier was placed below the sand filter and along the sides of the facility to insure that all percolation water was caught. Percolation water from the sand drain was collected in a 50 gallon drum.

Artificial rainfall was applied by a system of nozzles spraying into the air over the facility. The system had the capability of producing rainfall intensities from about 1/2 inch per hour to over 2.5 inches/hour.

Rainfall mass curves were obtained from a recording-type rain gage. The surface runoff was measured by an H-flume with a standard float gage. After passing through the flume, the runoff water was diverted to a small settling basin where it evaporated.

Three access tubes for use of a neutron moisture probe were installed in the middle of the shale at 20, 40, and 60 feet from the upstream end of the facility. Four thermistors were installed 60 feet downstream to monitor the temperature of (1) the air, (2) the surface of the shale, and (3) the shale at depths of one and two feet below the surface.

In the first 9 experiments (3 from natural rainfall, 6 from artificial rainfall), the total water applied amounted to over 26 inches in a 48 day period, or nearly two years of precipitation for the oil shale area.

From the first series of experiments, it was determined that the concentration and composition of total dissolved solids was dependent on several variables, including surface moisture, rainfall intensity, length of overland flow, kinematic viscosity of runoff water, slope, and time since beginning of runoff.

Table 4 gives results of chemical analyses conducted on samples obtained when the runoff rate had reached hydraulic equilibrium (hydraulic equilibrium is reached when runoff rate equals rainfall rate). Only the major constituents are given. Other ions analyzed for but not detected include Cu^+ , Zn^{++} , Al^{+++} , Fe^{++} , Cr^{6+} , Br^- , F^- , and I^- . The maximum concentration's observed were: K^+ , 30 mg/l; NO_3^- , 9 mg/l; and PO_4^{3-} , 5 mg/l.

Table 4 - Results of Chemical Analyses Conducted on Samples Taken at the Beginning of Hydraulic Equilibrium

Test No.	Rainfall and Runoff Rate, in/hr	Conductivity $\mu\text{mhos/cm @ } 25^{\circ}\text{C}$	Concentration, me/l					
			pH	Na ⁺	Ca ⁺⁺	Mg ⁺⁺	SO ₄ ⁼	HCO ₃ ⁻
4	0.55	223	8.203	0.34	1.17	0.20	1.46	0.32
5	0.44	785	8.048	0.67	4.71	0.94	6.04	0.31
6	1.00	425	7.875	0.40	2.37	0.34	2.97	0.34
7	1.72	745	8.167	1.68	3.20	0.62	5.53	0.31
8	2.20	430	8.241	1.70	1.80	0.42	3.81	0.32

Figure 1 shows the effect of drying (before a rainfall event) on the rate at which dissolved solids are leached from the oil shale residue surface during a simulated storm. After a simulated rainfall event, the surface moisture content of the oil shale retorting residue is a maximum (38% by weight). Subsequent drying of this wet surface causes the movement of water from the interior to the surface by capillary action. On reaching the surface, the water evaporates leaving behind a white deposit that is clearly visible on the black surface. This deposit is dissolved during the next rainfall event with the result that both concentration and composition of the dissolved solids in the runoff water vary with time and depend on the amount of drying prior to the rainfall event.

A 10 gram sample of this white deposit was dissolved in a liter of water, and an analysis was made for the major constituents with the following results:

Conductance, $\mu\text{mhos/cm at } 25^{\circ}\text{C}$	Concentration, me/l			
	Na ⁺	Mg ⁺⁺	Ca ⁺⁺	SO ₄ ⁼
28,500	580	30	10	740

The hydrologic parameters include rainfall intensity, length of overland flow, kinematic viscosity of runoff water, and surface slope. For the model used in this study, the surface slope was the same for all runs. All of these hydrologic parameters are included in the average depth of overland flow, \bar{D} . The average depth of overland flow (in feet) is given by

$$\bar{D} = 3/4 \left[\frac{3iLv}{43,200 \text{ gs}} \right]^{1/3} \quad (2)$$

where

- i = rainfall intensity, inches/hr
- L = length of overland flow, feet
- v = kinematic viscosity, ft²/sec (v = 1.088x10⁻⁵ ft²/sec at 20°C)
- g = acceleration of gravity, 32.2 ft/sec²
- s = slope, dimensionless (s = 0.0075 for all experiments)

43,200 is a unit conversion factor, $\frac{(\text{inch})(\text{seconds})}{(\text{foot})(\text{hour})}$

In order to develop a relationship between \bar{D} and the dissolved solids concentration, the following approach was used. On reciprocal paper the time since beginning of runoff was plotted versus conductance for each run and the value of conductance for the respective runs at infinite time obtained. This value was then plotted versus \bar{D} and using the approximation developed from the data that

dissolved solids in mg/l (0.6) (specific conductance @ 25°C in μmhos/cm), the relationship given by equation (3) was developed.

$$(\text{dissolved solids concentration @ infinite time}) \approx \frac{1.0 \times 10^{-3}}{D} \cdot \frac{1}{1.86} \quad (3)$$

As mentioned previously, both the concentration and composition of the runoff water varied with time. In general, at the beginning of a run, Na⁺ constituted the greatest portion of the cations, while near the end of the run (all experiments extended over approximately four hours) the runoff water approached 100% Ca⁺⁺ in cation concentration. The anion concentration was due almost entirely to SO₄⁼.

In order to determine the amount of sediment transported by the runoff water from the shale surface, the following procedure was adopted. An Imhoff cone was filled with 1 liter of runoff sample and allowed to settle for 24 hours. Assuming the settleable matter had a bulk density of 1.30 grams/cc, the settleable solids in mg/l could be determined. By plotting runoff volume times concentration versus time the amount of sediment moved during a given run could be determined. The sediment transported varied from 0.0081 lbs/[(ft²)(hr)] to 0.083 lbs/[(ft)²(hr)] for the series of runs. A particle size distribution was also obtained on the sediment. All of the sediment sampled passed the No. 200 sieve (0.074 mm opening) and had an average size of 0.032 mm.

To account for the water, a water balance was made on each run. These results are given in Table 5.

Table 5 - Water Balance Data

Run	Volume of Water Applied (ft ³)	Volume of Water Runoff (ft ³)	Volume of water Stored (ft ³)	
			Calculated	Observed
4	179	173	+ 6	+ 9
5	160	148	+12	+14
6	350	350	0	+10
7	480	500	-20	+20
8	780	755	+25	+19

The volume of water applied is simply the average rainfall intensity multiplied by the time of application times the area of application. The volume of runoff water can be determined from the hydrograph recorded by the stage recorder. Because no allowance was made for evaporation, the calculated volume of water stored is simply the volume of water applied minus the amount of runoff water. The observed volume of water stored was obtained by multiplying the area of application by the average rainfall intensity times the observed time for the surface of the shale to become wet (at best this observed time would be within ±10%).

As indicated from the data, the volume of water stored is quite small. This is also indicated by the change in moisture within the shale as determined by a neutron moisture probe. At one foot below the surface, the total change in moisture from the beginning of the first test (natural rainfall) to the last test (test No. 8) was less than 3% for those stations located 20 and 40 ft downstream, and less than 8% for the station located 60 ft downstream. At 1 foot 6 inches below the surface the change in moisture at the 20 ft and 40 ft stations was less than 2%, and for the station located 60 feet downstream the change was less than 12%.

Thermistors located 60 feet downstream indicated temperatures within the shale remained relatively constant between 20-24°C throughout the duration of the experiments. However, the dark color of the spent shale caused temperatures as high as 77°C to be measured on the surface. Temperatures this high could be lethal to germinating seeds.

After the series of nine tests were completed, the bulk density of the spent shale was increased by use of mechanical compacters, and another series of experiments conducted. Results of these experiments are not yet available.

Experiments using artificial snow will be conducted on the shale in late 1970 and early 1971. One natural snowfall has produced conductances in the runoff water as high as 450 $\mu\text{mhos/cm}$ @ 25°C. This conductance was obtained, however, when over half of the snow had melted. Thus, conductances higher than this may occur.

ACKNOWLEDGEMENTS

This paper is based on research supported by the Federal Water Quality Administration of the U.S. Department of Interior. Five percent of the total project cost was provided by Colorado State University. The extensive cooperation of the Union Oil Company, the U.S. Bureau of Mines, and the TOSCO organization was indispensable in making this study possible.

REFERENCES

1. "Turbulent Flow in Porous Media," by John C. Ward, (Closure), Journal of the Hydraulics Division, Proceedings of the American Society of Civil Engineers, July, 1966, page 116.
2. Corey, A.T., Fluid Mechanics of Porous Solids, Colorado State University, Fort Collins, Colorado, 1965.
3. Predicting the Quality of Irrigation Return Flows, Masters Thesis by G.A. Margheim, Department of Civil Engineering, Colorado State University, Fort Collins, Colorado, December, 1967.

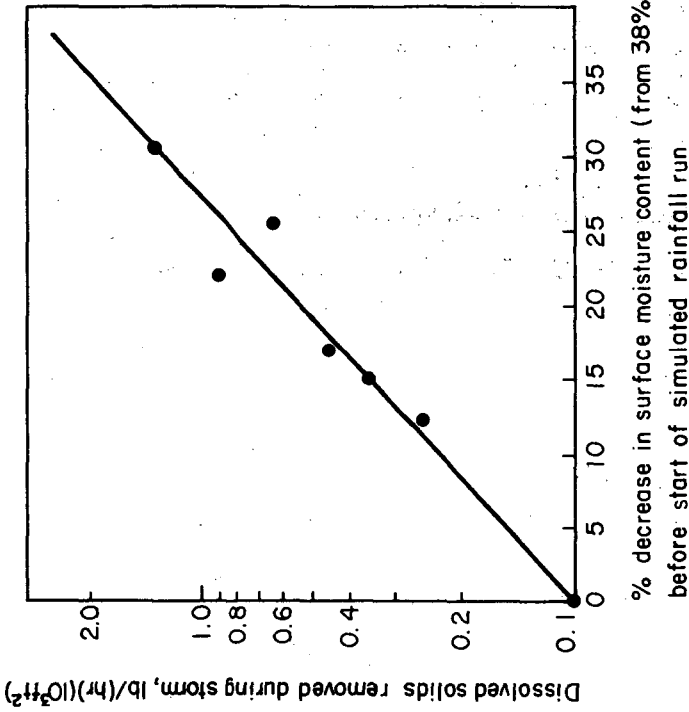


Figure 1 - Leachable Dissolved Solids versus Extent of Drying before Simulated Rainfall Event.

METHOD FOR RECLAIMING WASTE WATER FROM OIL-SHALE PROCESSING

Arnold B. Hubbard

U.S. Department of the Interior, Bureau of Mines
Laramie Energy Research Center, Laramie, Wyoming 82070

INTRODUCTION

Because the importance of industrial pollution abatement continues to grow, this work was initiated to develop possible solutions for environmental problems that an oil-shale processing industry may create (1).^{1/} Although the commercial production of fuel from oil shale is still in the future, it is realized that adequate disposal of waste products from a large oil-shale processing plant may present major problems. The Bureau of Mines, U.S. Department of the Interior, has initiated research to identify and propose solutions for the waste disposal problems in advance of industrial development as a guide to the incorporation of environmentally acceptable disposal processes in future plants.

The major waste products produced by an oil-shale processing industry are large quantities of spent shale, process gas, and process water. Because the process water formed during the production of shale oil contains considerable quantities of soluble organic and inorganic materials, it will present a major disposal problem.

The actual amount of water produced and the degree to which it is contaminated will depend upon the type and operating condition of the retorting process used and the nature of the oil shale. The amount of process water formed may equal 20 to 40 percent of the oil produced. This means that a plant producing 100,000 barrels of oil per day may also produce from 20,000 to 40,000 barrels of contaminated waste water that will require treatment before it can be used or discharged to the environment.

This paper describes a method for successively removing the contaminants so that water of different qualities may be obtained at the end of each step in the process. Hence, if water needs only partial treatment for plant use, the purification process may be stopped at any step.

Because most of our oil shale is located in arid country, possibly all of the retort water produced will be reclaimed and used to extinction, thus eliminating the necessity for discharge to the environment. Deciding factors in selecting the method described were (1) to use materials that can be regenerated or discarded, and (2) to try to obtain a product or products that may be of value to offset the reclaiming costs.

The method found to be the most promising makes use of a combination of (1) chemical treatment with lime to remove carbonates, most of the ammonia, and a portion of the organic materials; (2) adsorption on activated carbon to remove the remaining organic material; and (3) cation and anion exchange resins to remove the balance of the cations and anions.

EXPERIMENTAL

Process water produced by the Bureau's Gas Combustion Retort No. 2 operated by the Colorado School of Mines Research Foundation, Rifle, Colorado (2), and water

^{1/} Underlined numbers in parentheses refer to items in the list of references at the end of this report.

that separated from shale oil obtained by in situ retorting near Rock Springs, Wyoming (3), were studied. The process waters were obtained from the bottoms of the oil storage tanks after settling from the shale oils. Residual suspended oil was allowed to separate further from the waters in separatory funnels, and the waters were drained off. The remaining suspended oil and suspended solids were removed by filtering through water-wet filter paper. The filtrates were highly colored solutions of organic and inorganic materials.

Two slightly different water treatment methods were used. In the first method, Step A, sufficient lime to release the ammonia in the water plus a 10 percent excess was added to 1 liter of the colored, filtered water, and the mixture was boiled with constant stirring for 1 hour. This precipitated some of the organic material and essentially all of the carbonates, and liberated most of the ammonia. In Step B, the water, still colored, was passed through a column of activated carbon (Calgon Corporation, Filtrasorb 300),^{2/} 2.5 cm in diameter by 100 cm long. The effluent from the carbon-packed column was colorless and clear. In Step C, the water was passed through a 2.5 cm by 80 cm column of cation exchange resin (Rohm and Haas IRC-84). This removed the ammonium and other cations by exchanging them for hydrogen ions, which changed the pH of the water from basic to acidic. In Step D, the water was passed through a similar column of anion exchange resin (Rohm and Haas IR-45). This replaced the anions with hydroxyl ions to produce a relatively pure effluent.

In the second method, Steps A and B were reversed. The organic material was removed by passing the colored filtrate through the activated carbon column first, and the lime and ion exchange resin treatments followed.

The effectiveness of removing the soluble organic material was estimated by color reduction and carbon analysis by a Beckman Model IR-315 Infrared Carbon Analyzer. Activated carbon removed essentially all of the soluble organic material (4). Ion analyses were made by standard chemical and instrumental methods.

RESULTS AND DISCUSSION

The gas combustion retort water was selected for this study because it contains more total dissolved components than any other water tested, and it was produced by a process likely to be used in the future. The in situ water was selected because of its special origin and its high sodium, carbonate, and chloride ion content.

Analytical results for waste waters derived from Colorado and Wyoming oil shale produced by gas combustion and in situ retorting, respectively, show the presence of essentially the same components. However, the amounts and proportions of the components can vary widely.

The components include both organic and inorganic compounds. The organic material consists of amines, acids, bases, and neutral compounds. The actual number of organic compounds expected to be found in process water could be in the hundreds, but no specific compound identifications were made in the current study. The bulk of the inorganic components consists of ammonium, sodium, bicarbonate, carbonate, sulfate, and chloride ions. While the ions listed are not all of the ions in the water, they are the major ones. Spot analyses showed that minor ions were decreased in proportion to the others and generally were eliminated completely.

Tables 1 and 2 give the concentrations of the principal inorganic ions found in the two waters used and the concentrations remaining after the application of

^{2/} Reference to specific brand names is made for identification purposes only and does not imply endorsement by the Bureau of Mines.

each step of the two treatment methods. The ammonia concentrations of 8.91 and 4.80 grams per liter may be sufficiently high for economic recovery.

Table 1 shows the effectiveness of the two methods in removing the following ions from gas combustion retort water: ammonium, sodium, carbonate, chloride, and sulfate. Both methods removed these ions to an acceptable level with one pass (5, 6). The main advantages of Method 1 over Method 2 are emphasized in Step A (columns 1, 3, and 4). When the water was treated with lime first, 7.77 grams per liter (87%) of the ammonium ion, 12.78 grams per liter (88%) of the carbonate ion, and 3.20 grams per liter (59%) of chloride ions were removed from the water. When the water was passed over activated carbon first, the carbon removed 2.44 grams per liter (27%) of the ammonium ion, 1.92 grams per liter (13.3%) of the carbonate ion, and 0.32 gram per liter (5.9%) of the chloride ion. In general, the final products from both methods are comparable, but since treating the water with lime first (Method 1) is more economical because it reduces the load on the activated carbon and ion exchange resins, this method will be selected for future study.

In column 5, the sulfate values are inconsistent, particularly in that there appear to be more sulfate ions in the water after it is passed over the activated carbon in both methods. This could be caused by converting soluble sulfur-containing ions to sulfate but will require further study. The pH values shown in column 6 are all basic with the exception of Step C where the water was passed over the cation exchange resin. At this point in the process, the cations are exchanged for hydrogen ions and the pH changes to acid. This change in pH from basic to acidic causes unstable sulfur-containing ions to decompose. In so doing, free sulfur is precipitated, and the solution becomes cloudy in appearance. The removal of this finely precipitated sulfur presents a problem. It is too fine for filtration and settles very slowly. Flocculants may be useful, but they have not yet been investigated.

Table 2 shows similar results obtained for a water produced by in situ retorting near Rock Springs, Wyoming. The sodium, carbonate, chloride, and sulfate contents of this water are particularly high, but the process appears to work equally well on this water and, in general, the comments concerning table 1 are applicable to table 2.

In both methods, the ions were decreased successively in steps. The first method is preferable because its final product generally has slightly lower ion contents for each ion considered. Also, by treating the water with lime first to remove most of the ammonium, carbonate, and other ions present, along with some organic material, the load on the activated carbon and ion exchange resins is reduced. This will substantially reduce the cost of the treating process. Ion reductions of 90 percent and better were obtained by one passing, and this should be sufficient for most water uses. Further purification can be accomplished by utilizing a second set of ion exchange resin columns.

CONCLUSION

The procedure described can be used to reclaim waste water from oil-shale processing by (1) treating the water with lime, and heating to remove ammonia, carbonates, and some organic material; (2) passing over activated carbon to remove the balance of the organic material; and (3) passing over ion exchange resins to remove anions and cations. The effluent from any step can be diverted for plant use where further purification is not necessary. It may be possible to recover from this process ammonia and ammonium salts.

ACKNOWLEDGMENT

The work upon which this report is based was done under a cooperative agreement between the Bureau of Mines, U.S. Department of the Interior, and the University of Wyoming.

REFERENCES

1. Holcomb, R. W. Science, v. 169, July 1970, pp. 457-459.
2. Ruark, J. R., H. W. Sohns, and H. C. Carpenter. BuMines Rept. of Inv. 7303, 1969, 109 pp.
3. Burwell, E. L., H. C. Carpenter, and H. W. Sohns. BuMines Tech. Prog. Rept. 16, 1969, 8 pp.
4. Rizzo, J. L., and R. E. Schade. Water and Sewage Works, August 1969, pp. 307-312.
5. Committee on Water Quality Criteria, Federal Water Pollution Control Adm., Dept. of the Interior. Water Quality Criteria, 1968, 234 pp.
6. State Water Quality Control Board (California), Water Quality Criteria. Publication No. 3-A, 1963, pp. 258-273.

TABLE 1. - Removal of components from gas-combustion process water by methods 1 and 2

Method	6					
	1 Ammonium, g/l	2 Sodium, g/l	3 Carbonate, g/l	4 Chloride, g/l	5 Sulfate, g/l	6 pH
Untreated water	8.91	1.04	14.44	5.43	1.68	8.61
1 Step						
A	1.14	1.02	1.66	2.23	1.48	9.70
B	.57	.63	.42	1.52	1.90	9.10
C	.11	.15	.65	.35	.77	2.40
D	.00	.06	.18	.01	.00	9.34
2 Step						
A	6.47	.77	12.52	5.11	2.71	8.72
B	1.73	.73	.89	1.14	.57	12.11
C	.52	.28	.52	1.12	.76	1.35
D	.50	.27	.08	.03	.10	9.29

TABLE 2. - Removal of components from in situ retort process by methods 1 and 2

Method	6					
	1 Ammonium, g/l	2 Sodium, g/l	3 Carbonate, g/l	4 Chloride, g/l	5 Sulfate, g/l	6 pH
Untreated water	4.80	3.10	19.22	13.41	4.45	8.69
1 Step						
A	.52	2.83	5.26	3.11	3.98	8.79
B	.33	2.03	4.36	2.22	1.18	9.08
C	.25	.55	.57	.81	2.90	3.98
D	.12	.48	.27	.38	.64	11.24
2 Step						
A	4.03	2.63	6.70	10.37	3.69	8.76
B	1.41	2.14	.82	4.54	3.32	9.53
C	.25	.58	.46	.88	2.84	4.07
D	.21	.56	.50	.75	3.11	11.20

HYDROCRACKING OF SYNTHETIC OILS

S. A. Qader and G. R. Hill
Mineral Engineering Department
University of Utah, Salt Lake City, Utah 84112

INTRODUCTION

Synthetic oils derived from coal, oil shale and tar sands differ significantly in composition from petroleum crudes. The coal oils contain large amounts of oxygenated compounds and aromatic hydrocarbons and the shale oils contain large quantities of nitrogen compounds. Because of the differences in composition the synthetic oils may pose some new problems in their processing as compared to the conventional processing of petroleum oils. Hydrocracking is a versatile processing method and it will play an important role in the processing of synthetic oils as evidenced by the published data (1-4). In the present communication, the data on some aspects of hydrocracking of coal, shale and tar sand oils are presented.

EXPERIMENTAL

MATERIALS: The coal oil was obtained by the hydrogenation of a high volatile bituminous coal from Utah. The shale oil was obtained by insitu retorting. The tar sand oil was prepared by solvent extraction of tar sands found in Utah. A dual functional Catalyst was used for hydrocracking the synthetic oils.

EQUIPMENT

Hydrocracking was carried out in a continuous bench scale fixed Reactor System (4). The products were evaluated by standard methods. The heat of the reaction was calculated from the heats of combustion of raw materials and products.

RESULTS AND DISCUSSION

The product distributions and the severities of hydrocracking mainly depends upon the composition of the feed stocks and the processing conditions. The data in Table I indicates that the coal oil is more aromatic in nature when compared to the shale and tar sand oils as shown by the H-C atomic ratios. The coal oil also contains more heterocompounds and asphaltenes. The data in Table II indicates that the coal oil is a more refractory feed stock when compared to the shale and tar sand oils. This appears to be due to the higher aromatic and asphaltene contents of the coal oil. The hydrocracking severities seem to be somewhat related to the aromaticity of the feed stocks. The data in Table III indicates that the yield of Naphtha depends upon the total conversion irrespective of the type of feed stock used. The three feed stocks yielded almost the same quantities of Naphtha at equal conversion levels. However, the gas yield was high in case of shale oil while the coal oil yielded relatively more coke. The composition of Naphtha and gas depend upon the nature of the feed stock as indicated by the data in Table IV. The coal of Naphtha is more aromatic and will have a higher octane rating when compared to the Naphthas from shale and tar sand oils. It is evident from the foregoing discussion that aromatic feed stocks need more severe process conditions but they produce better quality naphthas.

The data in Table V indicates that hydrogen consumption varies with the nature of the feed stock and is directly proportional to the conversion in all the three cases. The consumption of hydrogen in coal oil hydrocracking is higher than the consumption in tar sand oil processing which in turn is more when compared to shale oil processing. This again seems to be related to the aromaticity of the feed stocks. The hydrocracking reactions are exothermic and the heat of the reaction varies with the nature of the feed stock and conversion as shown by the data in Table V. Coal oil hydrocracking produces more exothermic heat when compared to tar sand oil which in turn gives more heat when compared to shale oil. The reaction heat seems to be also related to the aromaticity of the feed stock.

The first order rate constants of the hydrocracking of coal, shale and tar sand oils were found to be respectively represented by equations 1 to 3.

$$K_c = 0.52 \times 10^4 e^{-16,200/RT} \text{ hr.}^{-1} \quad (1)$$

$$K_s = 0.12 \times 10^5 e^{-14,300/RT} \text{ hr.}^{-1} \quad (2)$$

$$K_t = 1.05 \times 10^4 e^{-15,100/RT} \text{ hr.}^{-1} \quad (3)$$

Where K_c , K_s , K_t represent reaction rate constants for the hydrocracking of coal, shale and tar sand oils respectively.

ACKNOWLEDGEMENT

Research work supported by the Office of Coal Research and the University of Utah.

LITERATURE CITED

1. Katsobashvili, Ya. R., Elbert, E. A., *Coke and Chemistry, USSR*, 1, 41 (1966).
2. Zielke, C. W., Struck, R. T., Evans, T. M., Costanza, C. P., Gorin, E., *Ind. Eng. Chem., Process Design and Develop*, 5, 151, 158 (1966).
3. Cottingham, P. L., Carpenter, H. C., *Ind. Eng. Chem., Process Design and Develop*, 6, 212 (1967).
4. Qader, S. A. Hill, G. R., *Hydrocarbon Processing*, 48, No. 3, 141 (1969).

TABLE I - PROPERTIES OF FEED STOCKS

	Coal Oil	Shale Oil	Tar Sand Oil
Gravity, °API	0.75	20.2	17.3
Viscosity, SUS, 80°C	205	180	220
S, Wt. %	0.43	0.85	0.34
N + O, Wt. %	3.84	2.14	1.84
H/C (Atomic)	1.06	1.81	1.62
Asphaltene, Vol. %	30.0	2.0	2.5
<u>Distillation, °C</u>			
1. B. P.	200	200	200
50% distillate	348	334	319

TABLE II - HYDROCRACKING PRODUCT DISTRIBUTION

Temp: 480°C, Pressure: 2000 P.S.I.
Space Velocity: 0.96

	Coal Oil	Shale Oil	Tar Sand Oil
Yield of Products, Vol. %			
Naphtha	60.0	68.0	66.0
Gas	9.5	14.0	12.0
Coke	5.1	4.0	6.0
Recycle Oil	27.0	14.5	17.5
Severity	0.7	0.82	0.78

TABLE III - HYDROCRACKING PRODUCT DISTRIBUTION

Conversion, Vol. %	20	40	60	80
<u>Naphtha Yield</u>				
Coal Oil	15	32	48	65
Shale Oil	16.5	35	48	63.5
Tar Sand Oil	15.5	32	47.5	64.0
<u>Gas Yield</u>				
Coal Oil	2.5	5.0	8.0	10.5
Shale Oil	2.0	6.0	9.0	13.0
Tar Sand Oil	3.5	6.0	8.5	11.0
<u>Coke Yield</u>				
Coal Oil	0.5	2.0	4.0	5.6
Shale Oil	0.5	1.6	2.7	4.0
Tar Sand Oil	0.5	2.0	3.6	5.0

TABLE IV - COMPOSITION OF NAPHTHA AND GAS

Temp: 480°C, Pressure: 2000 P.S. 1.

Sp. Vel: 0.96

	Coal Oil	Shale Oil	Tar Sand Oil
<u>Composition of Naphtha, Vol. %</u>			
Saturates	75.2	40.2	49.5
Olefins	2.8	3.1	2.5
Aromatics	22.0	56.7	48.0
<u>Composition of Gas, Vol. %</u>			
CH ₄	16.0	13.0	12.0
C ₂ H ₆	28.0	27.0	28.0
C ₃ H ₈	42.0	40.0	37.0
C ₄ H ₁₀	14.0	20.0	22.0

TABLE V - HYDROGEN CONSUMPTION AND REACTION HEAT IN HYDROCRACKING

Conversion, Vol. %	30	50	60	80
<u>H₂ Consumption, SCF/BBL</u>				
Coal Oil	600	1020	1240	1660
Shale Oil	380	720	900	1230
Tar Sand Oil	350	720	910	1290
<u>ΔH X 10³, BTU/BBL</u>				
Coal Oil	47	80	96	130
Shale Oil	34	58	70	96
Tar Sand Oil	32	60	75	104

ANALYTICAL LABORATORY TECHNIQUES FOR OIL SHALE

B. L. Beck⁽¹⁾, David Liederman⁽²⁾, R. Bernheimer⁽³⁾

- (1) Enjay Chemical Company, Baytown, Texas
(2) Mobil Research and Development Corp., Paulsboro, New Jersey
(3) 21 Innes Road, East Brunswick, New Jersey

Introduction

From 1964 to 1967, the U. S. Bureau of Mines oil shale facilities at Anvil Points near Rifle, Colorado were reactivated for a cooperative industrial oil shale research program. Mobil Oil Corporation acted as manager for this project with five other major oil companies actively participating. These were Humble Oil and Refining Company, Continental Oil Company, Pan American Petroleum Corporation, Phillips Petroleum Company, and the former Sinclair Research, Inc. Technical people from these oil companies, supported by personnel from the Colorado School of Mines Research Foundation (CSMRF), carried out an intensive retorting and mining research program at the then named Anvil Points Oil Shale Research Center. This paper describes the activities of the analytical laboratory which supported the research program. These activities would probably be typical of any such oil shale laboratory in a remote location. Information on the research program may be found elsewhere (1).

The primary purpose of the analytical laboratory was to serve the retorting and mining research program as opposed to doing analytical research. Some supplementary research work actually was found necessary and was done. However, the scope of this paper is limited to the role of the laboratory as a support group.

The Laboratory and Staff

The Bureau of Mines building, laboratory furniture, and much equipment were available and used. Where necessary and justifiable, new equipment was added to complete the physical part of the laboratory. Our major concern was obtaining equipment and instrumentation that had a short delivery time, was reliable, and was as simple as possible. No skilled laboratory instrument repair service was available onsite.

The staff was headed by a supervisor and a chemist, both professional analytical chemists from the participating companies. From four to seven laboratory technicians were required during the project. These were hired specifically for this limited project by the CSMRF and had limited or no laboratory experience.

Training in oil shale laboratory techniques was required for both the technical staff and the technicians. For the technical people, this came from visits to the Bureau of Mines Station in Laramie, Wyoming and to the CSMRF in Golden, Colorado. The technicians were trained onsite by the chemists.

Analytical Methods

A variety of methods was used to analyze the samples generated by the research program. These are listed in Table I. Many are or are similar to ASTM methods and are so noted. Others are described below.

Fischer Assay

One of the most important tests was the Fischer Assay on raw and spent shale. A semiautomated apparatus was designed using the basic principles of the methods reported by the Bureau of Mines (2), and the CSMRF (3).

One control unit of the six-unit apparatus is shown in Figure 1. This control circuit provided the desired heating rate with an upper temperature limit

cutoff and indicator. Temperature was monitored with the pyrometer, and heating power with the ammeter. All six control units were mounted on an aluminum panel 24 in by 66 in.

When an assay was started, the variable transformer was set a full power (normally about 13.5 amperes), and the high set point of the pyrometer at 510°C. When the temperature reached 500°C, the variable transformer was adjusted to a pre-determined setting to maintain the final 500°C temperature. After retorting was complete, the main switch was opened.

A complete description of the Fischer Assay method is found in the Bureau of Mines paper.

Carbon and Hydrogen

Precision carbon and hydrogen determinations were made using the conventional high temperature oxidative combustion technique followed by weighing the CO₂ and H₂O formed. The apparatus was specifically designed and assembled for our needs. Three furnaces were used around a 19 mm by 36 in Vycor combustion tube, packed according to Steyermark (4). Temperatures of the furnaces were:

- 4 in Sample Furnace - Oil and Organic Standards 700 ± 10°C
Gas, Shale, and Inorganic Standards 950 ± 10°C
- 12 in Middle Furnace - 680 ± 10°C
- 8 in Exit Furnace - 190 ± 10°C

For all but gas samples, the sample furnace was motor driven to allow an hour for movement from its initial position to its final position next to the middle furnace. When the final position was reached, a timer was activated to give 45 minutes additional combustion time before an end-of-run alarm sounded.

For gas samples, the sample furnace was positioned next to the middle furnace. A roll of copper gauze was inserted in place of the combustion boat and a special adapter (Figure 2) added to the combustion tube inlet. A 25% brine solution was used to displace the gas sample from a 1-liter gas sample tube in about 40 minutes. The combustion tube was then oxygen purged for an additional 20 minutes.

Gas Chromatography of Gas Samples

Retort gases were routinely analyzed for CO₂, O₂, N₂, CH₄, CO, and H₂. A Fischer Gas Partitioner Model 25V with two columns in series was used. Column 1 was 30 in of hexamethylphosphoramide on 60-80 mesh Columpak; Column 2 was 6.5 ft of 42-60 mesh activated 13X molecular sieve. A Sargent Model SR-25 recorder with a 1.0-mv range plug recorded the chromatographic peaks. Both instruments provided the remote laboratory with the high reliability required. Helium was used as carrier gas for determining all components except hydrogen; nitrogen was used for determining hydrogen. Analyzed standard gas mixtures were used for calibration.

To obtain a composite sample for an experimental retort run, a continuous sample was sent to a brine-displacement gas-holder at the laboratory. Approximately 3 cu ft of gas were collected via a heat-traced line. After a complete sample was obtained, it was then routed through a drying tube directly to a 0.5 ml sample loop at the chromatograph.

Water Analysis

Retort water produced by the retorting of oil shale was analyzed because of interest in corrosion, pollution, disposal, and possible future utilization. Analyses were made for NH₃, Cl⁻, CO₂, solids, ash, and pH.

Shale Richness Distribution

Shale richness, or assay, can be predicted from its density. Consequently the richness distribution of a sample can be determined from the density distribution. Seven solutions of carbon tetrachloride and tetrabromoethane were prepared to cover the density range of interest, 1.6 to 2.4. The volumes of measured shale

samples floating in graduates of the various solutions were normalized to 100% followed by application of a richness-density relationship (5).

Sampling

Obtaining representative samples of raw and spent shale, and liquid and gaseous retort products were always of major concern. Crushed shale, especially raw shale, shows variations in richness with particle size. Liquid product from retorts is a mixture of oil, water, and solids. Gaseous product from retorts has entrained oil, solids, and water.

The various phases of the liquid and gaseous samples were normally separated, measured, and then analyzed individually.

Sampling and sample size reduction of the raw shale were very important. The Fischer Assay and other tests on raw shale samples were the bases of material balances for each experimental retort run.

Several steps of size reduction take place from the tons of raw shale mined to the 100 grams of raw shale charged to the laboratory retort for Fischer Assay. However, the minus eight-mesh shale fed to the laboratory retort must be representative of the sample of interest. When raw shale is crushed, the leaner, more brittle material concentrates in the finer particles, while the richer, tougher material resists crushing and concentrates in the larger particles. To dramatize this effect, Fischer Assays were run on various particle sizes of a crushed sample. The results are shown in Table II.

All shale samples submitted to the laboratory needed to be reduced in quantity and particle size before analyses could be made. A rigorous splitting procedure was developed to reduce the initial quantity received to a basic 775 to 825 gram portion. This portion was crushed to pass an eight-mesh screen. Then another specific splitting and combining procedure was used to reduce this quantity to the amounts required for the individual tests.

Records

As previously noted, this project involved the U. S. Bureau of Mines, the CSMRF and six oil companies. Under these circumstances, accurate and complete records of samples and their analyses were essential. All samples received by the laboratory were sequentially numbered and recorded in bound notebooks. Their identity, date received, date analyses completed, and analyses made were also recorded. Bound calculation books were used and retained for each test, so that the original basic data were available if required.

Nine forms for data workup and reporting were developed for consistency and simplification. All of these were color coded for ease of identification.

Before the completed analyses on any sample were officially released from the laboratory, they were checked by one of the analytical chemists. The philosophy maintained by the laboratory was to report no result in preference to a questionable result.

Quality Control and Crosscheck Programs

A planned and effective quality control program was maintained throughout the research project. A schedule was posted for the technicians showing what tests each was to run on the quality control samples each week. At the end of the week they submitted a form with their results. These were recorded and any abnormal variations noted and investigated.

Every three months standard deviations for all tests in the quality control program were updated. Final statistics for some of the key tests in the program are shown in Table III. The number of quality control tests run depended upon the

frequency of each test normally requested and its importance. They averaged about 5% of the normal work load. Fischer Assays were run most frequently.

The internal quality control program took care of the precision of the tests. However any laboratory, especially a remote and relatively inexperienced laboratory, is also concerned about the absolute accuracy of its results. Standards and synthetic samples were used where possible. In addition, during the program several samples were crosschecked with other laboratories. Most of the comparisons were made with the Bureau of Mines at Laramie. Data were also exchanged with the CSMRF, Mobil, and Humble. Some of the typical crosscheck data are shown in Table IV. The Fischer Assay data are averages of several determinations. Agreements were from satisfactory to excellent.

Participating oil company laboratories were also requested to perform analyses for which this laboratory was not equipped. Examples of these were mass spectrometer gas analyses, and detailed analyses of oil and distillation fractions.

Correlations Among Analyses

During the course of analyzing several hundred samples, some correlations among the results from several methods were developed. Most of these were with the Fischer Assay of raw shale. A computer regression analysis program developed the equations for the relationships, as well as the correlation coefficient and standard deviation. These data are given in Table V.

These relationships compared well with those previously obtained by the Bureau of Mines, and were very useful to internally check analytical results for consistency.

Termination of Program

The Anvil Points Oil Shale Research Center Laboratory was in operation three years, and satisfactorily performed its function as a support group. At the end of the program, all equipment and supplies were appropriately deactivated, stored, or otherwise disposed of. All notebooks and records were filed and a final summary report was prepared. With this experience and newer instrumentation available, a laboratory today could be significantly improved. Undoubtedly much of the success of the laboratory was due to the high staff ratio of two analytical chemists to four-to-seven technicians for mostly routine analyses. The chemists were able to closely supervise the routine work and develop and improve methods. In addition, they were still able to keep familiar with and contribute to the research program.

Acknowledgment

The authors appreciate the permission granted by the six participating companies to publish this report.

References

- (1) Lawson, J. E., et.al., "Gas Combustion Retorting Performance in a Large Demonstration Retort" This Symposium.
- (2) Hubbard, A. B., "Automated Modified Fischer Retorts for Assaying Oil Shale and Bituminous Materials, U. S. Bureau of Mines Report of Investigations No. 6676, (1965).
- (3) Reeves, W. H., "Investigation of Methods for the Determination of Crude Shale Oil in Oil Shales," Colorado School of Mines Research Foundation, Report No. 64-1, (1964).
- (4) Steyermark, A., Quantitative Organic Microanalysis, pp. 221, Academic Press, New York, 2nd edition, (1961).
- (5) Smith, J. W., "Applicability of a Specific Gravity-Oil Yield Relationship to Green River Oil Shale," Ind. Engr. Chem, 3, 306 (1958).

TABLE I

ANALYTICAL METHODS

<u>Name</u>	<u>Procedure</u>
Ash Content of Oil	ASTM D 482
Ash Content of Shale	950°C with air
Benzene Extractables in Shale	ASTM D 473 s
C and H (total) in Shale, Oil, or Gas	See Text
Density of Shale	Loose, packed, solid
Distillation of Oil (10 mm.)	ASTM D 1160
Fischer Assay of Shale	See Text
Gas Analysis by Gas Chromatography	See Text
Gravity of Oil	ASTM D 287
Mineral CO ₂ Content of Shale	ASTM D 1756 s
Moisture Content of Shale	Volatiles at 105°C
Nitrogen (Kjeldahl) in Shale and Oil	ASTM E 258 s
Particle Size Distribution of Shale	Sieve analysis
Pour Point of Oil	ASTM D 97
Ramsbottom Carbon Residue of Oil	ASTM D 524
Saybolt Viscosity of Oil	ASTM D 88
Shale Richness Distribution	See Text
Water Analysis	See Text
Water in Oil	ASTM D 95
Water and Sediment in Oil	ASTM D 1796 s

s - method used similar to ASTM method

TABLE II

VARIATION OF RICHNESS OF RAW SHALE WITH SIZE

<u>Size (mesh)</u>	<u>Gal/Ton (Fischer Assay)</u>
+4	31.8
-4, +8	30.6
-8, +20	28.6
-20, +48	28.0
-48, +100	23.9
-100, +200	20.8
-200	19.6

TABLE III
INTERNAL QUALITY CONTROL PROGRAM STATISTICS

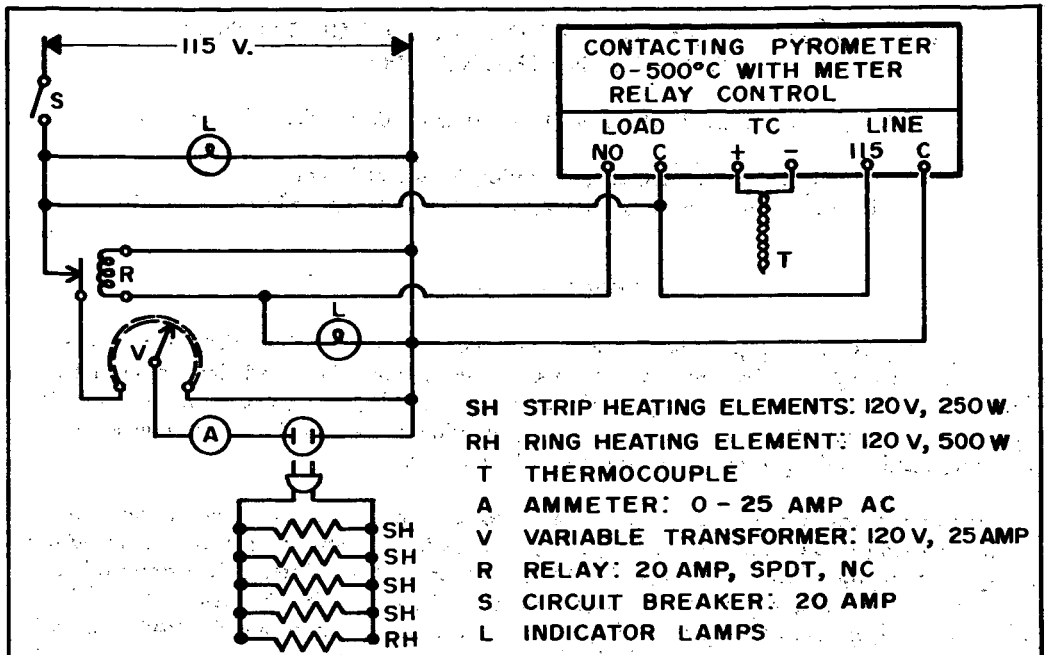
<u>Material</u>	<u>Test</u>	<u>Level</u>	<u>95% Confidence Limit</u>
Raw Shale	Fischer Assay	28 gal/ton	0.48
	Mineral CO ₂	17 Wt%	0.32
	Ash	69 Wt%	0.19
	Moisture	0.2 Wt%	0.034
	Carbon	16 Wt%	0.16
	Hydrogen	2 Wt%	0.063
Shale Oil	Carbon	84 Wt%	0.35
	Hydrogen	11 Wt%	0.55
	Nitrogen	2 Wt%	0.11
Retort Gas	Carbon	10 lb/MSCF	0.48
	Hydrogen	0.3 lb/MSCF	0.13

TABLE IV
SUMMARY OF CROSSCHECK DATA

<u>Test</u>	<u>Laboratory</u>		
	<u>Anvil Points</u>	<u>B of M</u>	<u>Humble</u>
Fischer Assay	26.7	27.0	-
	30.7	30.4	-
Specific Gravity (Oil)	0.917	0.917	-
Carbon (Raw Shale)	16.3	16.2	-
(Spent Shale)	6.77	6.78	6.77
(Oil)	83.9	84.8	84.0
Hydrogen (Raw Shale)	1.70	1.70	1.72
(Spent Shale)	0.30	0.27	0.28
(Oil)	11.1	11.6	11.4
Mineral CO ₂ (Raw Shale)	16.5	16.2	-
(Spent Shale)	14.9	14.5	-
Ash (Raw Shale)	68.2	68.4	-
(Spent Shale)	82.7	82.8	-

TABLE V
CORRELATIONS AMONG ANALYSES

	<u>Equations of Relationships</u>		<u>Correlation Coefficient</u>	<u>Standard Deviation</u>
	<u>(R - Raw Shale)</u>	<u>S - Spent Shale)</u>		
R	Total Carbon = (0.404)(FA) + 5.58		0.97	0.15
R	Organic Carbon = (0.444)(FA) - 0.25		0.97	0.16
R	Hydrogen = (0.0499)(FA) + 0.39		0.93	0.03
R	Ash = (-0.372)(FA) + 77.70		0.92	0.24
R	Ignition Loss - CO ₂ = (0.511)(FA) + 1.085		0.92	0.33
S	Mineral CO ₂ = (-0.809)(Ash) + 82.20		0.99	0.23



FISCHER ASSAY CONTROL CIRCUIT

FIGURE 1

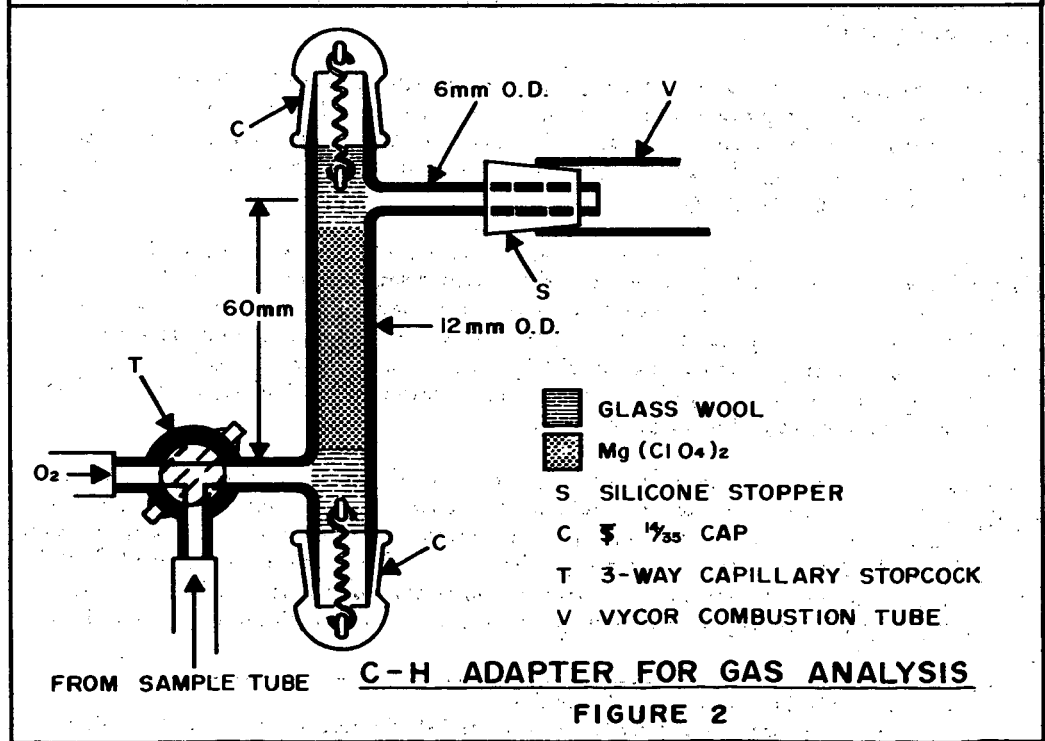


FIGURE 2

A RAPID METHOD FOR ESTIMATING OIL YIELDS OF OIL SHALES BY BROAD-LINE NMR SPECTROMETRY

A. W. Decora, J. P. Flaherty,¹ F. R. McDonald, and G. L. Cook

U.S. Department of the Interior, Bureau of Mines
Laramie Energy Research Center, Laramie, Wyoming 82070

INTRODUCTION

The Bureau of Mines, U.S. Department of the Interior, has been involved for many years in research work on oil shales. One phase of the work is a study of the characteristics, composition, and properties of Green River Formation oil shales in Colorado, Wyoming, and Utah. Of particular interest to a future oil-shale industry is the determination of the quantity of organic matter and of recoverable shale oil that is represented in these deposits.

There are two methods that are the most commonly used to estimate the organic matter and the recoverable shale oil present in oil shales. The standard method for estimating total organic matter is by determining organic carbon contents by the combustion method. The most common method for estimating the recoverable shale oil from oil shales is the modified Fischer assay method (1).² This method involves controlled heating of a sample of oil shale in a small metal retort. Both of these methods have become standard methods of assay for their particular purposes. The methods, however, are time consuming. For example, a typical Fischer assay may take 1-1/2 hours to complete and organic carbon determinations by combustion may take 4 hours to complete. It would be of great utility if a method were available that could increase the number of samples that could be processed per unit time.

Broad-line NMR spectrometry offers advantages for such a method. The NMR instrument may be tuned to observe only proton resonances. The principle of the method is that the quantity of organic hydrogen in the oil shales is related to the organic carbon contents and thus to the potential oil yields. Correlations of the NMR signal strengths can then be made with Fischer assay oil yields and organic carbon contents.

In the present work, it was necessary to test if the correlations of the proton broad-line NMR signal strengths were independent of the depths of the oil-shale samples; that is, is the hydrogen-to-carbon content and the hydrogen-to-potential oil yield sufficiently independent of depth so that the NMR correlations may be used in an analytical method? It was also necessary to show if the correlations hold over the limited area of an oil-shale deposit under development. The usual questions regarding other possible interferences had to be answered, particularly the possible interference from water protons and inorganic protons.

The results of the present research show that the proton broad-line NMR signal strength can be correlated with both the Fischer assay oil yield and the organic carbon contents of five oil shales from Colorado, Utah, Wyoming, and Kentucky. The correlations were shown to be independent of depth. The similarities of correlation parameters for cores of oil shales from the Green River Formation nearly 100 miles apart indicate that only one set of calibration data need be obtained for one oil-shale deposit under commercial development. The method is rapid, and the oil yields and

¹ U.S. Bureau of Mines Graduate Fellow in Physics.

² Underlined numbers in parentheses refer to items in the list of references at the end of this report.

organic carbon contents can be estimated on as many as 30 samples per hour. The spectrometric results can be used to supplement the standard methods so that the desired data may be rapidly measured on large numbers of samples expected in a future oil-shale industry.

EXPERIMENTAL PROCEDURE

Oil Shales Studied

Five oil shales from different geographic locations were used in this study. Four of the oil shales were from the Green River Formation in Colorado, Wyoming, and Utah, and one oil shale was from the New Albany Formation in Kentucky. Two oil shales from Wyoming were selected for this study--one from the Green River Basin and one from the Washakie Basin. These two Wyoming shales are designated Wyoming (GRB) and Wyoming (WB) in the discussion that follows.

Samples were selected from one core of each oil shale. Fischer assay oil yields and organic carbon contents were determined on the samples. The samples chosen had a range of Fischer assay oil yield from about 0-50 gal/ton and an organic carbon content range of about 0.5-25 weight percent.

The oil-shale samples were selected so that a test of the correlation of the NMR data with depth could be made. Accordingly, 20 samples of the Wyoming (WB) core were chosen that represented 2,500 feet of the core; 17 samples of the Colorado core were chosen that represented 719 feet of that core; 26 samples were chosen that represented 76 feet of the Utah core; 15 samples of the Kentucky core were chosen that represented 56 feet of that core; and 19 samples were chosen that represented 36 feet of the Wyoming (GRB) core.

Each oil-shale sample was prepared for NMR analysis by grinding it to yield powdered oil shale with the following approximate sieve analysis:

<u>Mesh size³</u>	<u>Wt pct of sample</u>
- 80 + 100	3
-100 + 200	30
-200 + 325	46
-325	21

Preparation of Sample Tubes

Each oil-shale sample was poured into a 4-inch x 1/2-inch-bore test tube. The weight of sample in the tube was approximately 7-8 g. The sample tube was then tapped until the shale sample would settle no further. The oil-shale samples, packed in this way, had bulk densities of about 1.10 g/ml. The sample in the tube completely occupied the sensitive volume of the NMR probe.

Instrumentation

The broad-line NMR spectrometer used in this work was put at our disposal by Major John C. Balogh of the Physics Department of the U.S. Air Force Academy, Colorado Springs, Colorado.

³ Plus signs on mesh sizes indicate that the sample is retained by that screen. Minus signs indicate the sample passes through the screen.

This instrument was a Varian V-4200B unit⁴ utilizing a 15-inch Varian magnet with a Varian Fieldral Mark III regulator; a Varian Model 4210A, 2-16 megahertz RF unit; appropriate sweep and detection electronics; a Varian F-80 X-Y recorder; and a Varian V4230B, 8-16 MHz probe. A Leeds and Northrup Speedomax G, 0-5 mv recorder fitted with a digital integrator (Instron Corp., Quincy, Mass.) was also electrically connected to the spectrometer output to give the area under the NMR adsorption curve.

Measurement of NMR Signal Strengths

NMR spectra were obtained on the various oil shales for two purposes: (1) To determine the location and number of resonance peaks, and (2) to use the absorption peak corresponding to the organic protons for signal strength and oil-yield correlations. For the first purpose, three probes were used: A 2- to 4-megahertz probe, a 4- to 8-megahertz probe, and an 8- to 16-megahertz probe. For the second purpose, an 8- to 16-megahertz probe was used.

A typical set of conditions for measurement of NMR signal areas for the correlation work follows. A sample tube containing an oil-shale sample was centered in the 8- to 16-megahertz probe and placed between the pole faces of the NMR spectrometer. The magnetic field, which had been on for several hours, stabilized at 2.320 kilogauss. The RF unit was turned on and set at a frequency of 10.003 MHz, and the RF field strength was adjusted to a fixed value. The sawtooth modulation unit was adjusted to a frequency of 40 hertz, phasing of 1.7, and field strength of 6.3×100 which corresponds to approximately 2.4 gauss. The output control unit was set at a signal level dependent on signal strength, filter at 40, reference phase 3.8, response 3, and balance at 5.2. The steady-state magnetic field was then swept through 50 gauss centered at 2.320 kilogauss in a sweep time of 2.5 min. The paddles of the probe were adjusted to give the first derivative absorption mode signal. The instrument was adjusted so that the richest oil-shale sample gave a peak of almost full scale on the recorder chart paper. The Instron integrator was used to record the positive area of the absorption curve (a base line was chosen that eliminated two small negative area components of the first derivative curve from the total area). All oil-shale samples in a set were run using constant instrument operating parameters. The areas under the broad-line signal of the absorption mode were recorded.

Three sets of correlation runs were made several months apart. In Run I the paddles of the NMR probe were adjusted to give the dispersion mode signal. In this case, the areas under the dispersion curve were obtained by counting squares under both the positive and negative areas of the dispersion plot on the chart paper. The paddles of the NMR probe were adjusted to give the first derivative of the absorption mode in Runs II and III. Areas for Runs II and III were obtained using the electronic integrator. The NMR signal areas were expressed as either integrator counts or as "square counts" and were different owing to changes in integrator constants. These three sets of areas were used to test the repeatability of linear regression correlations of the data.

Test for Interferences

The nuclear magnetic resonance conditions were set to obtain the proton resonances of the organic protons in the oil-shale samples; therefore, it was necessary to prove that the signal measured was due only to organic protons. One experiment was performed with a set of oil-shale samples having a relatively high concentration of nahcolite (NaHCO_3), dawsonite [$\text{NaAl}(\text{OH})_2\text{CO}_3$], and illite

⁴ Reference to specific brand names is made for identification purposes only and does not imply endorsement by the Bureau of Mines.

(a complex mineral substance containing 4-1/2 to 6 percent water as lattice hydroxyl groups). The experiment showed that the inorganic-associated protons did not interfere with the organic-associated proton resonance.

A second set of experiments was performed to test for the interference of free water. In this set of experiments, three samples of each oil shale were placed in a sealed chamber containing pans of water. The oil-shale samples were allowed to remain in this chamber (75 percent relative humidity) for 48 hours. The samples were found to absorb from 2 to 5 weight percent water in that period. The wet shale was placed in one of the test tubes, and the NMR signal area was measured. The signal area of the wet sample was compared to the signal area of the sample before wetting. The water proton was found to contribute to the NMR signal strength measured for the organic protons. The interference due to water was found to be easily avoided by air-drying the sample at room temperature for about 2 hours.

Treatment of Data

The mathematical relationships between two pairs of data were established in this study. These pairs were:

1. Fischer assay (gal/ton) and NMR signal area.
2. Organic carbon (wt pct) and NMR signal area.

A curve-fitting computer program was used to test the fit of the pairs of data to six common linear and nonlinear regression equations.

A second linear regression computer program was used to fit the pairs of data to a least-squares straight line and to compute other statistical parameters of the pairs of data. The second computer program also provided statistical data on the "goodness-of-fit" of the pairs of data to the least-squares straight line. The parameter used in this study as the measure of fit is the index of determination which is the square of the correlation coefficient. This index has the property that a perfect fit of the pairs of data to the straight line exists when the index of determination equals 1. An index of determination of zero means that no linear functional relationship exists.

RESULTS

The curve-fitting computer program was used to find which of six common linear and nonlinear regression equations best represented the pairs of data. The pairs of data were found to fit a simple straight line of the form:

$$Y = AX + B.$$

Figures 1 and 2 show representative plots of the two pairs of data for the Colorado oil shale. The figures show plots of Fischer assay and organic carbon contents vs. NMR signal area from Run II. These plots show that good straight-line correlations are obtained from the NMR method. The correlations for the four other oil shales are as good as those for the Colorado oil shale.

A second computer program was used to perform a linear regression analysis on the various pairs of data for each of the oil shales. The results of the regression analysis for the fitting of the Fischer assay oil yields and the organic carbon contents of the five oil shales are given in table 1. Table 1 lists the slopes (A) and the intercepts (B) of the least-squares straight lines together with the indexes of determination for the test of "goodness-of-fit" of the data for one correlation run.

TABLE 1. - Regression equation parameters and the indexes of determination for Fischer assay oil yields and organic carbon contents as a function of NMR signal area for five oil shales¹

Oil shale	Fischer assay vs. area		Index of determination	Organic carbon vs. area		Index of determination
	A	B		A	B	
Colorado	0.068	-1.0	0.91	0.026	1.2	0.95
Wyoming (GRB)	.054	1.7	.92	.021	1.8	.85
Wyoming (WB)	.045	-4.7	.97	.021	-1.5	.98
Utah	.053	-.9	.98	.024	-.7	.99
Kentucky	.045	-6.1	.95	.042	-5.5	.97

¹ The data listed in this table are the parameters calculated for Run III. The dependent variable, Y, in the straight-line equation, $Y = AX + B$, is the Fischer assay oil yield or the organic carbon content. The independent variable, X, is the broad-line NMR signal area.

Table 2 lists the indexes of determination obtained from the linear regression analysis of the Fischer assay vs. area and for the organic carbon vs. area for the five oil shales. The table lists this index for the three runs on the oil shales run several months apart. These three runs were made to test the repeatability of the correlations between the two pairs of data using different instrument operators and different methods (absorption and dispersion curves) of NMR strength integration. Table 2 shows that nearly the same correlations of the data points were obtained from the various pairs of data for the three runs.

TABLE 2. - Repeatability of linear regressions for five oil shales as shown by the index of determination

Oil shale	Index of determination					
	Fischer assay vs. area			Organic carbon vs. area		
	Run I ¹	Run II ²	Run III ²	Run I ¹	Run II ²	Run III ²
Colorado	0.90	0.91	0.91	0.91	0.98	0.95
Wyoming (GRB)	.96	.91	.92	.94	.88	.85
Wyoming (WB)	----	----	.97	----	----	.98
Utah	.96	.95	.98	.95	.97	.99
Kentucky	.89	.92	.95	.91	.97	.97

¹ Using NMR signal strength integrated from counting squares under the dispersion curve.

² Using NMR signal strengths integrated from the positive area under the first derivative of the absorption curve using an electronic integrator.

DISCUSSION OF RESULTS

Summary of the NMR Method

The wide-line NMR instrument in these experiments was adjusted to observe the proton resonance of the organic material of the oil-shale samples. The purpose of the study was to seek a correlation between the proton signal strength and the Fischer assay oil yields and the organic carbon contents of the oil shales. Because the proton signal strength was measured, it is necessary for the proton concentration to be related in some definable way to the Fischer assay oil yields and to the

organic carbon contents of the oil shales for the NMR technique to be useful in estimating the oil yields and organic carbon contents. It is also necessary for the inorganic protons and water protons to be noninterfering in the method. For the correlations to be useful, it is also necessary for the NMR signal strength to be independent of the depth of the oil shales studied and the area of an oil-shale deposit under development.

For the purposes of this study, five oil shales were chosen from five different geographic locations. The samples within each of the five sets were selected to give a range of oil yields, organic carbon contents, and depths.

The experiments gave the following results. The wide-line NMR signal strengths correlate well (indexes of determination generally better than 0.90) with the Fischer assay oil yields and the organic carbon contents of the five oil shales. The NMR signal strength is independent of the inorganic protons present in the samples. Free water protons, though interfering with the organic proton NMR signal area, can be effectively removed by air-drying the oil-shale samples for 2 hours at room temperature. The data for these oil shales correlated equally well for samples of oil shale that represented 719 feet of the Colorado oil shale, 36 feet of the Wyoming (GRB) oil shale, 2,500 feet of the Wyoming (WB) oil shale, 76 feet of the Utah oil shale, and 56 feet of the Kentucky oil shale. It was also observed that the correlations were repeatable at time intervals involving several months, utilization of different operators, and integration of NMR strengths by integration of either the absorption or dispersion mode of the NMR signal. These correlations are sufficient to allow the use of wide-line NMR spectrometry to rapidly estimate the potential oil yields and the organic carbon contents of the five oil shales of this study.

In general, the correlation of NMR signal area with organic carbon content was better than with Fischer assay oil yield. This better correlation is most likely due to the better accuracy of the combustion method for measuring organic carbon.

Different NMR correlations were obtained for the five oil shales. That is, least-squares lines of different slopes and intercepts were obtained for the five oil shales studied. Because different correlations were obtained, it is important to obtain calibration data for application to a specific oil-shale area under commercial development. Once calibrations are made, many oil-shale samples can be assayed per unit time to estimate potential oil yields and organic carbon contents. The experimental data indicate that calibration curves need be determined but once for a limited area under development. For example, the correlation parameters for cores of oil shales from the Green River Formation nearly 100 miles apart are similar and indicate that these parameters are probably the same over the limited area that may be involved in a commercial development. Sufficient cores were not available to test this possible similarity more completely.

Use of the NMR Method

Two different sets of oil-shale samples were selected to illustrate the use of the NMR method. Thirteen Colorado oil-shale samples and eight Wyoming (WB) samples were used. Both sets of samples were taken from the same cores that had been used to establish the linear regression parameters.

The NMR signal areas of the samples were obtained during Run III. The linear regression parameters listed in table 1 were used to calculate the Fischer assay oil yields and the organic carbon contents, respectively, from these NMR areas. The calculated results from the NMR method, together with the oil yields by Fischer assay and the organic carbon contents by the combustion method, are listed in tables 3-6. The tables also list the difference between the values calculated from the NMR method and the values obtained from Fischer assay and organic carbon by the combustion method.

TABLE 3. - Comparison of oil yields for 13 samples of Colorado oil shale determined by the broad-line NMR method and by the Fischer assay method

Fischer assay	Oil yield, gallons per ton	
	NMR ¹	Difference
7.2	8.4	0.8
11.6	11.2	.4
11.8	12.7	.9
15.8	18.1	2.3
22.1	21.5	.6
23.9	28.2	4.3
24.5	29.1	4.6
26.1	27.5	1.4
27.4	26.1	1.3
32.3	39.0	6.7
35.9	39.4	3.5
36.9	34.0	2.9
48.3	45.6	2.7

¹ The oil yields were calculated from the relationship:

$$\text{Oil yield, gallons per ton} = 0.068 \times (\text{NMR signal area}) - 1.0.$$

TABLE 4. - Comparison of organic carbon contents for 13 samples of Colorado oil shale determined by the broad-line NMR method and by the combustion method

Combustion	Organic carbon contents, wt pct	
	NMR ¹	Difference
3.8	4.8	1.0
5.8	6.4	.6
6.2	5.9	.3
7.8	8.5	.7
10.2	9.8	.4
11.6	12.1	.5
11.8	12.7	.9
12.6	11.6	1.0
13.2	12.4	.8
14.9	16.5	1.6
15.0	14.6	.4
15.7	16.6	.9
20.6	19.0	1.6

¹ The organic carbon contents were calculated from the relationship:

$$\text{Organic carbon, wt pct} = 0.026 \times (\text{NMR signal area}) + 1.2.$$

TABLE 5. - Comparison of oil yields for eight samples of Wyoming (WB) oil shale determined by the broad-line NMR method and by the Fischer assay method

Oil yield, gallons per ton		
Fischer assay	NMR ¹	Difference
5.8	9.5	3.7
6.9	9.5	2.6
10.5	11.5	1.0
15.0	12.9	2.1
16.8	15.7	1.1
26.8	25.1	1.7
30.2	30.9	.7
42.7	41.9	.3

¹ The oil yields were calculated from the relationship:

$$\text{Oil yield, gallons per ton} = 0.045 \times (\text{NMR area signal}) - 4.7.$$

TABLE 6. - Comparison of organic carbon contents for eight samples of Wyoming (WB) oil shale determined by the broad-line NMR method and by the combustion method

Organic carbon content, wt pct		
Combustion	NMR ¹	Difference
3.7	5.1	1.4
4.1	5.1	1.0
5.6	6.1	.5
8.0	6.7	1.3
8.2	8.0	.2
13.2	12.4	.8
14.9	15.1	.2
20.8	20.3	.5

¹ The organic carbon contents were calculated from the relationship:

$$\text{Organic carbon, wt pct} = 0.021 \times (\text{NMR signal area}) - 1.5.$$

The NMR method is not independent of the Fischer assay and combustion organic carbon methods because the latter two methods are used to establish the correlations with broad-line NMR signal strengths. Therefore, the oil yields and organic carbon contents calculated by NMR and listed in tables 3-6 indicate the amount of spread that may be obtained in estimations of the sought values by the NMR method when compared to the standard methods. The NMR method gives values that compare favorably to those used to obtain the correlations.

The closer comparison of the NMR results for the Wyoming (WB) oil shale than for the Colorado oil shale is directly related to the better correlation curves obtained for the Wyoming (WB) oil

shale (Fischer assay vs. area = 0.97; organic carbon vs. area = 0.98) than for the Colorado oil shale (Fischer assay vs. area = 0.91; organic carbon vs. area = 0.95).

The broad-line NMR method can be used to estimate the oil yields and the organic carbon contents many times faster than the conventional methods. The broad-line NMR method can be used to supplement the standard methods in a future oil-shale industry where many samples will need to be assayed per day.

CONCLUSION

Broad-line NMR spectrometry can be used to give a rapid estimation of the Fischer assay oil yields and organic carbon contents of oil shales. The broad-line NMR data give results that are a little less precise than the Fischer assay method and the combustion method, but the NMR method is many times faster than the other methods. The broad-line NMR method will have utility in a future oil-shale industry where many samples must be assayed in an area under development.

ACKNOWLEDGMENT

The work upon which this report is based was done under a cooperative agreement between the Bureau of Mines, U.S. Department of the Interior, and the University of Wyoming.

REFERENCES

1. Stanfield, K. E., and I. C. Frost. Method of Assaying Oil Shale by a Modified Fischer Retort. BuMines Rept. of Inv. 3977, 1946, 11 pp.

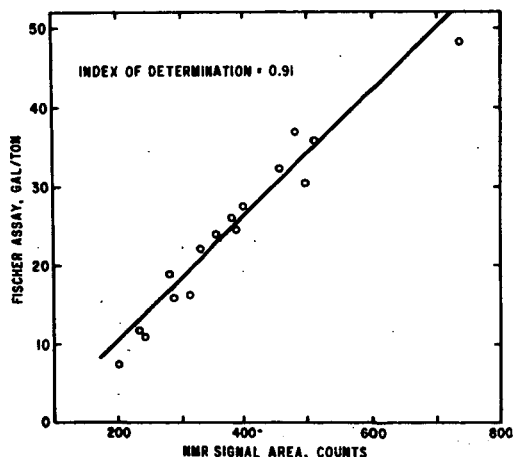


FIGURE 1.-Plot of Fischer Assay Oil Yield Vs NMR Signal Area for Colorado Oil Shale.

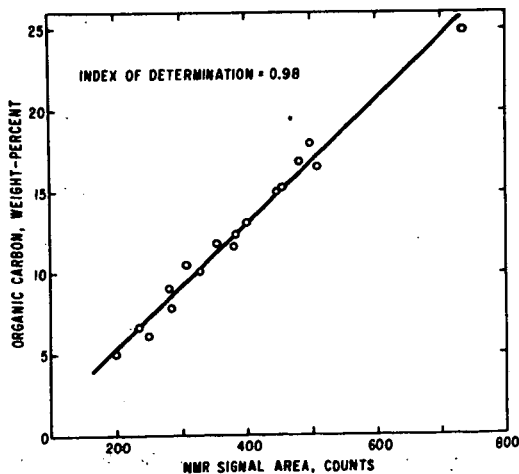


FIGURE 2.-Plot of Organic Carbon Content Vs NMR Signal Area for Colorado Oil Shale.

-47-
ESR OF BITUMENS: TEMPERATURE DEPENDENCE STUDIES.

T. F. Yen and D. K. Young

University of Southern California
2025 Zonal Avenue
Los Angeles, California 90033

Introduction

Electron spin resonance (ESR) provides a convenient method for the structural elucidation of complex macromolecules. It may, therefore, be utilized as a probe in the exploration of the micro-environment within large molecules, without the danger of either chemical decomposition, physical deformation, or dissolution from a solvent system. For bituminous materials (1,2), two different sources of ESR absorption are expected: that resulting from the presence of free radicals, and that arising from vanadium chelates. Considerable efforts have been directed toward the investigation of the latter; viz., nitrogen superhyperfine splittings due to the inherent paramagnetic vanadium moieties (3), the isotropy-anisotropy nature of vanadium (4), the ligand types of vanadium complexes (5), spectral parameters from petroporphyrins (6), vanadium chelate model systems (7,8,9,10), calculation (11), and synthesis (12) of anisotropic vanadium spectra in asphaltenes, and the enhancement and separation of vanadium signals (13,14) have been studied. Conversely, little research into the nature of free radical bitumens has been completed, with the exception of work performed concerning spin concentrations (15) and relaxation times (16), and examination of the ESR spectra of various gel permeation chromatography fractions of bitumens (17). Only recently have the g -values of a large variety of bituminous materials been collected and correlated with their structural properties (1).

It has been previously concluded (15,3) that the free radical in bitumens is located in a large aromatic ring system in such a manner as to optimize its stabilization by resonance of the delocalized π -electron. g -Value studies further reveal that these free spins resemble neither the semiquinone-quinone system (L- or H-forms of carbon) nor any other localized, heteroatom-bearing radical. Since both spin numbers (Ng) and g -values have been correlated with structural differences (2) and other physical properties of bitumens (15), basic investigation into the area of spin correlation or spin excitation will reveal information about the nature of the spins, especially regarding their interactions with their nearby host, the condensed aromatic systems. Information concerning the transfer and mobility of the spin and charged particles is essential to an understanding of the chemistry of bitumens.

Naturally occurring bituminous materials fall into two categories: the bitumens (including petroleum compounds) and the pyrobitumens. The former may be further subdivided into mineral waxes, asphalts, and asphaltides, and the pyrobitumens into asphaltoids and coals. These materials may be fractionated on the basis of solubility characteristics in various common solvents. Thus, resins are defined as n -pentane soluble, propane insoluble fractions; asphaltenes as benzene soluble, n -pentane insoluble fractions, carbenes as carbon disulfide soluble, benzene insoluble fractions, and carboids as the carbon disulfide insoluble fractions. The sequential progression from resin to carboid is associated with an increase in macromolecular size. These bitumens are characterized by condensed aromatic nuclei associated either intra- or intermolecularly and substituted with aliphatic or naphthenic substituents at their peripheries.

Previously, investigations into the dependence of certain physical properties of bitumens on temperature have yielded valuable information. Hence, methylene rocking-vibrational bands arising from paraffinic groups (18), measurements of gap energy (19), magnetic susceptibility (6) as affected by odd numbers of nitrogen ligands, and vanadium

51 nuclear-spin interaction in states of molecular association or dissociation with the bitumen matrix (4), are all temperature dependent. The present study will investigate the nature of the dependence of the ESR signal intensity with temperature in bitumen samples. The relative intensity of ESR spectra bands is expected to yield fairly high precision, if the detection systems are provided with suitable modulation amplitude and utilized at correct power levels (i.e., not causing saturation). It is anticipated that further information concerning the nature of the free radicals in bituminous materials, especially those under excited conditions, will be obtained. However, the immediate objective of this paper is to find whether there are any spins that are thermally accessible (e.g., singlet to triplet transitions); if so, then the fate of the doublet spins is examined. The next question that should be considered is the effect that is exerted on the spins by the host (stacked aromatic discs) in the micro environment.

Data Treatment

In the study of the variation of ESR intensity with temperature (20), two types of dependence are usually found. When there is negligible interaction between the adjacent spins, and the free radical behaves as a paramagnetic molecule (with 1/2 spin per molecule), as in the case of the Banfield and Kenyon's radical for example, then the Curie-Weiss law is followed and the intensity (I) expressed as that of a doublet state,

$$I_d = xN_d w/2kT \dots \dots \dots (1)$$

where x is a constant, N, the particle number of the doublet type, w, the energy level being split by the magnetic field, k, the Boltzmann constant and T, the absolute temperature. On the other hand, if there is significant interaction between the unpaired electrons, the fourfold level will be split into a diamagnetic singlet state (spins anti-parallel) and a magnetic triplet state (spins parallel). In this particular case, the temperature dependence is exponential and the ground state is a singlet. Consequently, the triplet state will lie at an energy J, above the ground level. In this case,

$$I_{st} = 2xN_{st} w/kT \exp \left[\frac{J}{kT} + 3 \right] \dots \dots \dots (2)$$

where N is the particle number of the singlet-triplet transition. For simplicity, the abbreviation,

$$E = \left[\exp \left(\frac{J}{kT} \right) + 3 \right]^{-1} \dots \dots \dots (3)$$

will be used.

Assuming that both temperature dependent processes, of spin-spin interactions and non-interaction, are operative within the system, then

$$I = I_d + I_{st} = c/T + aE/T \dots \dots \dots (4)$$

where c and a are constants. Their ratio is an indication of the number of doublet spins to that of the singlet-triplet spins. The fraction of doublet spins can thus be evaluated, e.g.,

$$\frac{N_d}{N_d + N_{st}} = 4c/(a+4c) \dots \dots \dots (5)$$

J, for a given sample may be determined as follows: a set of calibration curves is prepared (Fig. 1) by plotting the normalized E values, E_N, vs. T in which J is varied from 0.02 to 0.12 eV in 0.1 eV increments. The function is then normalized by setting E=0 at 123°K and E=1 at 400°K, so that

$$E_N = (E - E_{123}) / (E_{400} - E_{123}) \dots \dots \dots (6)$$

The raw intensity data are treated by plotting $(IT)_N$ vs. T. The normalization expression is similar to Equation 6

$$(IT)_N = \left[IT - (IT)_{123} \right] / \left[(IT)_{400} - (IT)_{123} \right] \dots \dots \dots (7)$$

In this manner, J is estimated by matching the normalized data curves $(IT)_N$ vs. T with the calibration curves having predetermined J values. This E_N vs. T curve is then vertically shifted by the addition of a constant quantity, $c' = (IT)_{123} / \left[(IT)_{400} - (IT)_{123} \right]$ to E_N , as in Fig. 2. Finally, point by point, the quantity, $E_{N+c'}$, is multiplied by $\left[(IT)_{400} - (IT)_{123} \right] / T$, to obtain I, so that,

$$I = (E_{N+c'}) \left[(IT)_{400} - (IT)_{123} \right] / T \dots \dots \dots (8)$$

Subsequently, the curve I vs. T is plotted (Fig. 3), allowing the individual components to be constructed from the following:

$$a = \left[(IT)_{400} - (IT)_{123} \right] / (E_{400} - E_{123}) \dots \dots \dots (9)$$

$$c = (IT)_{123} - a E_{123} \dots \dots \dots (10)$$

It is evident that, when IT is plotted vs. T, the quantity c is constant, shifting the curve in a direction parallel to the y-axis toward the experimental points (refer to Equation 4).

Results

Results obtained from the asphaltene fraction of four different crude oils and phthalocyanine are listed in Table I. Data from a number of charge-transfer complexes were used as an internal check of the validity of this treatment. The J-values obtained for both $NH_4^+TCNQ_2^-$ and Na^+TCNE^- complexes, according to the present graphic methods, are in excellent agreement with published results. For the chloranil-diaminodurene complex, however, $J=0.15$ fits more appropriately in the low temperature range and $J=0.25$ fits more appropriately in the high temperature range. All doublet concentrations agree well with published results for the low temperature range (Table I). No published result is available for $NH_4^+TCNQ_2^-$, although the doublet concentration for this compound is anticipated to be nil.

Table I PARAMETERS OF SPIN EXCITATION
FROM TEMPERATURE DEPENDENCE

No.	Sample	J (eV) x 10	$a \times 10$	c	$N_d / (N_d + N_{st})$ (%)
a [#]	Mara*	5.2	1.7	180	30
b	Ragusa*	9.5	5.3	120	8.0
c	Wafra*	9.0	5.0	100	7.6
d	Baxterville*	8.8	4.9	89	6.7
e	Phthalocyanine	8.0	2.4	220	27
f	$NH_4^+TCNQ_2^-$	3.4	2.4	-19	--
g	Na^+TCNE^-	25 (16)**	450.0 --	83 --	0.07 (0.03)
h	Chloranil-DAD	15 (16)	32.0 --	4.1 --	0.04 (0.04)
		20	130.0	4.1	0.01
		25	560.0	4.1	0.003
i	Etioporphyrin II	2.7	2.3	-21	--

#Identification of the lower case alphabets see curves in Fig. 4.

*Asphaltene

##TCNQ, 7,7,8,8-Tetracyano-p-quinodimethan; TCNE, Tetracyanoethylene; DAD, Diaminodurene.

**Quantities in parentheses are literature values.

The computed curves of the bitumen sample and phthalocyanine, match favorably with the experimental data points as can be seen from Fig. 4. It is evident that two different trends occur. The upper two samples (a and e) form a different trend than those of the lower three asphaltenes (b,c,d). These differences might very well be attributed to the constants, a and c , and may not result from the J -values.

In order to correlate the J values obtained from ESR, with those from magnetic susceptibility measurements, the corrected magnetic susceptibility (6) of an enriched petroporphyrin fraction from Boscan crude was treated, and a J value of 0.033 eV gave a perfect fitting (Fig. 5). However, the J value obtained by ESR measurement of the pure etioporphyrin II, is 0.027 eV. This indicates that there is fair agreement. So far, the lowest J value is, among asphaltenes, that of Mara ($J=0.025$ eV), which contains the highest amount of porphyrin (21). The fact that the J value of phthalocyanine is higher has not been accounted for, but it is suggested that contaminants, such as dimeric or polymeric species, may affect the energy separation.

Finally, in order to check the validity of the assumption that asphaltene exhibits singlet-triplet transitions, which typify many known charge-transfer complexes, e.g., TCNQ triethylammonium salt, a log-log plot, as in Fig. 6, was constructed for an asphaltene sample and a TCNQ complex. In Fig. 6, the points were obtained from experimental IT data, while the curves were computed from the J value of $4/(e^{J/kT}+3)$. The coincidence of the experimental points with the computed curves, together with the specific shape of the curve, suggests that asphaltenes exhibit singlet-triplet excitations.

Discussion

Condensed-ring aromatic molecules are disk-like in shape, and, not surprisingly, tend to orient themselves into crystallites of stacks or chains. Highly oriented, organic, free radicals are of significant interest, since the paramagnetism of the system is dominated by the presence of a strong antiferromagnetic exchange interaction directed axially through the center of the disks (Heisenberg chain) (22). This one-dimensional array of stacked, exchange-coupled, planar molecules, each with a spin of 1/2, can exhibit a spin of either one (doublet) or two (singlet-triplet) per repeating unit.

The layer diameter (L_a) of most bitumen aromatic crystallite sheets is approximately 8.5-15 Å, the cluster diameter (L_c) being within the range of 16-20 Å. The charge-transfer process in asphaltics is favored by the motion of electrons or holes axially to the plane of the disks (23). Infrared evidence suggests that these disks are held in stack formation by π - π associations of the donor-acceptor type (24). Hence, it is possible that excitation processes such as those manifested by some known donor-acceptor charge-transfer complexes could exist (Table II).

Table II LOW-LYING SINGLET-TRIPLET ENERGY INTERVALS AND ACTIVATION ENERGIES FOR CONDUCTION OF SOME CHARGE-TRANSFER COMPLEXES IN eV

Complex	J	$\Delta\epsilon$	Ref.
$\text{NH}_4^+\text{TCNQ}_2^-$	0.034	0.14	32
$3\text{AsMe}^+\text{TCNQ}_2^-$	0.065	0.30	34
4-Cyano-N-methyl-quinolium TCNQ_2^-	0.018	0.08	34
K TCNQ	0.2	0.35	34
p-Chloranil-DAD	0.15	0.25	33

Table II LOW-LYING SINGLET-TRIPLET ENERGY INTERVALS
AND ACTIVATION ENERGIES FOR CONDUCTION
OF SOME CHARGE-TRANSFER COMPLEXES IN eV (cont.)

<u>Complex</u>	<u>J</u>	<u>$\Delta\epsilon$</u>	<u>Ref.</u>
p-Chloranil-p PDA*	0.13	0.43	35
TMPD ⁺ ClO ₄ ^{-**}	0.0305	--	36

*p-Phenylenediamine

**N,N,N',N',-Tetramethyl-p-phenylenediamine

Treatment of spin excitation in petroleum asphaltene indicates that excitons may be raised from the ground singlet state to a thermally accessible triplet state, in addition to the usual doublet state. Furthermore, there is an apparent lack of spatial correlation; probably due to the random orientation of the crystallites in the mesomorphic medium. This independent, delocalized spin excitation may be accounted for by Wannier spin excitons rather than the Frenkel excitons, the latter being characterized by TCNQ radical ions, or Wurster's blue perchlorates (25).

The fact that the doublet concentration in phthalocyanine, as well as in Mara asphaltene (V=2370 ppm., highest vanadium content), is higher than those of the remaining samples suggests that paramagnetic impurities may inhibit the spin excitation. The four-fold difference in doublet concentration between high-vanadium and low-vanadium samples may indicate certain degrees of localization due to nuclei-spin interaction. In addition, the excitons inherent in bituminous materials are not associated with paramagnetic metal complexes. However, the gap energy of high-vanadium bitumens is generally small, suggesting that potential electron donors, such as heteroatom centers, may be present in these bituminous structures.

The Russell effect (thermal luminescence) has been observed in metal-free asphaltene and resin fractions of bitumens (26). Specifically, strong infrared luminescence and reflectance (27) were observed for coal-hydrogenated and benzene-suspended asphaltene. It is doubtful that, as reported earlier (27), this type of luminescence may be attributed to the presence of polynuclear aromatic hydrocarbons alone. It is possible that charge-transfer complexes play a significant role.

The enhancement of the asphaltene ESR signal was observed during the course of intra muros electrolytic redox experiments. It is possible that excitons are also responsible for this type of reaction. Other observations of asphaltene, such as the ease of induction of the Overhauser effect (proton polarization enhancement) (28), the Seebach effect (29) and charge-transfer nature in the presence of polar solvents (38) may be accounted for by exciton behavior. Charge carriers observed in electronic resistivity studies may also be of exciton origin.

The selection of phthalocyanine and etioporphyrin as model compounds in this experiment is based on the fact that both compounds exhibit exciton behavior. It is known that both compounds, when arranged in stacks, have an overall structure similar to those of crystallites in bitumens with approximately the same interplanar distances ($d=3.4$ Å). ESR signals, close to $g=2$, have been detected in metal free α - and β -phases of phthalocyanine (30); the nature of these radicals is most likely due to spin excitations. Recently, it has been noted that porphyrins exhibit chemoluminescence, the energy transfer of such excitation being demonstrated by the decomposition of tetralin peroxide (31).

The small differences in J-values and doublet concentration among the remaining asphaltene, excluding the high vanadium-containing sample, (Mara) indicates that these parameters are perhaps constant, within the range of experimental error. However, a careful examination of the parameters reveals that both (last two columns, Table III)

vary proportionally with each other, and inversely with aromaticity values (Table III). This trend also agrees with the electronic conductivity of native asphaltene (Room temperature resistivity ρ_{25} and $\Delta\epsilon$ are listed for a number of asphaltenes) (Table III). Considering the above, the nature of the charged particles within bitumens are influenced by their interaction with the polyaromatic systems present.

Table III RESISTIVITY PARAMETERS AND AROMATICITY OF ASPHALTENES

Asphaltene	f_a^*	$\rho_{25} \times 10^{-15}^{**}$ (ohm-cm)	$\Delta\epsilon^{**}$ (eV)	$J \times 10^2$ (eV)	$N_d / (N_d + st)$ (%)
Baxterville	0.53	3.1	1.2	8.8	6.7
Laquillas	0.41	590	1.5	--	--
Wafra	0.37	10000	1.7	9.0	7.6
Ragusa	0.26	--	--	9.5	8.0

*Ref. 37

**Ref. 19

In order to further understand the nature of the singlet species within the bitumens, photoexcitation experiments should be conducted with these samples. Due to the interference of the vanadium hyperfine absorptions, ENDOR would prove to be an excellent tool for this work. The location of the $\Delta_m = \pm 1$ and $\Delta_m = \pm 2$ lines and of zero-field splitting parameters will be reported in a subsequent paper.

Experimental

A Varian V 4502 x-band spectrometer equipped with a 12 in. V 4013 A magnet and a V 4532 dual cavity (100 KHz modulation at sample and 400 Hz at reference) was employed. The temperature level in the range between 123° and 400°K was precalibrated and held within $\pm 3^\circ$ by use of a Varian variable temperature accessory. The relative intensity of the free radical absorption was reproducible in repeated trials to within 4%. Raw data of the intensity together with the corresponding temperature for the bitumens and phthalocyanine can be located as points in Fig. 4.

References

1. T. F. Yen and S. Sprang, ACS, Div. Petroleum Chem., Preprints 15(3), A65-A76 (1970).
2. T. F. Yen, Chemistry in Space Research, R. F. Landel and A. Rembaum, editor, Elsevier Publishing Company, New York, New York, 1971, in press.
3. T. F. Yen, E. C. Tynan, G. B. Vaughan, and L. J. Boucher, Spectrometry of Fuels, R. A. Friedel, editor, Plenum Publishing Corp., New York, New York, 1970, Chap. 14, pp. 187-201.
4. E. C. Tynan and T. F. Yen, Fuel (London) 43, 191 (1969).
5. L. J. Boucher, E. C. Tynan, and T. F. Yen, Electron Spin Resonance of Metal Complexes, T. F. Yen, editor, Plenum Publishing Corp., New York, New York, 1969, pp. 111-130.
6. T. F. Yen, L. J. Boucher, J. P. Dickie, E. C. Tynan, and G. B. Vaughan, J. Inst. Petroleum 51, 87 (1969).
7. L. J. Boucher, E. C. Tynan, and T. F. Yen, Inorg. Chem. 7, 731 (1968).
8. L. J. Boucher and T. F. Yen, Inorg. Chem. 7, 2665 (1968).
9. L. J. Boucher and T. F. Yen, Inorg. Chem. 8, 689 (1969).
10. G. B. Vaughan, E. C. Tynan, and T. F. Yen, Chem. Geol. 6(3), in press (1970).
11. J. H. Mackey, M. Kopp, E. C. Tynan, and T. F. Yen, Electron Spin Resonance of Metal Complexes, T. F. Yen, editor, Plenum Publishing Corp., New York, New York, 1969, pp. 33-57.
12. E. C. Tynan and T. F. Yen, J. Magnetic Resonance 3, in press, (1970).

13. J. E. Beasely, R. L. Anderson, J. P. Dickie, F. R. Dollish, E. C. Tynan, and T. F. Yen, Spectroscopy Letters 2(5), 149 (1969).
14. T. F. Yen, E. C. Tynan, G. B. Vaughan, and L. J. Boucher, ACS, Div. Fuel Chem., Preprints 11(4), 264-275 (1967).
15. T. F. Yen, J. G. Erdman, and A. J. Saraceno, Anal. Chem. 34, 694 (1962).
16. A. J. Saraceno and N. D. Coggeshall, J. Chem. Phys. 34, 260 (1961).
17. J. Q. Adams, K. H. Altgelt, R. L. LeTourneau, and L. P. Lindemen, ACS, Div. Pet. Chem., Preprints 11(2), B140 (1966).
18. T. F. Yen and J. G. Erdman, ACS, Div. Anal. Chem., Abstract, 29B-30 (1965).
19. G. A. Sill and T. F. Yen, Fuel (London) 43, 61 (1969).
20. D. Bijl, H. Kainer, and A. C. Rose-Innes, J. Chem. Phys. 30, 765 (1959).
21. E. W. Baker, T. F. Yen, J. P. Dickie, R. E. Rhodes, and L. F. Clark, J. Am. Chem. Soc. 89, 3631 (1967).
22. P. L. Nordio, Z. U. Soos, and H. M. McConnell, Ann. Rev. Phys. Chem. 17, 237 (1966).
23. J. P. Dickie and T. F. Yen, Anal. Chem. 39, 1847 (1967).
24. T. F. Yen, ACS, Div. Petroleum Chem., Abstract, paper 35 (1969).
25. B. M. Hoffman and R. C. Hughes, J. Chem. Phys. 52, 4011 (1970).
26. G. R. Yohe, Fuel (London) 29, 163 (1950).
27. R. A. Friedel and H. L. Gibson, Nature 211, 404 (1966).
28. E. H. Poindexter, J. Chem. Phys. 31, 1477 (1959).
29. G. A. Sill and T. F. Yen, Rev. Sci. Inst. 41, 878 (1970).
30. S. F. Harrison and K. H. Ludewig, J. Chem. Phys. 45, 343 (1966).
31. E. H. White, D. R. Roberts and D. F. Roswell, Molecular Luminescence, E. C. Lim, editor, W. A. Benjamin, Inc., New York, New York, 1969, p. 479.
32. D. B. Chesnut, H. Foster, and W. D. Phillips, J. Chem. Phys. 34, 684 (1961).
33. D. B. Chesnut and W. D. Phillips, J. Chem. Phys. 35, 1002 (1961).
34. R. G. Kepler, J. Chem. Phys. 39, 3528 (1963).
35. A. Ottenberg, C. J. Hoffman and J. Osiecki, J. Chem. Phys. 38, 1898 (1963).
36. D. D. Thomas, H. Keller, and H. M. McConnell, J. Chem. Phys. 39, 2321 (1963).
37. T. F. Yen and J. G. Erdman, Encyclopedia of X-rays and Gamma-rays, G. L. Clark, editor, Reinhold Publishing Corp., New York, 1963, pp. 65-68.
38. T. F. Yen, ACS, Div. Fuel Chem., Preprints, in press (1971).

Acknowledgement

Partial support of a grant from Gulf Research and Development Company is acknowledged. Thanks are due to Steve Sprang and Massoud Davar for their valuable assistance.

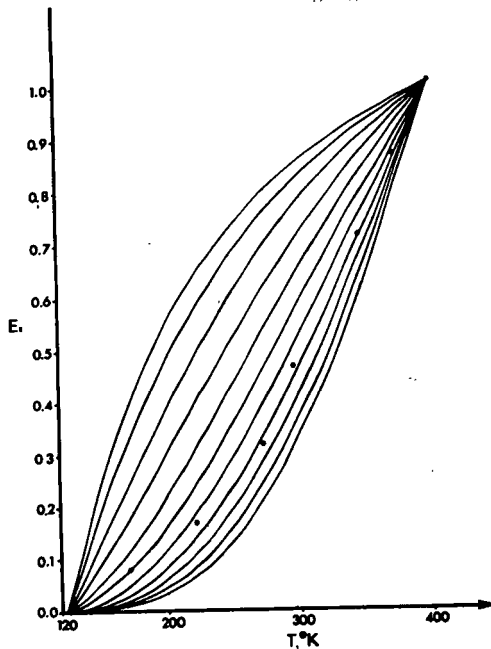


Fig. 1. A series of calibration curves of the general type, $E = \exp(JkT + 3)^{-1}$ with known values for J . (E is normalized so that $E_{123^{\circ}\text{K}} = 0$ and $E_{400^{\circ}\text{K}} = 1$. From left to right, J increases from 0.02 eV to 0.12 eV with 0.01 eV increments. The points indicate the values for the Baxterville asphaltene, $J = 0.088$ eV).

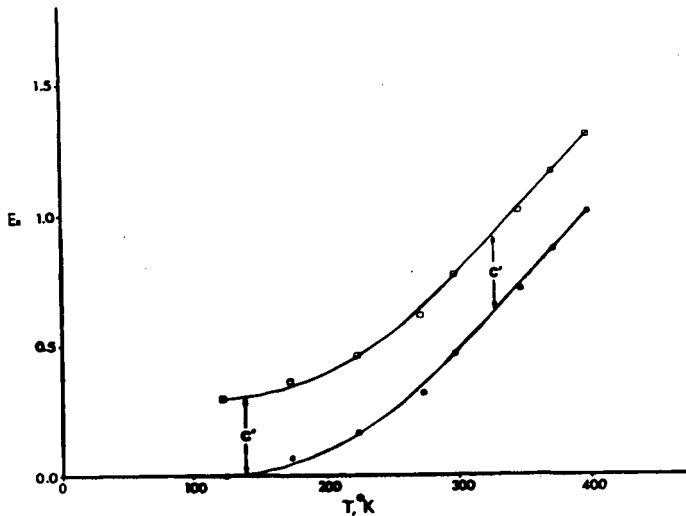


Fig. 2. Graphical Matching Procedure of the Baxterville Asphaltene: The lower line represents $(E - E_{123}) / (E_{400} - E_{123})$; the upper line indicates that the lower line has been shifted up by an amount of c' , where $c' = 0.292$.

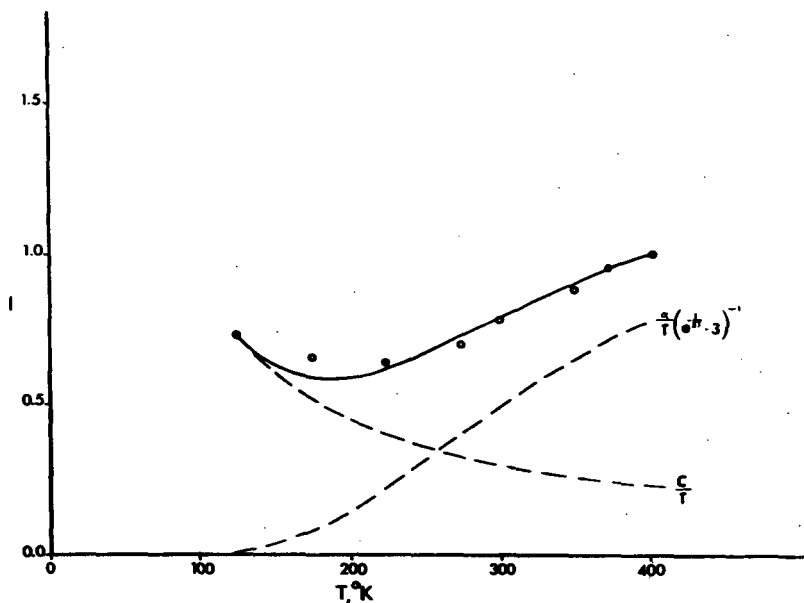


Fig. 3. Two Components for a Baxterville Asphaltene. (The circles indicate experimental data. The continuous line represents a theoretical curve with $J=0.088$, $c=89$, $a=4900$. The C/T curve is the doublet contribution; the E/T curve is singlet-triplet contribution).

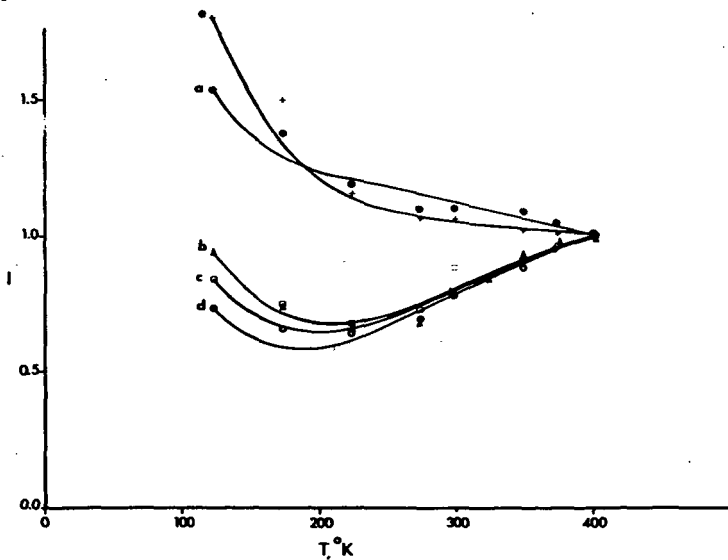


Fig. 4. Intensity Data of Asphaltenes (see Table I for sample identification).

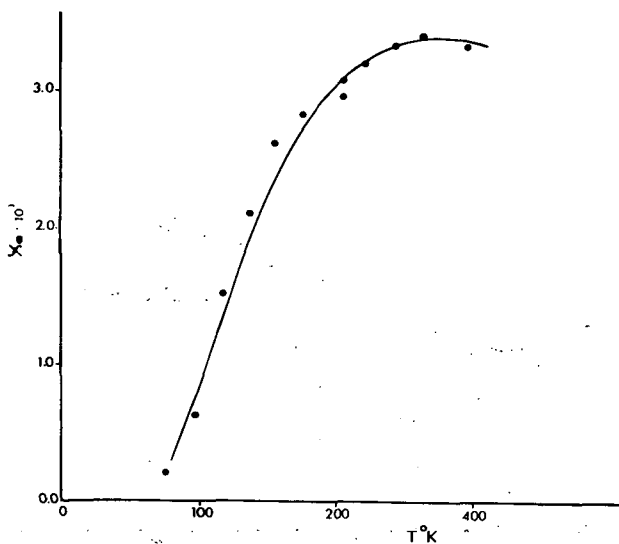


Fig. 5. Magnetic Susceptibility of a Boscan Petroporphyrin (J is approximately 0.038 eV).

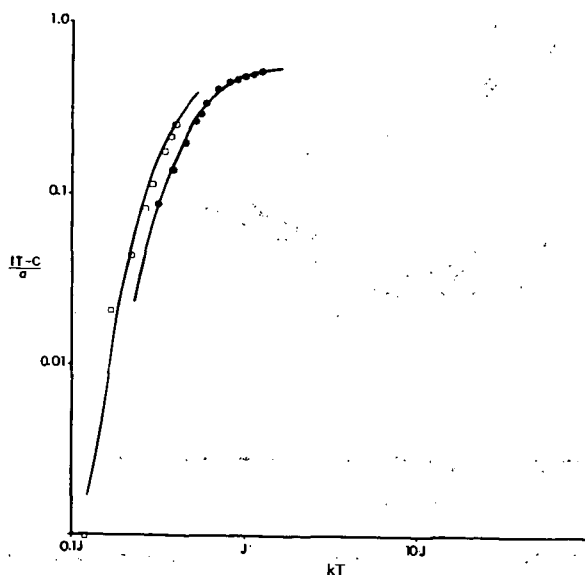


Fig. 6. Double Log Plot of $4E$ vs. kT for a TCNQ Salt (round) and a Baxterville Asphaltene (square). Curves are computed with known J values obtained by graphical procedure. The points are obtained from experimental IT data, i.e., the y-axis can be plotted as $(IT-c)/a$.

HIGH TEMPERATURE MASS SPECTROSCOPY OF ATHABASCA ASPHALTENES AND THE RELATIONSHIP TO CRACKING PROCESSES

By

James G. Speight
Research Council of Alberta
Edmonton, Alberta, Canada

INTRODUCTION

In a previous communication (1), it was shown that Athabasca asphaltenes are composed predominantly of peri-condensed aromatic systems, varying from six to fourteen rings per sheet, bearing alkyl and naphthene substituents. The present paper represents a further facet of a systematic investigation into the properties and potential uses of the Athabasca bitumen and fractions arising therefrom. More particularly, the work described herein is a preliminary attempt to elucidate the predominant mechanisms involved in the cracking of asphaltenes. The thermal treatment of Athabasca bitumen has been the subject of several earlier publications. For example, Ball (2) described the bitumen in general terms as being susceptible to heat and, therefore, to refining processes; Peterson and Gishler (3) investigated the recovery of oil from the bituminous sand by feeding the sand directly into a hot fluidized bed; Kriebel and Seyer (4) investigated the fractional distillation of the oil at reduced pressures; Pasternack (5-7) studied the partial thermal cracking of the bitumen and noted changes in such properties as molecular weight and carbon residue of the bitumen; Erdman and Dickie (8) noted the changes in viscosity and density during the mild thermal alteration of the bitumen; and McNab and his co-workers (9) calculated activation energies for cracking of the bitumen and concluded that the bitumen was more thermally labile than a conventional crude oil.

EXPERIMENTAL

Materials and General Techniques

The asphaltene fraction was isolated by diluting dry Athabasca bitumen with 40 volumes of technical pentane (containing 93% n-pentane), followed by agitation of the mixture for not less than 5 hours. The asphaltenes were separated by filtration and washed thoroughly with fresh portions of pentane until the washings were colourless and evaporation of an aliquot failed to leave any residue.

Cracking Procedure

The apparatus consisted of standard Pyrex glass equipment fitted with B14/23 ground glass joints. The asphaltenes (50.0 ± 0.2 g) were cracked in a round-bottomed flask (100 ml capacity) which was heated by an alloy bath. Products passed through an air-cooled condenser

(25.4 cm long) and liquids were collected in a water-cooled receiver. Gases were collected in a series of traps cooled to -78°C , -130°C , and -196°C which were protected from the atmosphere by a mercury lock attached to the -196°C trap. In order to commence distillation, the apparatus was flushed with dry helium (75 ml/min) for five minutes whilst the temperature was raised to 200°C . The helium flow was discontinued and the temperature was then (a) in one experiment, raised rapidly to 455°C over fifteen minutes and maintained there for two hours by which time all of the distillate had been collected, (b) in a separate experiment, raised to 455°C over a period of two hours by which time distillation was complete.

At the end of each distillation, the distillate was raised, *in situ*, to 150°C for one hour to remove any dissolved gases. Spectroscopic and physical examination prior to and after the thermal treatment indicated no change to the distillate itself.

The residues were insoluble honeycombed coke-like materials from which small amounts of resinous materials could be extracted with benzene during 24 hours. The insoluble coke had no appreciable absorption in the infrared. For convenience, the products from these distillations are designated as oil, resins, and coke.

The proportions of *n*-paraffins in the oil fractions were determined by formation of an insoluble complex between the *n*-paraffins and urea (10). The uncomplexed oil was then treated with 35 volumes of acetone and chilled to -23°C (-10°F), whereby the branched paraffinic material was precipitated (11).

Analytical Procedures

Gaseous materials were handled in a conventional glass vacuum apparatus equipped with storage reservoirs.

Gas-chromatographic analyses of the paraffinic fractions of the light oils were carried out with a 5751B F and M gas chromatograph equipped with a dual flame ionization detector. The chromatographic column was a 6-foot by 1/8-inch column loaded with 10% silicone rubber on 80-100 mesh Diatoport S. Gaseous mixtures were analysed at room temperature and for distillates the temperature was programmed to rise from 100°C to 280°C at the rate of 6°C per minute. Each analysis was carried out twice. Distillates were diluted with an equal volume of benzene. In each repeat analysis, samples of standard hydrocarbons were added to the mixture which enabled a more accurate determination of the peaks in the mixtures corresponding to known materials.

Proton magnetic resonance spectra were obtained using a Hitachi Perkin-Elmer R20 High Resolution NMR Spectrometer. All spectra were run using tetramethylsilane (TMS) as an internal standard. The samples were prepared as approximately 25%-by-volume solutions in spectroscopically pure carbon tetrachloride and the spectra were recorded immediately over the interval of 0-600 c.p.s. from TMS.

Mass spectra were recorded on a Perkin Elmer 270 Mass Spectrometer. Solids were introduced directly into the ionisation chamber whilst liquids were vapourised in vacuo into the ionisation chamber by preheating in a small oven.

Infrared spectra were recorded on a Perkin Elmer 221 Infrared Spectrometer; liquids were recorded as a film and solids at a concentration of 0.4% in potassium bromide.

RESULTS

The foregoing work shows that the asphaltenes can be cracked, under conditions similar to those employed for visbreaking (i.e. $\sim 470^{\circ}\text{C}$) to afford a near aliphatic oil ($\text{H/C} = 1.65$) containing higher paraffins with lower molecular weight paraffins occurring as gases. There are marked similarities between products of the slow and rapid cracking processes with the interesting exceptions that the amount of light oil is increased significantly, yields of gases are reduced (Table I) and whilst paraffins are products of both cracking processes there are higher proportions of *n*-paraffins in the light oil from the slow distillation. In each case, reduction in hetero-atom content, occurring as water, hydrogen sulphide, and ammonia (traces), is especially noticeable in the oxygen analyses (Table II). This, and infrared spectroscopic evidence, indicates that whilst nitrogen and sulphur are not in dominant functional groups, and probably have thermal stability conferred upon them by incorporation into ring systems, the majority of the oxygen is located in thermally labile, e.g., carbonyl, groups. If this is indeed the case, the results may serve as a guide to illustrate the relative occurrence of the hetero-atoms in heterocyclic structures.

TABLE I Destructive Distillation of Athabasca Asphaltenes

<u>Products</u>	<u>--Distillation --</u>	
	<u>Rapid</u>	<u>Slow</u>
Light oil (Yield, wt. %)	35.2	43.9
Resins (Yield, wt. %)	4.5	4.5
Coke (Yield, wt. %)	48.4	49.0
Gases [wt. % (by difference)]	11.9	2.6
[wt. % (found)]	11.2	2.3

TABLE II Loss of Hetero-Elements during Cracking

	<u>----- % (w/w) Loss -----</u>	
	<u>Rapid Heating</u>	<u>Slow Heating</u>
Oxygen	81.3	80.1
Nitrogen	1.0	1.0
Sulphur	23.4	17.1

Proton magnetic resonance and mass spectroscopy indicated an overall dealkylation of the aromatics to methyl (predominantly) and ethyl (minority) groups. There was also the indication that the predominant aromatics in the cracked products were based on the naphthalene nucleus. Other investigations showed that higher temperatures ($>500^{\circ}\text{C}$) promote the formation of benzene, in place of naphthalene, nuclei as the predominant aromatics in the cracked material but this is accompanied by an increase in coke formation.

The formation of the paraffins can be ascribed to the generation of hydrogen within the system which occurs during the pyrolysis of condensed aromatic structures (12,13). Indeed, it (14) has been demonstrated that a surprisingly low amount of hydrogen is required to upgrade the Athabasca bitumen and other experiments by the present author with reduced* Athabasca asphaltenes show that increased yields of the lower molecular weight paraffins are produced during cracking of the hydrogenated asphaltenes. Thus, one of the major effects is a transfer of hydrogen within the system either by repeated condensation of aromatic material to coke or by complete aromatization of the naphthenes. The overall result is a highly saturated fraction - the light oil - and a highly condensed aromatic ring system - the coke.

Mass spectroscopic examination of the asphaltenes showed a whole range of fragmentation ions up to at least m/e 700. The particular fragmentation patterns will be discussed in detail in a later publication. However, more pertinent to the present work, there were several significant details which emerged from the spectra. There was a marked increase, with increasing temperature (from 60°C-350°C), of ions attributable to low molecular weight hydrocarbon fragments (m/e - 29, 43, 57, 71, 85), monocycloparaffins (m/e - 69, 83), alkylbenzenes (m/e - 91, 105), and naphthalenes (m/e - 125, 127, 141, 155). In fact, the mass spectra of the cracked products up to m/e 220 were very similar to the spectrum produced from the asphaltenes at 350°C. There is the suggestion here that the cracking processes involve predominant formation of fragments of the above types (presumably as free radicals) which then interact with the hydrogen produced to yield the end-products. Indeed, the identification of paraffins, methyl and, to a lesser extent, ethyl benzenes and naphthalenes among the products lends credence to this view.

The facile elimination of oxygen, predominantly as water, during cracking was confirmed in part by the intense peaks at m/e 17, 18 whilst sulphur elimination in elemental form or hydrogen sulphide was also confirmed by peaks at m/e - 32, 33, and 34. Peaks due to the elimination of nitrogen as ammonia were not so prominent but there was the suggestion of nitrogen occurring in pyridine nuclei and also sulphur in benzothiophene nuclei. This would confirm the postulate that these elements are not liberated as readily as oxygen during the cracking because of the stability conferred on them through location in ring-systems. In addition, the majority of nitrogen and sulphur remaining in the products occurs in the coke.

It is apparent from these results, that carbon-carbon bond fission occurring during thermal degradation of the asphaltenes is greatest at the bond β to an aromatic ring. Intramolecular condensation of the aromatic moieties yielding coke and generating hydrogen within the system are also dominant reactions. At present, it is not known whether the hydrogen so generated, and also by aromatisation of naphthene structures, exists as free hydrogen or merely participates in the processes in the form of an intramolecular hydrogen transfer.

In addition, the facile elimination of oxygen as water and, to a lesser extent, sulphur and nitrogen as hydrogen sulphide and ammonia, respectively, affords a convenient means of eliminating these elements from the products. It would appear, therefore, that high proportions of the sulphur and nitrogen originally present in the asphaltenes are located in ring-systems and are largely incorporated into the coke during cracking.

* Using lithium metal/ethylenediamine or elemental hydrogen/catalyst or lithium aluminum hydride.

ACKNOWLEDGEMENTS

The author is indebted to Syncrude Canada Ltd. for gifts of dry bitumen, to Dr. N. Berkowitz for his comments on the manuscript, to Mr. J. Barlow for valuable technical assistance, to Mr. M. Anderson for recording the proton magnetic resonance spectra, and to Mr. G. Spratt for recording the infrared and mass spectra.

REFERENCES

1. Speight, J. G., companion paper presented at the Symposium on Oil Shale, Tar Sands, and Related Material presented before the Division of Fuel Chemistry and the Division of Petroleum Chemistry, American Chemical Society, Los Angeles, California, March 28 - April 2, 1971.
2. Ball, M. W., Can. Inst. of Mining and Met., Trans. 44, 58 (1941).
3. Peterson, W. S. and Gishler, P. E., Canadian J. Research, 28, 62 (1950).
4. Krieble, V. K. and Seyer, W. F., J. Amer. Chem. Soc., 43, 1337 (1921).
5. Pasternack, D. S., Can. J. Petrol. Tech., 3, 39, Summer (1964).
6. Pasternack, D. S., Can. J. Petrol. Tech., 3, 1, Fall (1964).
7. Pasternack, D. S., Can. J. Petrol. Tech., 3, 1, Winter (1964).
8. Erdman, J. G. and Dickie, J. P., Div. Petrol. Chem., Am. Chem. Soc., Philadelphia, B-69 (1964).
9. McNab, J. G., Smith, P. V., and Betts, R. L., Ind. Eng. Chem., 44, 2556 (1952).
10. Marquart, J. R., Dellow, G. B. and Freitas, E. R., Anal. Chem., 40, 1633 (1968).
11. Traxler, R. N. and Schweyer, H. E., Oil and Gas Journal, 52, 158 (1953).
12. Madison, J. J. and Roberts, R. M., Ind. Eng. Chem., 50, 237 (1958).
13. Lewis, I. C. and Edstrom, T., J. Org. Chem., 28, 2050 (1963).
14. Parsons, B. I., Mines Branch Technical Bulletin TB100, Canada Dept. of Energy, Mines and Resources (1968).

EXOTHERMAL METAMORPHOSIS OF COAL PRECURSORS

George Richard Hill, Don Carlos Adams

College of Mines and Mineral Industries
University of Utah
Salt Lake City, Utah 84112

The genesis of high rank coals, those containing more than 86 percent fixed carbon, has been a matter of conjecture since coal classification schemes were invented. The classical model for the transition of cellulose, lignin and other plant materials into coals of various ranks is described by Wilson and Wells (1);

"The chemical changes taking place in transition from wood to peat and progressively through the successive ranks of coal to anthracite are suggested...Such changes, which may have taken hundreds of thousands or millions of years, are believed to have converted peat to lignite and progressively through successively higher ranks of coal, to anthracite."

Pressure is used to help account for the difference in rank. Wilson and Wells state further "In deeply buried coals pressures of 1500 atm may have been reached.

The advanced state of transformation typified by Pennsylvania anthracite is probably due to the enormous pressures to which the deposits were subjected when the Appalachian Mountains were formed."

X-ray diffraction of high rank coals demonstrates a distinct peak corresponding to (002) graphite lattice spacing. This peak is weak or absent in lower rank coals. (2) The polymerization of carbonaceous material to graphite requires temperatures in the range 600° to 800°C, well above the 200°C maximum temperatures to which some coals have presumably been exposed.

The possibility that coalification could be rapid is suggested by a discovery made by Petzoldt (3) in 1882;

Upon unearthing a wooden pile which had been rammed into the ground, he found it to have been metamorphosed to a coal like substance. From the center, it exhibited a continuum of material from black through dark brown, and light at the surface. This he analyzed and found to resemble anthracite in the center portion, and the outer part resembling brown coal.

Teichmuller and Teichmuller (4) after studying systematically the geological factors related to the coals of western Europe concluded "according to our observations in different coal-bearing foredeeps the effect of pressure on rank increase is purely physical. The chemical reactions are caused by temperature increase, and according to the experimental observations, pressure actually retards them." They cite many examples of conflicting data where an increase in age does not correspond to higher rank. Their general conclusion respecting time is: "time has relatively small influence on the coalification process." and, "The effect of time upon coalification depends on the temperature to which the coal has been exposed during burial. If this temperature is low, the time factor is hardly important. With higher temperatures, however, the length of heating

has a marked effect."

Research in our laboratory has been concerned with the determination of the pressure coefficient and the temperature coefficient of the conversion of cellulose type materials to coal. This research and that of Pan (5) demonstrated that high pressure decreases the rate of conversion of cellulose into coal-like materials and of low rank coals into coals of higher rank. The temperature coefficient of formation of coal-like materials is positive and high. But perhaps of greater importance is the serendipitous discovery that cellulose type materials confined at high pressures when heated slowly to temperatures in the range 200° to 240°C decompose exothermally, raising the temperature of the material to the graphite forming range, i.e., above 600°C.

APPARATUS AND EXPERIMENTAL PROCEDURE

High Pressure

This high pressure work was carried out in a hexahedral, 200 ton press, designed by H. T. Hall. The rams of the press have an 8" diameter piston, which at 8000 psi hydraulic pressure, exert a force of 400,000 lbs. or 200 tons. The anvils used were the 15/16" anvils. Pressure calibrations for this anvil set were made using the bismuth I-II and II-III transitions and the change of resistance of bismuth with pressure.

Differential Thermal Analysis

A description of the Differential Thermal Analysis (DTA) system will be published in a second paper. All DTA samples were pelletized as ¼", right-circular sections. This was accomplished by melting the sample, in the case of the glucose, xylose, and inositol, and pressing the melt into ¼" diameter teflon tubes (all done under a vacuum). The cellulose powder and wood samples were pelletized at approximately 5 kb in a ¼" diameter piston and cylinder die system, which was equipped with "o-ring" seals, above and below the sample, to facilitate the evacuation of the sample material.

Thus pelletized, the sample was assembled in the pyrophyllite-cube-furnace-DTA system, with thermocouples. The cube assembly was evacuated in a closed vessel for one hour. The vessel was then pressurized to 100 psi with pure N₂ gas and maintained for a minimum of one hour at this pressure. Thereafter the sample was placed immediately in the press to minimize the diffusion of air into the cube and into contact with the sample.

All DTA samples were enclosed in a teflon capsule to insulate the sample from any possible mineral or catalytic effect.

Temperature Recording

Differential, and actual temperature traces were made simultaneously on a Honeywell Electronik 194, dual-pen recorder.

Constant Temperature Pyrolysis

One sample was pyrolyzed at constant temperature (after reaching reaction temperature). The equipment used was a Fisher system with both thermogravimetric analysis as well as DTA accessories (but not equipped to be used simultaneously). The Fisher Model 360 temperature programmer was used as the temperature controller and a Cahn Electrobalance monitored the weight (and weight change).

The above specified Honeywell recorder was used to record the electrobalance output.

Temperature Programmer

An Assembly Products "Temptendor" model 732, calibrated for an Iron-Constantan thermocouple, was used as a temperature programmer. This was accomplished by attaching a variable-gear train to drive the controller potentiometer at a predetermined rate. The potentiometer was connected to a digital readout dial calibrated in degrees C. and readable to approximately $\pm 0.2^{\circ}\text{C}$. Temperature agreement between the control thermocouple and any other thermocouple at the same temperature was usually within one (1) degree C. As shown in figure 1, the programmer operated a servo-system which automatically adjusted a variable transformer for the correct power requirement to satisfy a balanced bridge condition in the temperature controller.

An additional feature of the power system was a stepdown transformer to accommodate the low resistance furnace elements. This system was rated for a continuous output to $\frac{1}{2}$ kw. It was subsequently equipped with a water-cooling coil which allowed a continuous output of approximately 1.2 kw.

X-ray Analysis

A General Electric XRD-5 diffractometer was used to obtain X-ray diffraction patterns on the sample residue. The radiation was Cu K α (Ni filtered). Samples were ground in an agate mortar from two to three minutes, mixed to a slurry with ethyl alcohol and spread in a thin film on the glass sample slide.

C, H, O, Analyses

Ultimate analyses were performed by the Utah Engineering Experiment Station on an F & M 180 C H N analyzer to obtain the percentage of carbon and hydrogen. The oxygen analysis was performed with a Coleman Oxygen Analyzer. Accuracy is estimated to be within $\pm 5\%$ for all samples.

Infra-Red Analysis

Infra-Red analyses were performed on a Model 521, Perkin-Elmer dual-beam recording spectrophotometer. KBr absorption windows were prepared, using approximately 200 mg of mixture (1:200, sample to KBr ratio). These were ground together with an agate mortar and pestle. Nujol mixes were prepared by grinding the sample in nujol with the agate mortar and pestle. The spectra of the nujol mixtures were not very satisfactory, presumably because the samples were not ground fine enough to observe the differences in absorption spectra.

Mass Spectrometry

Mass spectra were obtained from the gas samples desorbed from the product residue plus that collected directly from the blow-out of sample #134. These were analyzed on a CEC 21-620 mass spectrometer. This unit has a resolution limit of 300, and an accuracy on the order of 5 to 10%.

Pyrolysis Materials

Chemicals and materials used in these experiments were as follows:

1. Absorbent cotton (used for X-ray diffraction only).
2. Chromatographic grade cellulose pulp, Schleicher and

- Schuell #2200.
3. Anhydrous glucose
 4. Xylose, Eastman Organic Chemicals #542
 5. i Inositol (meso), Nutritional Biochemical Corp. #1338
 6. Yellow pine wood

RESULTS AND DISCUSSION

Anomalous High Pressure Effects

Low Pressure DTA

Typical of the Differential Thermal Analysis (DTA) of a cellulose in a vacuum, is an endothermal trace corresponding to thermal degradation. Figure 2 by Akita and Kase (6), compares the DTA of cellulose in air, in N_2 , and in a vacuum. Here it is noted that in the presence of O_2 , the effect of combustion of the pyrolyzate causes an exothermal peak immediately succeeding the endothermal degradation.

The atmosphere of N_2 can be observed to inhibit the extent of the endotherm probably due to the retarded transfer of the product from the reaction zone.

Exothermal Reaction

Figures 3,4, and 5 are modified high pressure DTA traces or plots of ΔT vs. the program or reference temperature for the various samples studied. The original traces were ΔT vs. time. The heating rate was a constant, for each DTA trace, and since reaction temperature was the parameter of greater interest than time, the abscissa was converted to temperature. One further change was made to facilitate the comparison of curves, the baseline was set at $\Delta T = 0$ so that (except for differences in thermal conductivity of sample and reference) the peak height essentially represents the temperature difference between samples and reference.

The high pressure DTA of cellulose demonstrates the occurrence of an anomalous exothermal reaction, quite unlike the typical vacuum DTA of pure cellulose, as illustrated in figure 2. Figure 3 shows several exothermal reactions of cellulose at pressures of 7, 16, 23, and 28 kb. Precautions were taken to exclude oxygen from the sample, however, no difference was noted between sample 121, which was prepared in an atmosphere of oxygen, and those which were excluded from oxygen. The amount of oxygen which would remain entrapped after pressurization, in contact with the sample, is reasonably very low and insufficient to effect any sustained, observable oxidation. Lipska and Parker (7) have shown that at one atmosphere of N_2 plus O_2 , oxygen content below 0.5% had no effect on the pyrolysis.

As a consequence, the observed exotherm cannot be attributed to oxidation. The intimate confinement of reactants and activation states, however, could produce a different mechanism with different products and therefore a different thermal effect.

"Positive" and "Negative" Effects of Pressure

It can be observed from figure 3 that at 29 kb, a slightly higher temperature is required to effect the reaction than at 7 kb. Thus, the high-pressure reaction is slightly more temperature resistant.

This pressure effect might be considered as a negative effect, as it inhibits certain reactions. On the other hand, the intimate product confinement could be thought of as a positive effect, since it favors reactions which otherwise might occur infrequently or not at all.

An important effect, which might be categorized as a positive pressure effect, can also be noted by comparing figure 2 (the data of Akita and Kase) with our thermograms of the same heating rate in figure 4. The initiation temperature of the cellulose exotherm at high pressure is lower than that which occurs during vacuum pyrolysis. The low-pressure reaction begins at approximately 290°C. However, at 7 kb it occurs considerably lower, near 227°C (three-sample average of #122, 123, and 141, see Table I).

Fast vs. Slow Reaction

At least two types of reactions are observed during DTA under a confining pressure. These can be described as slow (figure 3) and fast reaction (figure 4 except #99). Note that the cellulose peak of the fast reaction is more than 400°C above the reference ($\Delta T=0$) while the slow reaction peaks of cellulose are between 2° to 3°C high. This different effect is obtained simply by varying the heating rate.

It is natural to expect that a fast heating rate would effect a higher peak, but an increase from ½°/min. to 5°/min. could not be supposed to account for a ΔT increase from 2° to 400°C. Heating rates on the order of ½ to 1° per minute will unpredictably be the fast or slow reaction type. Note that at ½°/min., sample 101 was a fast reaction (see Table I). The range of unpredictability should be a function of the temperature-control accuracy during the programmed heating. The unexpected high peak of sample 101 went off scale and so it is not plotted, but this does show that the faster and higher-temperature reaction causes a more complete and more exothermal reaction. Table I shows that the peak area of sample 101 is >5 units while the peak area of other samples heated at the same rate was approximately 2 units.

The reason for this difference may be as follows. The slow reaction corresponds to a delicate condition of programmed heating which must be slow enough to allow for the removal of the heat of reaction. If the heat of reaction cannot transfer from the reaction zone as rapidly as it is generated, the temperature climbs, accelerating the exothermal reaction, and runs out of control to completion. The sample size is important here and a larger sample would produce a higher temperature and require a slower heating rate to maintain the control of the slower reaction.

A major problem encountered in the rapid heating rates is the retention of the gases generated by the reaction. Excessive volatility in the sample cube leads to violent rupture of the cube and explosive loss of product.

Sample rupture and the escape of product gases was never a problem at the lower heating rate with the slower reactions.

I-R Analysis of Residue

Figure 6 shows the IR absorption spectra of the various sample residues, illustrating the effects of variation in pressure, heating rate, and type of molecular structure.

Samples 95 and 121, pyrolyzed at $\frac{1}{2}^{\circ}$ /minute and at 28 and 7 kb, respectively, produced almost identical spectra, indicating very little difference in the product residue due to this pressure difference.

Cellulose-sample 123, with the heating rate of 5° /minute (which produced the very rapid reaction and high temperature) showed a very different absorption. The 1700 cm^{-1} band, (generally thought to be due to C=O) is very much reduced. The 2860 to 2950 cm^{-1} bands, attributed to naphthenic-CH, CH_2 , and CH_3 groups is so completely reduced that it would almost appear that CH groups are essentially all that are left (near the 2920 peak). Aromatic absorption in the bands 750, 820, and 860 cm^{-1} show up very well.

Sample 149, (yellow pine wood) compared with #123, shows the same or slightly more absorption in the 750 to 860 bands, slightly more absorption in the 1590 band (also attributed to aromatic structure and perhaps C=O groups), much less at 1700; and about the same or less absorption in the 2920 area. All of this seems very natural in spite of the fact that #123 reached a higher temperature (670°C vs. 513°C) since the aromatic content of wood is high to begin with.

For the most part, the difference between #142, glucose, and #146, xylose, can be explained on the basis of the difference in the peak temperatures (440°C for #146, vs. 322°C for #142).

The inositol was not completely reacted and gave adsorption spectra very similar to pure inositol and for that reason is not included here. (For a very excellent discussion on IR band assignments see reference 8.)

X-ray Diffraction

Ergun (2) has shown a correlation of vitrinite coal rank with the general peak form particularly in the $2\theta = 20^{\circ}$ to 27° range (i.e., $s-(2\sin\theta)/\lambda$ range of approximately .23 to .33). He states, "With decrease in rank the most pronounced band becomes broader, and its position is shifted to lower 2θ values ... peak position could serve as a simple but reliable index of coal rank." (Lower s values corresponds with lower 2θ value.)

Figure 7 is a comparison of the X-ray diffraction patterns of several different samples which were investigated. They are: 1) metamorphosed samples of cellulose (124, 105, 148, 132, 58); 2) metamorphosed anhydrous glucose (142); 3) metamorphosed xylose (146); 4) samples of high volatile bituminous (HVB), low volatile bituminous (LVB), and graphite (all reproduced from reference 5); and 5) ball-milled and natural cotton.

These curves have been arranged in order of decreasing 2θ value, from top to bottom (i.e., high rank at the top). This arrangement also turns out to be a function of the heating rate. Samples which were heated rapidly and which reached a high temperature are high on the chart. Sample #123 heated to 670°C at the exotherm peak; #149, to 513°C ; #105 (slow heating rate) heated to approximately 225°C at the exotherm peak.

Cellulose sample #58 is the highest on the scale of synthetic coals. This sample was heated very rapidly, without the use of DTA and at 28 kb pressure. It was heated to 225°C in 3 minutes and

continued at a rough rate of 10°/minute, to 300°C (manual temperature control). That this sample (#58) exhibits a distinct (002) graphite peak of 26.5° 2θ, (probably the most pronounced graphite peak of all those compared here, except pure graphite) is thought to be very significant. The coal sample which was heated to 850°C at 30 kb for 30 minutes does not approach the graphite peak as well. This would appear to show that the heat generated during the exothermal metamorphosis is a more effective graphitization heat than externally applied heat on a previously coalified sample.

High Oxygen Content in Press Samples

One important effect on high pressure, which would be considerably different in coalification of large vegetal accumulations is this: the confining pressure acts to retain a very high percentage of oxygen. One probable reason for this, in the fast reactions, is that the small, ¼-gram samples cool very rapidly after attaining peak temperature. Not only would a larger sample be likely to reach higher temperatures but it would also remain heated for longer periods allowing for diffusion of volatiles away from the reaction zone, perhaps to condense in a cooler locality. After attaining maximum temperature, slow cooling would probably encourage growth of the more stable molecular structure and the elimination of oxygen.

Stability From Inter-Ring and Intra-Ring Effects

It is obvious that the 1,4-glycosidic linkage helps in the stabilization of cellulose. This can be seen by a comparison of the thermogram of anhydrous glucose with that of cellulose (see figures 4 and 5). The initiation temperature is approximately 141°C for glucose. This is more than 80°C below that observed for cellulose at the same heating rate of 5°/min.

By comparing the exotherm of anhydrous glucose (#142) with that of xylose (#146), the effect of the pendant -CH₂OH group becomes apparent. Pendant groups have been observed to detract from the thermal stability of a molecule. The xylose reaction began approximately 45°C (i.e., 186°C) above the glucose reaction temperature.

The -CH₂OH is likely the site of the reaction initiation. Xylose reacted slower than cellulose (at the same heating rate) until it reached approximately 215 to 220°C whereupon it converted very rapidly to the fast reaction similar to the cellulose (and at a temperature nearly as high as with cellulose). This seems to imply that the 1,4-glycosidic linkage (and perhaps other stabilizing factors) inhibits the decomposition of the cellulose chain until the temperature is sufficiently high to open the ring.

Without the C-O-C bond nor the pendant -CH₂OH, inositol is seen to be remarkably more stable than either anhydrous glucose or xylose. Note that even at the high initiation temperature of 270°C the sample did not overheat and run out of control. The uniformity of the inositol ring is a strong stabilizing effect. It appears that inositol began a very rapid exotherm but was suddenly checked perhaps by an endothermal reaction (or a series of endothermal reactions) such as dehydration.

Analysis of Low-Pressure-Pyrolyzate Gases

Sample #124 (see figure 8) was pyrolyzed at 300°C to analyze

the evolved gases of the early stages of pyrolysis of cellulose. This was carried out with the TBA equipment but at constant temperature (after about eight minutes required to reach 300°C). The pyrolyzate was collected in four bottles during the periods of 0 to 5, 5 to 10, 10 to 20, and 20 to 165 minutes. Mass spectrometric analysis of the gas is included in the same figure. Here it can be observed that: 1) almost pure H₂O is evolved initially (below 260°C). 2) The very low initial fraction of CO₂ gradually increases. 3) Short-chain hydrocarbons were observed, but only in the initial moments of the 300°C period. 4) The initial irregularity of the rate of weight-loss curve, is probably due to the time required for the sample and container to come to reaction temperature. The effect of an immediate 300°C reaction temperature could correspond to the extrapolated, dashed line.

Small amounts of CO are thought to have been present but were unobservable due to the masking effect of the contaminating air (M/e = 28, due to N₂). Experiments by Madorsky (9,10) show that there is about one-third as much CO as CO₂ during pyrolysis at temperatures between 280 to 400°C.

Rapid, Mature Stabilization

The case of the sudden, out of control, high-temperature reaction, and the resulting high temperatures (exceeding 670°C in the non-blow-out sample 123) could allow a very complete reorientation of the molecular structure. The hot reactive mass of many short chain segments would favor elimination of oxygen, particularly where it occurs as a pendant hydroxyl group. Benzene ring structurization which would probably form infrequently at low temperature would be favored. Note that figure 6, showing the IR spectra of sample 123, has accordingly the most prominent absorption in the 750, 820, and 860 cm⁻¹ region, which have been attributed to benzoid aromatic structure (7). At very high temperatures for example during coalification of a clean concentration of vegetal material, the graphite structure should be favored. Here again this effect can be noted: Figure 7, showing the X-ray diffraction for various samples, illustrates how samples 58, 123, and 149 (sample of wood which autogeneously heated above 520°C) most nearly approach the high-rank coal patterns and diffraction of the (002) graphite peak at 26.5° 2θ.

Factors Responsible for Maximum Temperature

Among the factors determining the maximum temperature attainable by a coalifying exotherm, are mass, concentration of reactive groups in the deposit, and initiation temperature. A very small sample (e.g., ¼ gram, such as those used in this work) would probably lose heat very rapidly and not attain the maximum temperature. Reduced concentration of reactive groups, perhaps due to the rapid decay of cellulose from woody materials, would tend to diminish the maximum temperature, as would dilution with mineral matter. Thus, highly concentrated vegetal material might convert to anthracite or graphite, whereas, decayed material with significant mineral contamination, upon attaining initiation temperature might heat spontaneously and be converted to one of the intermediate ranks of coal. Low rank coals with considerable mineral content and/or those which were heated very slowly, say, due to gradual sinking and accumulation of overburden may have had an analogous metamorphosis of the slow, annealing or controlled-temperature cellulose pyrolysis, without heating significantly above ambient

conditions. Some upranking may thus occur from high ground temperatures.

Possible Factors Influencing the Initiation Temperature

Factors which might account for elevating the temperature to reaction initiation could be combustion of overlying vegetation, earth-movement friction, magmatic heat sources, and perhaps natural ground temperatures. If the ground temperature increased very slowly it might tend to yield low-rank coals without the coal experiencing a significant autogenous heating.

Appreciation is expressed for the J. L. Dougan fellowship and to the Equity Oil Company for support of this research.

REFERENCES

1. P. J. Wilson, Jr., and J. H. Wells, Coal, Coke and Coal Chemicals. New York: McGraw-Hill Bk. Co., Inc., 1950, pp. 42-3.
2. S. Ergun, X-ray Studies of Coal and Carbonaceous Materials. Washington D. C.: U. S. Bureau of Mines Bull. 648, 1968.
3. A. Petzoldt, Quoted in O. Stutzer and A. C. Noe, Geology of Coal. Chicago; University of Chicago Press, 1940, p. 124.
4. M. Teichmüller and R. Teichmüller, "Geological Causes of Coalification." Coal Science, Vol 55 of Advances in Chemistry Series. R. F. Gould ed. Washington D. C.: American Chemical Society, 1966, pp. 133-155.
5. L. S. Pan, "Pressure Effects on Laboratory Coalification Processes." Ph.D. Dissertation, University of Utah, 1967.
6. K. Akita and M. Kase, J. Poly. Sci. Part A-1, 5 (1967), 833.
7. A. E. Lipska and W. J. Parker, J. Appl. Poly. Sci., 10 (1966), 1439.
8. R. A. Friedel, H. L. Retcofsky, and J. A. Queiser, Advances in Coal Spectrometry. U. S. Bur. Mines Bull. 640, 1967.
9. S. L. Madorsky, V. E. Hart, and S. Straus, J. Res. Nat. Bur. Stand., 56 (1956), 343.
10. S. L. Madorsky, Thermal Degradation of Organic Polymers. New York: John Wiley & Sons, Inc., 1964, chap. 12.

Table I. DTA DATA AND RESIDUE ANALYSIS

sample no.	material	pressure (kp)	sample wt. (mg.)	heat rate °C/min.	blowout	Initial Reaction Temp. (°C)	ΔT peak (°C)	Maximum Temp. (°C)	peak area (μV-min)	wt. % CHO	wt. % H	wt. % N	Residue % of total
90	cellulose	3	281	9	yes	233	high	high	-	73.6	3.5	22.8	42.7
94	"	28	269	10	no	210	high	high	-	87.5	3.1	9.5	64.3
95	"	28	230	k	no	215	2.8	300	1.3	72.6	4.3	23.1	56.5
96	"	23	284	k	no	200	2.9	237	2.3	67.3	4.0	28.7	77.8
99	"	7	299	k	no	188	2.7	237	-	67	4	29.6	77.0
100	"	23	305	k	no	-	-	300	-	71.6	2.7	25.7	65.9
101	"	16	300	k	no	210	>15	300	>5	72.6	2.7	24.7	-
105	"	16	271	k	no	207	1.1	308	2.20	74	4.0	23	51.3
120	"	7	307	k	no	192	1.85	300	2.22	61	3.4	25	53.2
121	"	7	295	k	no	198	1.2	276	2.20	-	-	-	52.2
122	"	7	285	5	yes	223	high	high	-	85.4	4.0	10.6	8.87
123	"	7	299	5	no	231	415	>454	-	-	-	-	40.5
141	"	7	300	5	yes	227	216	>454	2.4	incomplete reaction	-	-	54.4
129	inositol	7	285	5	no	287	9.7	350	1.2	incomplete reaction	-	-	-
135	"	7	292	5	no	270	-	-	-	-	-	-	-
142	glucose	7	263	5	no	141	10.1	322	6.1	79	5.8	15	26
146	xylose	7	233	5	no	175	185	440	-	82	4.8	13	37.5
149	wood	7	276	5	no	242	250	513	-	92	4.1	4	37.0
134	cellulose	5	290	-	-	-	-	-	-	-	-	-	-

Not DTA (blow-out gas collected for analysis: 50% H₂O, 20% CO₂, 2% acetone, 2% H₂ + CO % undetermined)

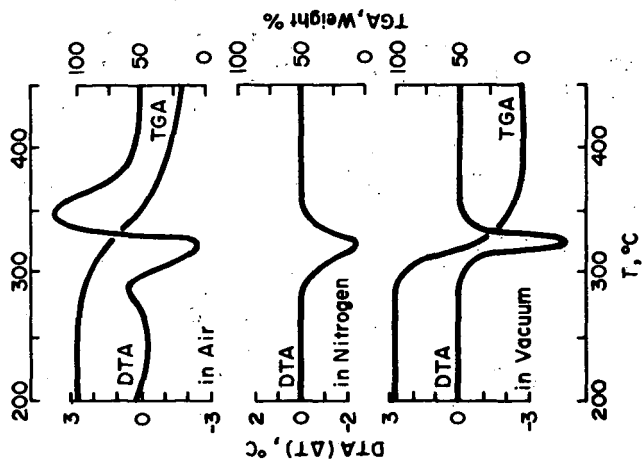


Fig. 2. DTA AND TGA CURVES OF CELLULOSE IN AIR, N₂, AND IN VACUO. ● = 5°C/MIN (6)

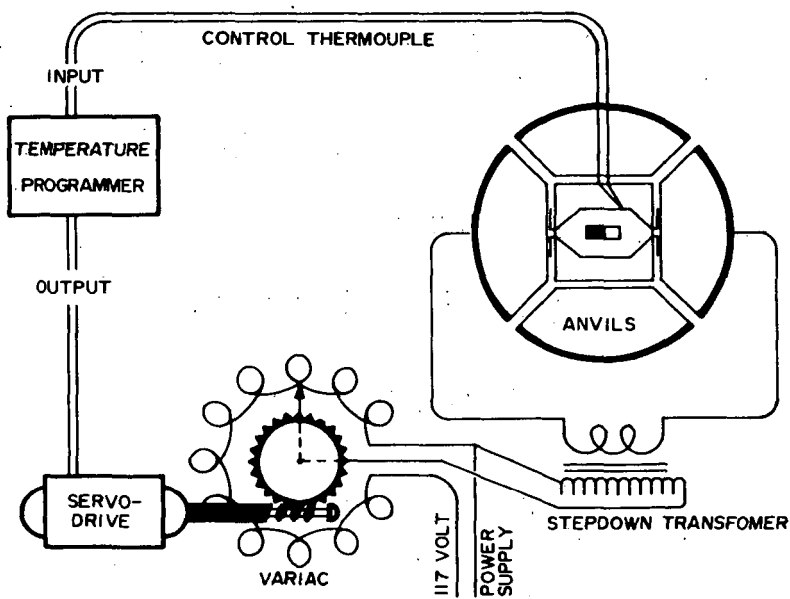


Fig. 1. TEMPERATURE PROGRAMMER AND POWER SYSTEM

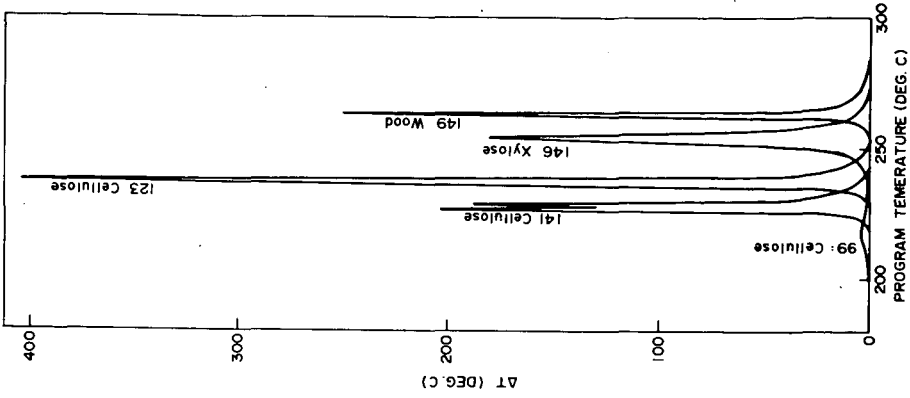


Fig. 4. DTA THERMOGRAMS AT 7 KB, HEATING RATE $6^{\circ}/\text{MIN.}$

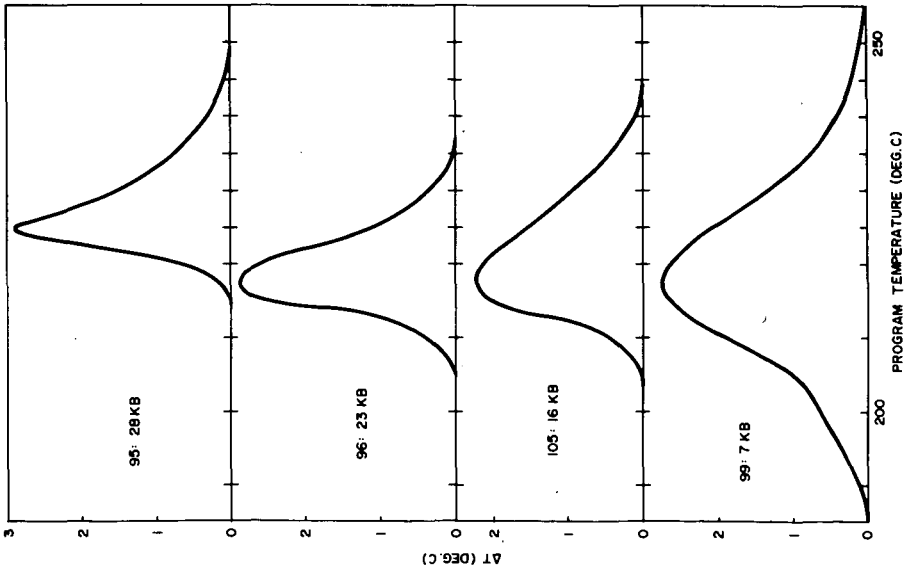


Fig. 3. CELLULOSE DTA EXOTHERMS AT VARIOUS PRESSURES HEATING RATE = $1/20^{\circ}/\text{MIN.}$

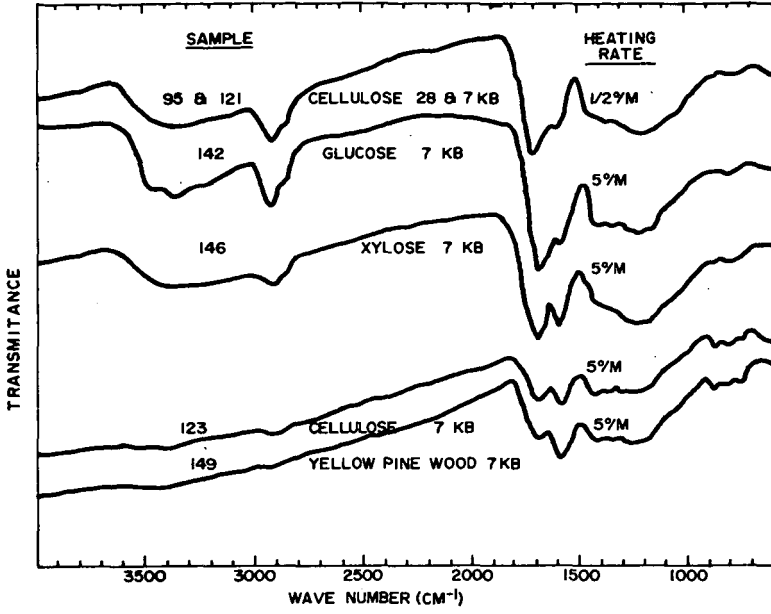


Fig. 6. I-R SPECTRA OF SAMPLE RESIDUE

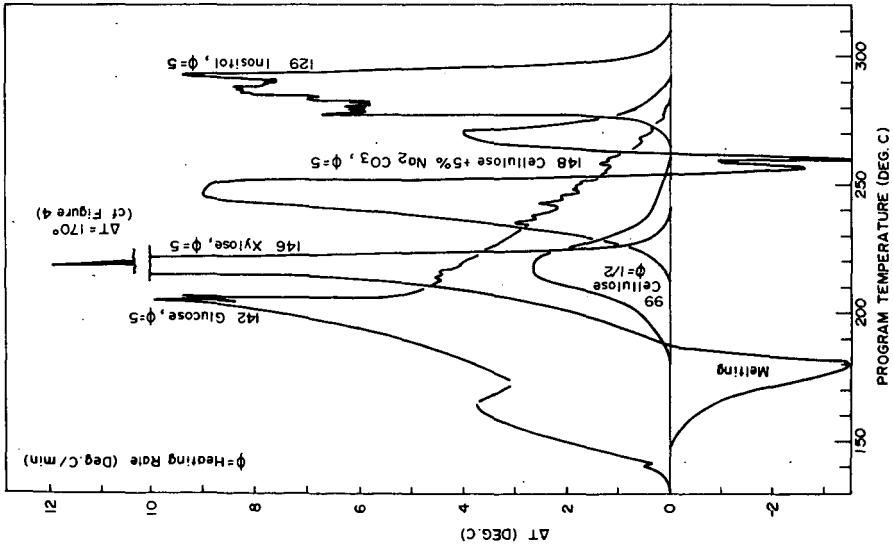
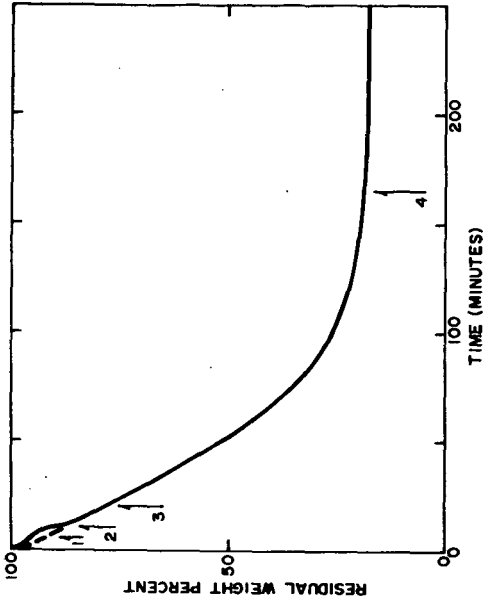


Fig. 5. DTA THERMOGRAMS AT 7 KB



INITIAL WT.: 124.0 MG.
AFTER 10 HRS.: 18.75 MG.

PYROLYZATE ANALYSIS	COLLECTION PERIOD	TEMP. (°C)
#1. 100% H ₂ O	0 - 5 MINUTES	Rm.T. - 160°
#2. 91% H ₂ O, 4% CO ₂ , 4% HC'S*	5 - 10 "	160° - 300°
#3. 82% H ₂ O, 15% CO ₂	10 - 20 "	300°
#4. 74% H ₂ O, 20% CO ₂	20 - 165 "	300°

*HC'S: PROBABLY 4% CH₄ + SMALL FRACTION ETHANE, ACETONE, AND ACETALDEHYDE.

CO PRESENCE NOT DISTINGUISHABLE DUE TO MASKING EFFECT OF H₂ (SAME W/E VALUE). PERCENTAGES ARE BASED ON VOLUME WITHOUT AIR.

Fig. 8. SAMPLE #124: VACUUM PYROLYSIS OF CELLULOSE AND ANALYSIS OF GASEOUS PRODUCTS

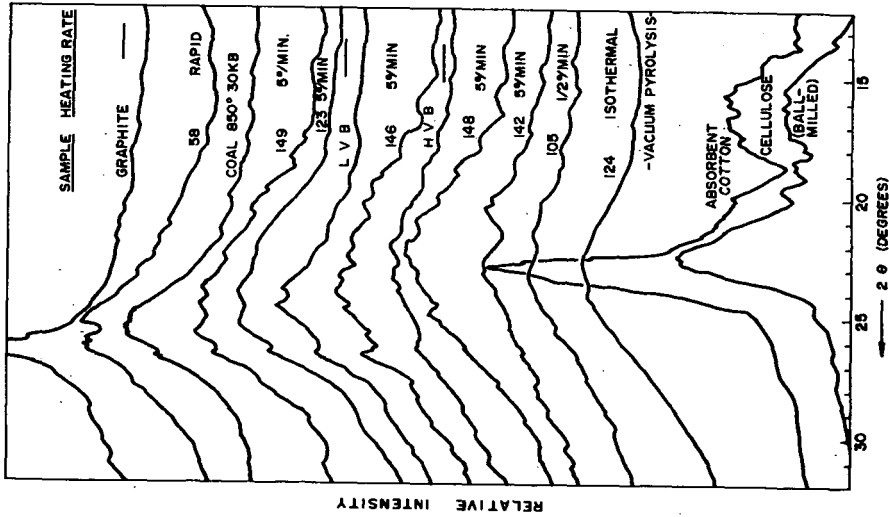


Fig. 7. A COMPARISON OF X-RAY DIFFRACTION PATTERNS

THE STRUCTURE OF ATHABASCA ASPHALTENES AND THE CONVERSION OF THESE MATERIALS TO USEFUL BY-PRODUCTS

By

James G. Speight
Research Council of Alberta
Edmonton, Alberta, Canada

INTRODUCTION

The last decade has seen phenomenal development of gas-chromatographic and spectroscopic techniques which has enhanced identification of the constituents of lower boiling fractions of crude oils. However, the heavy ends of petroleum, i.e., the asphaltenes, have not been so readily identified but by application of chemical and physical methods to the problem of asphaltene structure, a number of significant details have been gathered from which it has been possible to propose a general model of asphaltene structure. One of these methods, proton magnetic resonance (p.m.r.) spectroscopy, has recently been evaluated (1,2,3,4) as a tool in the structural analysis of fractions of petroleum oils and asphalts and the results indicated (5) that petroleum asphaltenes are basically peri-condensed aromatic ring systems, having six to twenty aromatic nuclei, bearing alkyl and naphthenic moieties, with the hetero-atoms liberally scattered throughout in a variety of locations, including heterocyclic systems.

Subsequent application of the p.m.r. method to fractions of Athabasca bitumen (6) allowed the average chemical structures of the constituents to be expressed in terms of carbon-type distribution. Moreover, it was also possible to estimate the average structures of the aromatics within the fractions of the bitumen by relating the ratios of peripheral aromatic carbons to total aromatic carbons to those of known fused ring compounds. In general terms, an average asphaltene molecule appeared to consist of four or more aromatic sheets, containing ten or more rings each. Each condensed aromatic ring system carried individual alkyl side chains (four or five carbon atom units), which may or may not be linked to other aromatic sheets, together with smaller proportions of naphthenic rings which were presumably fused to the aromatic ring system.

The desirability of removing the asphaltene fraction from a crude oil has been advocated many times, the principal reasons being the production of a cracking stock low in metal impurities, hetero-atom (i.e. nitrogen, oxygen, and sulphur) compounds, and having a low carbon residue (7). The present paper is the outcome of a more detailed structural analysis of the Athabasca asphaltenes describing the average structures of the constituents within sub-fractions of the asphaltenes, with passing reference to the structures of the asphaltenes from forty-five conventional Alberta crudes, and, in conjunction with the chemical evidence provided herein, affords an indication of the potential of these heavy ends of crude oils.

EXPERIMENTAL

Materials and General Techniques

Asphaltenes from Athabasca bitumen and from forty-five conventional Alberta crude oils were obtained by a standardized procedure described elsewhere (6). Fractionation of the Athabasca asphaltenes was achieved by treatment of the washed and dried asphaltenes with a series of higher molecular weight paraffinic solvents whereby, a soluble fraction (e.g. A₁) and an insoluble fraction (e.g. B₁) were obtained as shown below.

Fractionation of Athabasca Asphaltenes

	----- Fractions -----							
	A ₁	B ₁	A ₂	B ₂	A ₃	B ₃	A ₄	B ₄
% bitumen	1.0	16.0	1.8	15.2	3.4	13.6	6.0	11.0
% asphaltenes	5.9	94.1	10.6	89.4	20.0	80.0	35.3	64.7

Physical and Elemental Analyses

Elemental compositions of the fractions were determined by the Alfred Bernhardt Micro-analytical Laboratory, Elbach uber Engelskirchen, West Germany; the oxygen content of the samples was determined directly and not by difference. Molecular weights were measured osmotically. P.m.r. spectra were obtained in duplicate with a Hitachi Perkin-Elmer R20 High Resolution NMR Spectrometer using tetramethylsilane as internal standard as described previously (6). Furthermore, by means of the same principles as outlined previously (6) certain structural parameters were estimated which, with the exception of (e), are independent of the observed molecular weight, and are:

- (a) C_{SA}/C_p , the ratio of carbon atoms directly attached to an aromatic sheet to peripheral carbon atoms; C_{SA}/C_p is the average degree of substitution of the aromatic sheet.
- (b) C_S/C_{SA} , the ratio of saturated carbon atoms to carbon atoms attached to the edge of the aromatic sheet; the C_S/C_{SA} ratio indicates the average number of carbon atoms attached to a position on the edge of an aromatic sheet.
- (c) C_p/C_A , the ratio of peripheral carbon atoms per aromatic sheet to aromatic carbon atoms, i.e., an estimate of the average shape of the aromatic sheets.
- (d) $(C_S - C_{Me})/C_{Me}$, the ratio of methylene carbon to methyl carbon, i.e., an estimate of the degree of branching in the saturated moieties of the molecules.
- (e) R_A , the number of aromatic rings per molecule.

The results are illustrated in Table I and the C_p/C_A ratios for a series of standard condensed aromatics are presented in Table II in order to illustrate more clearly the closest possible ring structures of the aromatics.

RESULTS

Structures in Asphaltene Fractions

The structural parameters presented in Table I offer information about the average struc-

TABLE I Structural Parameters of the Constituents
in the Athabasca Asphaltene Fractions

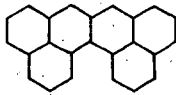
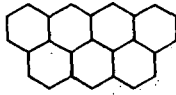
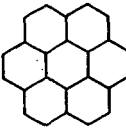
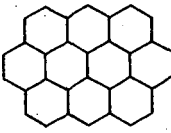
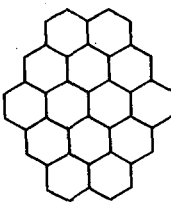
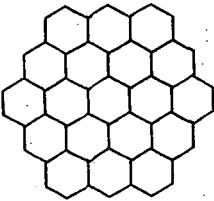
Sample	Molecular weight	-----Structural Parameters-----				Aromatic rings R_A
		C_{SA}/C_p	C_S/C_{SA}	C_p/C_A	$(C_S-C_{Me})/C_{Me}$	
A ₁	2,694	0.57	3.6	0.55	8.2	20.6
A ₂	2,704	0.62	3.5	0.54	8.2	20.7
A ₃	3,185	0.57	4.1	0.48	9.4	27.6
A ₄	4,338	0.65	3.1	0.46	4.4	40.8
B ₁	6,427	0.49	5.8	0.37	4.4	66.3
B ₂	6,530	0.48	6.0	0.37	4.6	67.8
B ₃	7,603	0.49	5.7	0.35	4.5	82.1
B ₄	8,158	0.52	5.0	0.35	4.6	90.3

tures of the Athabasca asphaltene fractions. For example, comparison of the C_p/C_A ratios with those of standard condensed aromatic compounds shows that the average structures of the asphaltenes vary from a dibenzonaphthacene, i.e., a six-ring unit in the lower molecular weight fractions to a least dinaphtho-ovalene, i.e., a fourteen-ring unit, in the higher molecular weight fractions. In keeping with this postulate of condensed aromatic structures, the asphaltenes form π -complexes with picric acid and with 1,3,5-trinitrobenzene which can be examined spectroscopically. Complexes of this type have been shown to be formed between condensed aromatics (e.g. pyrene, ovalene, etc.) and electron deficient nitro-aromatics (8).

From the C_{SA}/C_p parameters, 57-65% of the peripheral carbon atoms in the lower molecular weight asphaltenes (the A series) and 48-52% of the peripheral carbon atoms in the higher molecular weight fractions (the B series) carry saturated substituents. Moreover, the C_S/C_{SA} parameters show that these saturated substituents vary from a three to four carbon atom chain in the lower molecular weight fractions to a five to six carbon atom chain in the higher molecular weight fractions. In addition, the higher $(C_S-C_{Me})/C_{Me}$ parameters of the lower molecular weight asphaltenes suggest a lower degree of branching in the saturated moieties. It would appear that the aromatic portions of the lower molecular weight asphaltenes carry unbranched alkyl substituents and unsubstituted naphthenic moieties whereas the aromatic sheets of the higher molecular weight asphaltenes bear branched alkyl and alkyl-substituted naphthenic moieties.

From p.m.r. and molecular weight data, each individual asphaltene molecule contains more than one aromatic sheet. For example, in the lower molecular weight asphaltenes where the C_p/C_A parameters indicate a six-, seven- or ten-ring basic unit, molecular weights indicate twenty to forty aromatic rings per molecule (R_A , Table I) which requires three or more basic units per asphaltene molecule. Similarly, in the higher molecular weight fractions where the basic unit is at least a fourteen-ring system, molecular weight data indicate that four to seven of these units constitute an asphaltene molecule. However, data obtained by the determination of molecular weights of the asphaltene fractions in solvents having different dielectric constants and in benzene at various temperatures suggest that the high molecular weights of the asphaltene molecules are due, in part, to electrostatic association of the individual units. These data, presented in Tables III and IV, show that a decrease in the observed molecular weight occurs when a solvent of higher dielectric constant or higher temperature is employed for the determination which suggests breakdown of π -electron interactions between individual asphaltene units under these conditions. A similar concept has been invoked to explain the high molecular weights of other crude oil asphaltenes (9) and the association of asphaltene units in dilute solution has also been reported (10).

TABLE II C_p/C_A Ratios of Condensed Aromatic Compounds

-----Hydrocarbon-----		
<u>Name</u>	<u>Structure</u>	<u>C_p/C_A</u>
Dibenzo[de,hi]naphthacene		0.58
Anthro[defghi]naphthacene		0.52
Coronene		0.50
Ovalene		0.44
Dinaphtho[2,7-hijk·2,7-stuv]- ovalene(Circopyrene)		0.38
Circocoronene		0.33

The present results also afford an indication of the limiting size of the individual sheets in the asphaltene molecules. A comparison of C_p/C_A ratios with the molecular weight (Table V) and a plot of these values shows that the limiting value for C_p/C_A is approximately 0.35, i.e., close to the C_p/C_A ratio of a fourteen-ring unit. Thus, it appears that any higher molecular weight fraction of the asphaltens will be due to agglomerations of like, in this case dinaphtho-ovalene, nuclei and are probably approaching homogeneity. Larger units may approximate a coke-like structure.

Similar observations were recorded for asphaltens from the forty-five conventional Alberta crudes; viz. the ring systems varied from six to fourteen aromatic nuclei per sheet with a tendency to associate in solution but there appeared to be higher proportions of naphthenic and

TABLE III Molecular Weight Determinations of Asphaltene Fractions in Different Solvents

<u>Sample</u>	<u>Solvent</u>	<u>Dielectric Constant*</u>	<u>Observed Molecular Weight</u>
A ₁	benzene	2.3	2,694
A ₁	methylene dibromide	7.8	2,239
A ₁	pyridine	12.3	1,382
B ₁	benzene	2.3	6,427
B ₁	methylene dibromide	7.8	4,804
B ₁	pyridine	12.3	3,413

* Handbook of Chemistry and Physics, Chemical Rubber Co.

TABLE IV Relationship of Asphaltene Molecular Weight to Temperature of Solvent*

<u>Temp. (°C)</u>	<u>Observed Molecular Weight**</u>
35	6,427
40	5,780
45	5,570
50	5,290
55	4,710

* Solvent; benzene; sample: B₁

** Average of three determinations; the result of each determination was within $\pm 3\%$ of the mean.

TABLE V Relationship of Asphaltene C_p/C_A Ratios to Molecular Weights

<u>Fraction</u>	<u>Molecular Weight</u>	<u>C_p/C_A</u>
A ₁	2,694	0.55
A ₂	2,704	0.54
A ₃	3,185	0.48
A ₄	4,338	0.46
B ₁	6,427	0.37
B ₂	6,530	0.37
B ₃	7,603	0.35
B ₄	8,158	0.35

alkyl moieties in these asphaltenes. It was also evident that the asphaltene structure was related to the age and nature of the sediment in which the oil was located but there did not appear to be any strict relationship between asphaltene content (% w/w) and viscosity (or "heaviness") of the crude oil. These results will be discussed in detail in a forthcoming publication.

DISCUSSION

Chemical Modification of Athabasca Asphaltenes

It is evident from the data assembled here that Athabasca asphaltenes are not entirely homogeneous and consist of large molecules and significantly smaller ones, i.e., the six-ring species, which are probably in the asphaltene fraction because of their high polarity, presumably due to their hetero-atom content, and hence their ability to associate in organic solvents. Nevertheless, as well as the conventional conversion of the asphaltenes to good grade coke, there are several other possible uses of the asphaltenes which can be brought about by carrying out simple chemical conversions of these carbonaceous materials. The progress of these reactions can be followed spectroscopically and the observations, which will be published in detail at a later date, are in agreement with a condensed aromatic ring-system bearing alkyl and naphthene substituents.

Oxidation with nitric acid, or other common oxidising agents, renders the asphaltenes water-dispersible and soluble in aqueous alkali which, when followed by sulphonation or sulphomethylation, yields water-soluble products (11). Halogenation with elemental halogen produces halo-derivatives of the asphaltenes (12) which, when fused with alkali, afford alkali-soluble materials. Introduction of the halogen as *p*-halophenyl via the Gomberg reaction (13) also affords a means of indirectly introducing functional groups or even introduction of the functional group in this manner affords useful products. Other useful reactions include carboxylation of the halo-asphaltenes via lithium/carbon dioxide; oxidation with *m*-dinitrobenzene and subsequent preparation of the imines; low temperature carbonization of the halo-asphaltenes via a Wurtz-Fittig or Ullmann reaction; conversion of the halo-asphaltenes to hydroxy-asphaltenes by caustic fusion; treatment with maleic anhydride and alkaline hydrolysis of the product affords a water-dispersible material which when treated with ammonia affords an acid dispersible product.

The overall effect of these and many other simple chemical reactions is to produce derivatives of the asphaltenes which may be gainfully employed. For example the incorporation of nitrogen or phosphorus into the molecule via the Gomberg reaction affords potentially useful slow-release fertilisers and soil conditioners as does the reaction of the carbonyl-asphaltenes with hydroxylamine or amines. Water-dispersible derivatives are useful as drilling mud thinners and soil conditioners whilst hydroxyl-containing derivatives can be used as ion-exchange resins or heat transfer media. Halo-asphaltenes are adequately suited for this latter purpose.

ACKNOWLEDGEMENTS

The author is indebted to Syncrude Canada Ltd. for gifts of dry bitumen, to the Oil and Gas Conservation Board for samples of Alberta crude oils, to Dr. N. Berkowitz for critically reading the manuscript, to Mr. J. Barlow for valuable technical assistance, and to Mr. M. Anderson for recording the proton magnetic resonance spectra.

REFERENCES

1. N. F. Chamberlain, American Petroleum Institute Division of Refining, 29th Midyear Meeting, St. Louis, Mo. (1964).
2. T. F. Yen and J. G. Erdman, American Chem. Soc., Division of Petroleum Chemistry, Atlantic City, 99 (1962).
3. S. W. Ferris, E. P. Black and J. B. Clelland, American Chem. Soc., Division of Petroleum Chemistry, Pittsburgh, B-130 (1966).
4. J. W. Ramsey, F. R. McDonald, and J. C. Peterson, Ind. Eng. Chem., Prod-Res. and Development, 6, 231 (1967).
5. P. A. Witherspoon and R. S. Winniford in "Fundamental Aspects of Petroleum Geochemistry", Elsevier, Princeton, N.J. (1967).
6. J. G. Speight, Fuel, 49, 76 (1970).
7. B. J. Mair in "Chemical Technology of Petroleum", W. A. Gruse and D. R. Stevens (Editors), McGraw-Hill, New York, Chapter 8 (1960).
8. T. F. Yen, A. K. T. Lee and J. I. S. Tang, Chem. Comm., 762 (1969).
9. T. F. Yen, J. G. Erdman, and S. S. Pollack, Anal. Chem., 33, 1587 (1961).
10. R. S. Winniford, J. Inst. Petroleum, 49, 215 (1963).
11. S. E. Moschopedis and J. G. Speight, Fuel, in press (1970).
12. S. E. Moschopedis and J. G. Speight, Fuel, in press (1970).
13. S. E. Moschopedis and J. G. Speight, Fuel, in press (1970).

GAS CHROMATOGRAPHIC SEPARATION OF SULFUR COMPOUNDS FROM ATHABASCA BITUMEN

H. Sawatzky, G.T. Smiley, A.E. George and D.M. Clugston

Fuels Research Centre
555 Booth Street
Ottawa, Ontario, Canada

INTRODUCTION

In this work we have attempted to develop a simple separation method for investigating the sulfur compounds in the distillable portion of the Athabasca bitumen. This involves gas chromatographic techniques using a specific sulfur detector.

The Athabasca bitumen contains very little material boiling in the gasoline and kerosene ranges. Therefore, at this time, the sulfur compounds in these fractions are not of main interest.

The sulfur compounds in the gasoline and kerosene fractions in some crude oils have been intensively investigated by the workers involved in API projects and others (1, 2, 3). The methods for separating the sulfur compounds that were developed by these workers entail numerous steps, some of which have to be repeated several times. Also, these methods become more difficult to apply as the boiling temperature of the material under investigation increases. Most of these methods of separation were developed prior to the availability of specific sulfur detectors for chromatography.

It was clear that the separation of the sulfur compounds in the Athabasca bitumen would be difficult if the classical methods were used; therefore, simpler methods were sought. We decided to attempt to develop a separation procedure that consisted of subjecting narrow distillation fractions to gas chromatographic separation techniques. The fraction that was used had a distilling temperature corresponding to 333°C at atmospheric pressure and most of the work discussed in this paper deals with this fraction.

EXPERIMENTAL

The fraction of Athabasca bitumen used for this study was obtained by iso-propanol extraction (4). This extract was distilled in a rotary film molecular still (Arthur F. Smith Inc. model 50-2) in which the liquid contacted only glass and "Teflon" at 200°C and 20 μ pressure. The distillate from the molecular still was fractionated using a spinning annular still (Nester Faust model NFA-100) at a 10:1 reflux ratio and at a reflux rate of 15 drops/min. The estimated efficiency of this still is in the range of 125-200 plates at atmospheric pressure. The fraction that was used for developing our technique distilled at a temperature of 79.5°C under 10 μ pressure which corresponds to 333°C at atmospheric pressure.

Gas Chromatographic Separations

(a) Preparative

A "Varian Aerograph" model 2100 gas chromatograph was employed for the preparative separations. Two glass columns 3/8 in. ID and 20 ft long were used. One was packed with 10% Carbowax 20M on acid washed Chromosorb W, 60-80 mesh. The temperature was programmed at 1°/min from 150 to 245°C and then held isothermally at this level. The carrier gas was nitrogen and flow rate was 200 ml/min. The effluent was split and 1/9 of it was diverted into the "Melpar" detector.

The other column was packed with 15% Hyprose [octakis (2-hydroxypropyl) sucrose] on acid washed Chromosorb W, 60-80 mesh. The temperature was programmed at 0.5°/min from 125 to 190°C at which temperature it was held isothermally. The nitrogen carrier gas flow rate was 620 ml/min. Also 1/13 of the effluent was diverted into the detector.

The effluent not passing into the detector was led into traps; each containing 0.25g of packing consisting of 10% Carbowax 20M on acid washed Chromosorb W, 60-80 mesh. The sample size for both columns were 10 μ l per run. Repetitive runs were made until the packing in the traps contained sufficient material for rechromatography. Samples of the packing in the various traps that contained the various effluent cuts were then subjected to rechromatography on the analytical gas-solid chromatographic column.

(b) Analytical

In this case the gas chromatograph was a "Tracor" model MT 220 instrument. Two columns were employed. An inorganic column consisted of a glass column 4 mm ID and 22 ft long packed with 15% lithium chloride on acid washed Chromosorb W, 60-70 mesh. The packing was prepared by adding a solution of the salt to the Chromosorb and evaporating the water by heating with stirring. The dry solid mixture was then fired at 700°C for 30 min in a muffle furnace. This mixture was packed into the column, with suction, in a dry atmosphere. During the rechromatography the temperature of this inorganic column was programmed at a rate of 1°/min from 50°C to 200°C. The flow rate of the helium carrier gas was 65 ml/min. Each injected sample consisted of 18 mg of packing containing trapped material from the preparative chromatographic step. These samples were packed into thin-walled glass capillary tubes and injected with a solid injector purchased from Hewlett Packard. The glass tubes were crushed in the injection chamber during injection. The effluent stream was split diverting 80% to a mass spectrometer and the rest to the detector.

The other analytical column used for chromatography of other distillate fractions consisted of a 2 mm ID and 20 ft long glass column packed with 5% Carbowax 20M on acid washed Chromosorb W, 60-80 mesh. The column temperature was programmed at 0.8°/min from 100°C to 220°C and then

held isothermally at this temperature. Helium was the carrier gas and its flow rate was 30 mls/min. The distillate fractions analyzed on this column were injected as 0.5 μ l samples.

(c) Detector

A "Melpar" model FPD 100 AT consisting of both flame photometric and flame ionization units was used. The photometric unit was fitted with the filter required for sulfur detection. In the chromatograms shown the term "Melpar" refers to photometric sulfur detection.

Mass Spectrometry

Low resolution mass spectrometry was performed with a CEC 21-104 instrument connected to a "Tracor" MT 220 gas chromatograph through a Biemann-Watson stainless steel enriching device.

High resolution mass spectra were obtained on a CEC 21-110 mass spectrometer using the direct inlet and the photoplate detector.

RESULTS AND DISCUSSION

A preliminary survey of organic stationary phases was made in order to find suitable phases for separating sulfur containing components. As expected, non-polar phases gave little separation but the polar phases showed considerable promise. Many polar phases were tested and Carbowax 20M appeared to be the most suitable taking into account the separation achieved over the entire chromatogram. From Fig 1 it can be seen that the major portion of the sulfur-free material is eluted first, and then the sulfur trace follows showing two humps of peaks and shoulders. Although there were some differences, all the polar phases that were tested seemed to separate on a similar basis.

The Hyprose [octakis (2- hydroxypropyl) sucrose] containing column gave the best resolution of the second hump. The sulfur chromatogram obtained with Hyprose is shown in Fig 2. Unfortunately, very poor flame ionization responses were obtained using this stationary phase. This poor response is believed to be due to deposition of material bled from the column into the detector. The temperature of the detector was limited to 170°C. When a short Carbowax 20M after column was attached, the bleeding into the detector was reduced but the response was still poor.

The chromatograms shown in Fig 1 and 2 were obtained from the preparative columns. Narrower columns of the same length did not improve resolution. Fractions were collected using both columns. However, only the results from the Hyprose column are discussed because they were superior.

As all the polar organic stationary phases that were tested appeared to separate on similar basis, it seemed unlikely that the separations would be substantially improved by rechromatography on another organic phase. References dealing with gas chromatographic separations of hydrocarbons on column packings containing

inorganic salts have appeared in the literature (5, 6, 7). It was found that these salt containing packings can be used for our bitumen fractions and they seem to separate on a basis different from the polar organic phases.

Of all the combinations of different salts and supports tested, the one containing lithium chloride on acid washed Chromosorb W appeared to be the best. Neither the salt nor the Chromosorb W alone brought about any separation. The lithium chloride, when deposited on the Chromosorb by evaporation of an aqueous solution was fairly effective, but firing the dry packing at 700°C improved the separations substantially. The salt contents were varied from 0.1% to 25% and the optimum content was found to be about 15% by weight.

The material trapped out during the preparative chromatography was rechromatographed on the column containing the lithium chloride and the Chromosorb W. Poor results were obtained from fractions trapped out during the first hump period from both preparative columns. However, much better results were obtained from fractions collected during the second hump period with the one from the Hyprose being better than from the Carbowax 20M.

The fractions 7, 8, 9, 10 and 11, shown in Fig 2 were rechromatographed on the inorganic column. When Fraction 8 which is responsible for the large peak was chromatographed, it was further resolved as shown in Fig 3. It can be seen that more sulfur-free material was separated and that there is some, though not complete, agreement between the sulfur and Flame ionization chromatograms indicating that there is some sulfur-free material present together with that containing sulfur. It should be mentioned that the "Melpar" sulfur response is not linear and is partially masked by the presence of other materials.

The sulfur rechromatograms obtained from Fractions 9, 10 and 11, are shown in Fig 4. It can be seen that some of the peaks in the chromatogram from Fraction 8 are also evident in that from Fraction 9, but there are differences as will be discussed later with the mass spectral data. It should be mentioned that the detector response obtained during the chromatography of Fraction 8, as shown in Fig 3, was actually much greater than when the chromatograms in Fig 4 were obtained indicating that there was more material in Fraction 8.

The effluent from the salt-containing column was split and 80% of it was fed into a mass spectrometer. Scans were made of all materials causing significant sulfur peaks. Inorganic gas chromatographic columns are ideal for direct coupling to mass spectrometers since the spectra do not become complicated by column bleed.

Characterization, so far, has been made only on the basis of mass spectrographic data. From the data obtained from the low resolution mass spectrometer coupled with the gas chromatograph it was not possible to ascertain which of the ions contained sulfur. Therefore a sample of Fraction 8 as shown in Fig 2 was analyzed by high resolution mass spectrometry. The two most abundant parent ions had m/e ratios of 218.11380 and 212.15593 which correspond to empirical formulae of $C_{14}H_{18}S$ and $C_{16}H_{20}$ with errors of +0.00088 and -0.00056 respectively. There also were two minor parent ions with m/e ratios of 232.12764 and 226.17113 and these correspond

held isothermally at this temperature. Helium was the carrier gas and its flow rate was 30 mls/min. The distillate fractions analyzed on this column were injected as 0.5 μ l samples.

(c) Detector

A "Melpar" model FPD 100 AT consisting of both flame photometric and flame ionization units was used. The photometric unit was fitted with the filter required for sulfur detection. In the chromatograms shown the term "Melpar" refers to photometric sulfur detection.

Spectrometry

Low resolution mass spectrometry was performed with a CEC 21-104 instrument connected to a "Tracor" MT 220 gas chromatograph through a Biemann-Watson stainless steel enriching device.

High resolution mass spectra were obtained on a CEC 21-110 mass spectrometer with the direct inlet and the photoplate detector.

RESULTS AND DISCUSSION

A preliminary survey of organic stationary phases was made in order to find suitable phases for separating sulfur containing components. As expected, non-polar phases gave little separation but the polar phases showed considerable promise. Several polar phases were tested and Carbowax 20M appeared to be the most suitable. Taking into account the separation achieved over the entire chromatogram. From this it can be seen that the major portion of the sulfur-free material is eluted first, and then the sulfur trace follows showing two humps of peaks and shoulders. Although there were some differences, all the polar phases that were tested seemed to separate on a similar basis.

The Hyprose [octakis (2-hydroxypropyl) sucrose] containing column gave the best resolution of the second hump. The sulfur chromatogram obtained with Hyprose is shown in Fig 2. Unfortunately, very poor flame ionization responses were obtained with this stationary phase. This poor response is believed to be due to deposition of material bled from the column into the detector. The temperature of the detector was limited to 170°C. When a short Carbowax 20M after column was attached, the flow of sulfur into the detector was reduced but the response was still poor.

The chromatograms shown in Fig 1 and 2 were obtained from the preparative columns. Narrower columns of the same length did not improve resolution. Fractions were collected using both columns. However, only the results from the Hyprose column are discussed because they were superior.

As all the polar organic stationary phases that were tested appeared to separate on a similar basis, it seemed unlikely that the separations would be substantially improved by rechromatography on another organic phase. References dealing with chromatographic separations of hydrocarbons on column packings containing

-26-

inorganic salts have appeared in the literature (5, 6, 7). It was found that these salt containing packings can be used for our bitumen fractions and they seem to separate on a basis different from the polar organic phases.

Of all the combinations of different salts and supports tested, the one containing lithium chloride on acid washed Chromosorb W appeared to be the best. Neither the salt nor the Chromosorb W alone brought about any separation. The lithium chloride, when deposited on the Chromosorb by evaporation of an aqueous solution was fairly effective, but firing the dry packing at 700°C improved the separations substantially. The salt contents were varied from 0.1% to 25% and the optimum content was found to be about 15% by weight.

The material trapped out during the preparative chromatography was rechromatographed on the column containing the lithium chloride and the Chromosorb W. Poor results were obtained from fractions trapped out during the first hump period from both preparative columns. However, much better results were obtained from fractions collected during the second hump period with the one from the Hyprose being better than from the Carbowax 20M.

The fractions 7, 8, 9, 10 and 11, shown in Fig 2 were rechromatographed on the inorganic column. When Fraction 8 which is responsible for the large peak was chromatographed, it was further resolved as shown in Fig 3. It can be seen that more sulfur-free material was separated and that there is some, though not complete, agreement between the sulfur and flame ionization chromatograms indicating that there is some sulfur-free material present together with that containing sulfur. It should be mentioned that the "Melpar" sulfur response is not linear and is partially masked by the presence of other materials.

The sulfur rechromatograms obtained from Fractions 9, 10 and 11, are shown in Fig 4. It can be seen that some of the peaks in the chromatogram from Fraction 8 are also evident in that from Fraction 9, but there are differences as will be discussed later with the mass spectral data. It should be mentioned that the detector response obtained during the chromatography of Fraction 8, as shown in Fig 3, was actually much greater than when the chromatograms in Fig 4 were obtained indicating that there was more material in Fraction 8.

The effluent from the salt-containing column was split and 80% of it was fed into a mass spectrometer. Scans were made of all materials causing significant sulfur peaks. Inorganic gas chromatographic columns are ideal for direct coupling to mass spectrometers since the spectra do not become complicated by column bleed.

Characterization, so far, has been made only on the basis of mass spectrographic data. From the data obtained from the low resolution mass spectrometer coupled with the gas chromatograph it was not possible to ascertain which of the ions contained sulfur. Therefore a sample of Fraction 8 as shown in Fig 2 was analyzed by high resolution mass spectrometry. The two most abundant parent ions had m/e ratios of 218.11380 and 212.15593 which correspond to empirical formulae of $C_{14}H_{18}S$ and $C_{16}H_{20}$ with errors of +0.00088 and -0.00056 respectively. There also were two minor parent ions with m/e ratios of 232.12764 and 226.17113 and these correspond

to the formulae $C_{15}H_{20}S$ and $C_{17}H_{22}$ with errors of -0.00093 and $+0.00101$ respectively.

On the basis of these formulae it would appear that the most likely sulfur compounds in Fraction 8 consist mainly of isomeric benzothiophenes with six, and to a lesser extent, seven carbons in side chains. All the significant fragment ions that would be expected from these benzothiophenes were observed. The ions that appeared to be sulfur-bearing had m/e ratios of 217, 203, 189, 175, 161 and 147.

The sulfur-free parent ions would appear to be naphthalenes with 6 or 7 carbons in side chains. The sulfur-free fragment ions had m/e ratios of 197, 183, 169, 155 and 141. These are the ones expected for such naphthalenes.

The salt containing column seemed to cause some separation of isomers of both the benzothiophenes and the naphthalenes. Considerable hydrocarbon material was separated from the benzothiophenes but some still remained. When Fraction 8 was rechromatographed the most abundant sulfur-bearing ions had m/e ratios of 189 and 175 in the majority of scans. This might be interpreted as due to the presence of benzothiophenes with propyl and butyl side chains. In a few scans the ion with m/e ratio of 203 was quite abundant and in only one scan was the 217 ion prominent. The 161 ion was less prominent and the 147 considerably less, and sometimes not distinguishable from the background.

During rechromatography of Fraction 8 there appeared to be a minor series of ions that had not been noted in the high resolution mass spectra. The parent ions of this series had m/e ratios of 228 and 214 with the latter being the most abundant. The fragment ions had m/e ratios of 213, 199, 185, 171, 157, 143 and 129. Possibly these ions might have been derived from indenenes with 7 and 8 carbon atoms in side chains.

The benzothiophenes, naphthalenes and to some extent the indenenes appeared to persist during the rechromatography of Fractions 9, 10 and 11. It was noted that with the exception of the scans taken at E and F during rechromatography of Fraction 9 the main sulfur-bearing ion had a m/e ratio of 161. This indicates that the material in Fraction 9 was different from that in Fraction 8 although there was some overlapping. This 161 ion was not very prominent in Fractions 10 and 11.

During the later stages of rechromatography of Fraction 9 and then during rechromatography of 10 and 11 another ion series became evident. The parent ion had a m/e ratio of 210 and fragment ions were found at m/e ratios of 195 and 181. Possibly these ions might be derived from naphthalenes substituted with a third non-aromatic ring.

Unfortunately at this time there is insufficient mass spectral data on benzothiophenes for more comprehensive structure assignment. The fact that the naphthalenes and indenenes appeared to accompany the benzothiophenes is not considered a major problem. These hydrocarbons did not interfere with mass spectroscopy of the sulfur

compounds. Also, they would not be expected to interfere with characterization involving desulfurization because the products from sulfur compounds would be of lower molecular weight than the hydrocarbons. Also, these accompanying hydrocarbons must be similar to the sulfur compounds and can be considered as an aid in characterization.

The fact that a single chromatographic separation on Hyprose separated the benzothiophenes from the other sulfur compounds is considered to be a major achievement. Other workers (8), after a lengthy series of treatments, arrived at an inseparable mixture of benzothiophenes and naphthalenes. But these were of lower molecular weight and had fewer isomers than the benzothiophenes discussed in this presentation. Thus we have had some success in finding a method for separating sulfur compounds that is much simpler than those developed prior to the availability of specific sulfur detectors for gas chromatography.

Similar gas chromatographic separations can be applied to higher boiling fractions as shown in Fig 5.

CONCLUSIONS

A single gas chromatographic separation of a 333°C boiling distillate fraction of Athabasca bitumen on a Hyprose-Chromosorb W column could isolate the major portion of what appeared to be benzothiophenes with 6 and 7 carbon atom side chains from the other sulfur compounds.

Several peaks were obtained; all of them appearing to be due to benzothiophenes. Rechromatography of the fractions causing the sulfur peaks on a salt-containing column further resolved the apparent benzothiophenes. At the present time the bases for these separations are not clear.

ACKNOWLEDGMENT

The authors are indebted to Dr. D.S. Montgomery for helpful suggestions and discussions. Also, they wish to thank Dr. D.B. MacLean of McMaster University for the high resolution mass spectra.

REFERENCES

1. Drushel, H.V., "Sulfur Compounds in Petroleum", ACS Div. Petroleum Chem., Preprints 15 (2), C - 13 (1970)
2. Coleman, H.J., Hopkins, R.L., and Thompson, C.J. "Highlights of Some 50 Man Years of Petroleum Sulfur Studies at the Bureau of Mines", ACS Div. Petroleum Chem., Preprints 15 (3), A-17 (1970)
3. Dean, R.A., and Whitehead, E.V. "Status of Work in Separation and Identification of Sulfur Compounds in Petroleum and Shale Oil", Proceedings of the Seventh World Petroleum Congress 2, 165 (1967)

4. Millson, M.F., "An Investigation of the Asphaltenes from the Athabasca Tar Sand", Mines Branch Report FD 67/84-RBS
5. Geiss, F., Versino, B., and Schlitt, H., *Chromatographia* 1, 9 (1968)
6. Versino, B., and Geiss, F., *Chromatographia* 2, 354 (1969)
7. Gump, B.H., *J. Chromatographic Science* 7, 755 (1969)
8. Hopkins, R.L., Coleman, H.J., Thompson, G.J., and Rall, H.T., *Anal. Chem.* 41, 2041 (1969)

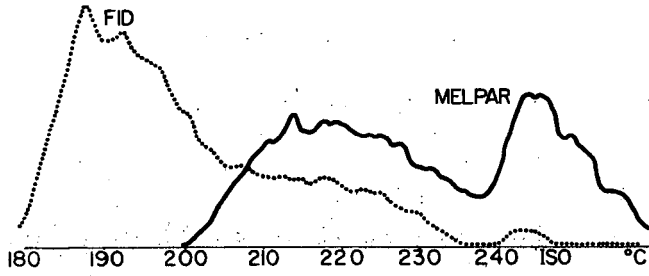


Figure 1. Chromatography Separation on Preparative Carbowax 20M Column

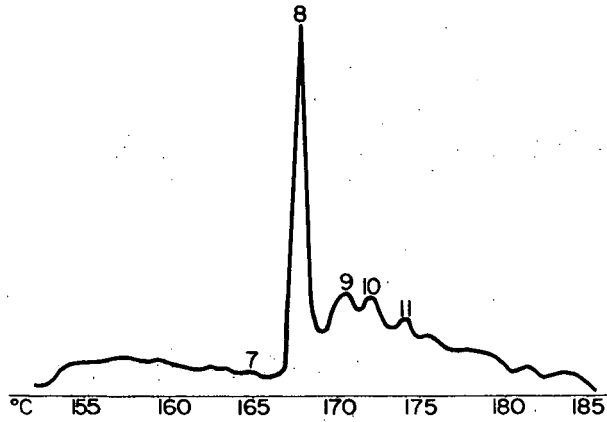


Figure 2. Separation on Preparative Hyprose Column

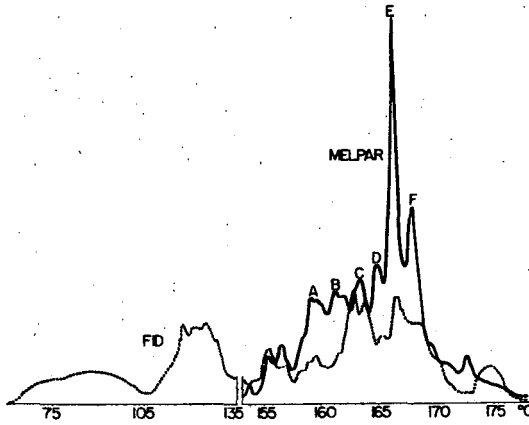


Figure 3. Rechromatography of Fraction 8 (Figure 2) on LiCl-Chromosorb W Column

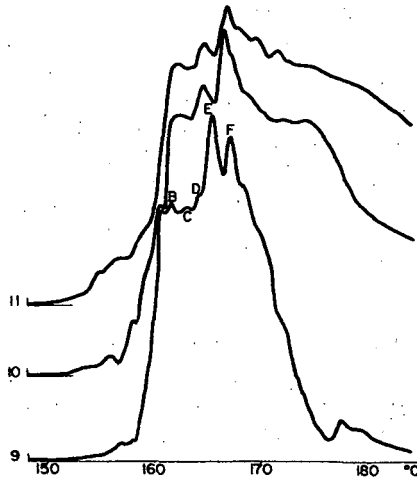


Figure 4. Rechromatography of Fraction 9, 10 & 11 (Figure 2) on the LiCl-Chromosorb W Column

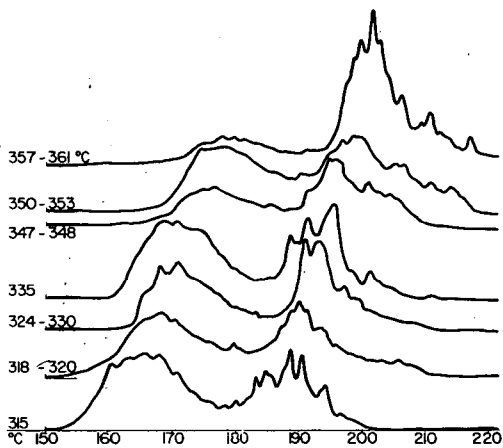


Figure 5. Sulfur Chromatograms of Various Distillate Fractions
(Analytical Carbowax 20 M Column)

THE STRUCTURE OF BITUMENS: CHARGE-TRANSFER NATURE

Teh Fu Yen

University of Southern California
2025 Zonal Avenue
Los Angeles, California 90033

Introduction

Most recently, we have been able to use the technique of electron spin resonance (ESR) (1,2) to elucidate the structure of native bitumens and have been able to reclassify the natural bitumens according to the differences in structure. The present work represents a portion of the continuous effort toward the correlation of structural features with the chemical and physical properties of these naturally occurring macromolecules.

X-ray diffraction (3,4), graphic densimetric methods (5,6), mass spectrometry (7,8,9), and ESR (9,10,11) have been used to show that naturally occurring bitumens contain large, fused-ring aromatic systems associated in stacked arrays. Generally, these aromatic systems consist of 2-dimensional disc-like planes, having a layer diameter ranging from 8.5-15.0 Å. These measurements correspond to the sizes of peri-condensed polynuclear aromatic hydrocarbons (PAH) of approximately 7-18 ring systems. Carbon chains assuming a zig-zag configuration are substituted on the edges of these individual planar discs in such a manner as to resemble those of paracyclophane molecules. These discs are associated in crystallites consisting of 5 or 6 layers in a stack with interlayer distances varying from 3.4-3.7 Å. These graphite-like crystallites are randomly distributed (although oriented) over a continuous mesomorphic media which contains both naphthenic and aliphatic structures (4,7).

Most of the molecules in the asphaltene fractions of bitumens are alkyl-substituted polycarbocyclic hydrocarbons (13). As to the resin or maltene fraction, most of its molecules contain heterocyclic systems and exhibit polarity due to functional substituents (8,14). Among the most frequently occurring and typical of these heteroaromatics is the petroporphyrin (15), an 18-diaza-annulene system (4). Hence, bitumens can be considered as being composed of polycyclic aromatic compounds bearing different functional groups. These individual components possess varying degrees of charge-transfer ability depending upon their relative donor or acceptor abilities.

For asphaltics, it has been possible to intercalate (16) a known acceptor such as iodine between the layers of alkyl-substituted polyaromatic systems which behave as donors. Experimentally, the interlayer distance of an iodine asphaltic complex increases from 3.5 Å to 8.7 Å, corresponding to the separation formed from the insertion of an axially intercalated iodine molecule (4x1.33 Å). Other evidence supporting this observation includes the occurrence of the 1080 cm^{-1} infrared donor-acceptor band, the increase in spin concentration of the iodine asphaltic complex and lowering of resistivity and gap energy in electrical measurements.

Up to the present, little work on the charge-transfer properties of bitumens has been published. This investigation represents the first reported experimental attempt at using infrared methods to study the charge-transfer characteristics of the polyaromatic molecules and to reveal the nature of their association within the bitumens.

Experimental

The asphaltene and resin fractions of bitumens were prepared by the conventional pentane/propane precipitation method described in an earlier paper (3).

The donor-acceptor complexes were made by dissolving the donor and the acceptor in boiling benzene; the molar ratio of acceptor to donor was, in all cases, 1 or slightly greater than 1. The reaction mixture was allowed to stand at room temperature for 24-48 hours to permit the separation of a solid. The product was then isolated, thoroughly washed with benzene and its melting point determined and checked with a literature value when available. The spectra were obtained with a Beckman IR-12 double beam instrument. For solid phase measurements, films, Nujol mulls, and potassium bromide pellets were prepared in the conventional fashion. Sets of matched cells of fixed thicknesses were used, for solution determinations, and, at the concentrations employed (0.50-0.25 g/ml), measurements were consistent with Beer's Law. High or intermediate resolution settings were used for scanning. The estimated error in the wavenumber based on repeated scans was $\pm 1 \text{ cm}^{-1}$.

Results

When bitumens are examined in the $1,000-625 \text{ cm}^{-1}$ region ($10-16\mu$), four bands located at approximately 865, 815, 760, and 730 cm^{-1} are observed. Examples of such spectra are shown in Fig. 1 and are represented by a visbreaker tar, two asphaltene fractions, and one resin fraction. These observations are generally unique to the naturally occurring or altered bitumens (17). The first three bands correspond closely to those for aromatic C-H out-of-plane bending vibrations (isolated, 2- and 3-adjacent C-H bonds), whereas the fourth band, occurring at a shoulder at $731-720 \text{ cm}^{-1}$, appears to be due to in-plane methylene rocking vibrations (18) of paraffinic nature.

Table I

OBSERVED SHIFT OF FREQUENCIES OF BENDING VIBRATIONS
FROM A WEST TEXAS ASPHALTIC IN VARIOUS MEDIA

<u>Media</u>	<u>Number of Bands</u>				<u>ϵ</u>	<u>$(\epsilon-1)/(2\epsilon+1)$</u>
	<u>(cm^{-1})</u>					
	<u>(1)</u>	<u>(2)</u>	<u>(3)</u>	<u>(4)</u>		
Film	874	816	753	724		
n-Hexane	873	815	752	----*	1.925	0.19
Carbon disulfide	873	816	755	725	2.641	0.26
1-Iododecane	876	816	---	---	3.93**	0.33
Chloroform	881	---	---	---	4.806	0.36
n-Heptyl acetate	---	---	767	---	4.81**	0.36
Methyl iodide	---	---	760	---	7	0.40
Benzonitrile	880	823	---	---	25.58	0.49

*Dashed line represents dead regions.

**Approximated values from homologous series.

The results summarized in Table I show the effect of the dielectric constant of solvents on the positions of the four bands as compared with the reference spectrum for the solid phase (without solvent) for a bitumen resin fraction. The sample was differentially scanned in the presence of seven solvents of varying degrees of polarity: n-hexane, carbon disulfide, 1-iododecane, chloroform, n-heptyl acetate, methyl iodide, and benzonitrile. When compared to the spectrum of a solid portion of this sample, shifts toward the blue were observed for the first three bands; these represent the aromatic C-H bending vibration (in this region,

there is no absorption by the solvents). No significant displacement was observed for the fourth band (methylene rocking). Spectra obtained in this manner were exemplified by 1-iododecane, as shown in Fig. 2. The shift of the first three bands becomes larger as the dielectric constant of the polar medium increases.

The extent of the shift becomes more striking when the sample is allowed to react with complexing reagents such as nitro- or cyano-bearing acceptors (picric acid, s-trinitrobenzene, p- or m-dinitrobenzene, tetracyanoethylene). Since the composite aromatic system in bitumens does not form well-defined complexes, a simple technique had to be devised for forming the donor-acceptor charge-transfer complex in situ. This was accomplished by adding the donor to an excess of the acceptor in a solvent and scanning the resulting solution against the pure acceptor in the same solvent. This procedure was tested with perylene and s-trinitrobenzene in a nitrobenzene-carbon disulfide solution and shown to yield peaks identical in position to those found with the Nujol mull scan of the solid complex of perylene-s-trinitrobenzene as shown in Fig. 3 (772 cm^{-1} instead of 773 cm^{-1} from the solid sample; 818 cm^{-1} instead of 821 cm^{-1} from the solid sample).

In this fashion, it was possible to obtain satisfactory spectra for different fractions of bitumens. Fig. 4 summarizes the results of these spectra for three different complexing media (5% tetracyanoethylene in benzonitrile; 2.5% s-trinitrobenzene in 1:10 nitrobenzene-carbon disulfide; 2.5% m-dinitrobenzene in 1:10 nitrobenzene-carbon disulfide) and one non-complexing solvent (methyl iodide). A similar shift pattern was also observed for a Wafra asphaltene in three different media (Fig. 5). The shifts were as anticipated, although, however, the bands became broader. The dashed line in Fig. 2 represents the "dead region" of the media (region of solvent absorption interferences).

Table II

Sample	Band Number	Solid Matrix	10% $\text{NO}_2\phi^1$ in carbon disulfide	5% TCE ² in benzo-nitrile	2.5% ₃ s-TNB ³	2.5% ₄ m-DNB ⁴	2.5% ₅ p-DNB ⁵	2.5% ₆ PA ⁶
					in $\text{NO}_2\phi$ -carbon disulfide (1:10)			
West								
Texas	(1)	874	891	886	885	890	890	887
Resin	(2)	816	825	835	822	828	825	825
	(3)	753	764	---	762	867	762	765
	(4)	724	727	---	726	---	727	---
Baxterville								
Resin	(1)	870	---	---	885	---	---	---
	(2)	812	---	---	824	---	---	---
	(3)	750	---	---	766	---	---	---
	(4)	725	---	---	---	---	---	---
Raudhatain								
Asphaltene	(1)	866	869	---	873	---	873	---
	(2)	817	823	---	820	---	824	---
	(3)	757	765	---	759	---	765	---
	(4)	732	730	---	---	---	---	---

1. Nitrobenzene
2. Tetracyanoethylene
3. s-Trinitrobenzene
4. m-Dinitrobenzene
5. p-Dinitrobenzene
6. Picric acid

Fractions of other bitumens gave similar results as indicated in Table II. The displacement for the first three bands was 10-15 cm^{-1} , while that for the fourth band was only 2-3 cm^{-1} . The extent of the shift of aromatic C-H bending vibration bands is of the same order of magnitude as observed for those of pure PAH (18,19). One such example is provided by the perylene-s-trinitrobenzene complex as shown in Fig. 3. The C-H bending of perylene shifted toward the blue from 767 cm^{-1} (3- γ) to 733 cm^{-1} . On the other hand, the C-H bending of the acceptor, s-trinitrobenzene shifted toward the red from 922 cm^{-1} (1- γ) to 909 cm^{-1} .

Discussion

The polyaromatic systems within the bituminous structures undergo charge-transfer processes readily. In the presence of a known acceptor, the aromatic system usually behaves as a donor; this is due to the fact that asphaltic molecules bear numerous short alkyl chains such as methyl or ethyl groups (13), which are known to be electron releasing. Association due to the π - π overlap usually occurs when there is a charge-transfer from a π -donor to a π -acceptor. Charge-transfer may occur to varying degrees, the extreme case being the formation of two separate ions.

The frequency shift of an absorption band arising from a substance in solution can normally be predicted by the Kirkwood-Bauer-Magat (KEM) rule, which states that the shift, $-\Delta\mu/\mu$, proportional to $(n^2-1)/(2n^2+1)$, $(\epsilon-1)/(2\epsilon+1)$ where n is the refractive index and ϵ is the dielectric constant of the solvent. In this manner, a red shift is expected, since both n and ϵ are greater than unity. The KEM relation was based on the concept of non-localized interactions between a simple oscillating dipole (solute) and an electric field within a spherical cavity, in a continuous dielectric (solvent). On the other hand, Kientz (20) and La Lau (21) have independently found that the aromatic C-H bending bands of aromatics in polar solvents are shifted in a direction opposite to that predicted by the KEM relation. They have explained their blue shift data on the basis of localized electrostatic interaction. The observations of the blue shifts reported in Table I are in agreement with those of Kientz and La Lau and are also consistent with the results obtained from pure PAH investigations (18). Localized interactions in a given charge-transfer process, involving π - π systems, are to be anticipated.

Hence, the strong effect of the frequency shift in the case of complexing media in Fig. 2 can be explained on the basis of an even stronger localized interaction between the donor and acceptor molecules. The energy for the donor-acceptor charge-transfer process usually consists of the ionization potential of the donor and the electron affinity of the acceptor; in terms of the molecular orbital theory (MO), the energy may be expressed as the difference between that of the highest, filled MO of the donor and the lowest, filled MO of the acceptor. The blue shift for the donor and the red shift for the acceptor have been found for PAH (19). For a given acceptor, the frequency shifts of the donors are proportional to their molecular orbital m -values. Presumably, in a charge-transfer process which is associated with a partial removal of electrons from the bonding orbitals of the donor to the antibonding orbitals of the acceptor, the change in vertical energy not only affects the extinction coefficient of a vibrational band, but also influences the force constant of certain modes.

The polyaromatic systems in bitumens consist of alkyl-substituted polynuclear aromatics, π -deficient heteroaromatics, π -excessive heteroaromatics and, electro-negatively substituted aromatics, etc. The association of polyaromatics can be visualized as a close approach of two different aromatic systems; for example, π -deficient and π -excessive heteroaromatic molecules. It is yet possible that there are associations between molecules of the same type e.g., the fully alkyl-substituted aromatics and the less alkyl-substituted aromatics. This type of π - π association

is the cause of stack formation in bitumens as observed by x-ray diffraction, both in high angle (4) and in low angle (22) ranges.

In general, molecular interaction is favored by the close proximity of orderly packed rod- or disc-shaped molecules. For mononuclear homocyclic aromatics (benzenes), optimum interaction is achieved when the molecules are in stacked positions so that the charge clouds can be superimposed. The layer-like configuration of the aromatic moiety in paracyclophanes having short folding polymethylene bridges, and for isotactic polystyrenes is achieved through the interannular interactions of π -electrons such that the flexibility of the polymethylene chains is inhibited, e.g., 3_1 -helix.

Since porphyrins are present in the composites of bitumens (14), a study of the nature of metalloporphyrins occurring in bitumens (11,23,24,25) could probe the nature of association among various aromatic molecules within bitumens. By ESR methods, the temperature dependence of the anisotropy of the vanadium hyperfine structures in different polar media results in a dissociation energy of approximately 10-14 kcal (26). Similarly, dissociation energy of the vanadyl stretching mode is about 17 kcal (27). This order of dissociation energy is a measure of the extent of association of the porphyrin (free) with other polyaromatic systems (fixed or bound) in bitumens. Very recently, the observation of nitrogen superhyperfine structures of vanadium chelates in bitumens also suggest the presence of this type of association behavior (12). In order to separate vanadyl porphyrin from polyaromatic molecules in bitumens, both elevated temperature and a polar solvent are required (28,29).

Many colloidal characteristics of bitumens such as its gel-sol conversion, temperature coefficient of viscosity, complex flow, and micelle stability, etc. may be explained on the basis of the charge-transfer nature of individual aromatic systems throughout the macrostructure (30,31). Consequently, the inter- and intra-cluster associations not only affect processing, treatment, and refining, but are also relevant to the problems concerning pollution, recovery, geochemistry, and genesis of all bituminous materials (32).

Acknowledgement

Partial support of a Gulf Grant is gratefully acknowledged. Thanks are due to James Tang, Albert Lee, and Steve Sprang for their assistance.

References

1. T. F. Yen and G. Sprang, ACS, Div. Petroleum Chem. Preprints 15(3), A65-A76 (1970).
2. T. F. Yen, Chemistry in Space Research, R. F. Landel and A. Rembaum, editor, Elsevier Publishing Company, New York, New York, 1971, in print.
3. T. F. Yen, J. G. Erdman, and S. S. Pollack, Anal. Chem. 33, 1587 (1961).
4. T. F. Yen and J. G. Erdman, Encyclopedia of X-rays and Gamma-Rays, G. L. Clark, editor, Reinhold Publishing Corporation, New York, 1963, pp. 65-68.
5. T. F. Yen, J. G. Erdman, and W. E. Hanson, J. Chem. Eng. Data 6, 443 (1961).
6. T. F. Yen and J. P. Dickie, J. Inst. Petroleum 54, 50 (1968).
7. J. P. Dickie and T. F. Yen, Anal. Chem. 39, 1847 (1967).
8. J. P. Dickie and T. F. Yen, ACS, Div. Petroleum Chem., Preprints 13(2), F140-F143 (1968).
9. J. P. Dickie and T. F. Yen, J. Mass Spectroscopy 1, 501 (1963).

10. T. F. Yen, J. G. Erdman, and A. J. Saraceno, Anal. Chem. **34**, 694 (1962).
11. L. J. Boucher, E. C. Tynan, and T. F. Yen, Electron Spin Resonance of Metal Complexes, T. F. Yen, editor, Plenum Publishing Corp., New York, New York, 1969, pp. 111-130.
12. T. F. Yen, E. C. Tynan, G. B. Vaughan, and L. J. Boucher, Spectrometry of Fuels, R. A. Friedel, editor, Plenum Publishing Corp., New York, New York, 1970, Chap. 14, pp. 187-201.
13. T. F. Yen and J. G. Erdman, ACS, Div. Petroleum Chem., Preprints **7(3)**, 99-111 (1962).
14. T. F. Yen, L. J. Boucher, J. P. Dickie, E. C. Tynan, and G. B. Vaughan, J. Inst. Petroleum **55**, 87 (1969).
15. E. W. Baker, T. F. Yen, J. P. Dickie, R. E. Rhodes, and L. F. Clark, J. Am. Chem. Soc. **89**, 3631 (1967).
16. G. A. Sill and T. F. Yen, Fuel (London) **43**, 61 (1969).
17. T. F. Yen and J. G. Erdman, ACS, Div. Petroleum Chem., Preprints **7(1)**, 5-18 (1962).
18. T. F. Yen, A. K. T. Lee, and J. I. S. Tang, J. Chem. Soc., D, Chem. **7**, 762 (1969).
19. T. F. Yen, A. K. T. Lee, and J. I. S. Tang, ACS Southwest Regional Conference, Anaheim, California, October 1969.
20. H. Kienitz, Naturwiss **42**, 511 (1955).
21. C. La Lau, Spectrochim Acta **14**, 181 (1959).
22. S. S. Pollack and T. F. Yen, Anal. Chem. **42(6)**, 623 (1970).
23. L. J. Boucher, E. C. Tynan, and T. F. Yen, Inorg. Chem. **7**, 731 (1968).
24. L. J. Boucher and T. F. Yen, Inorg. Chem. **7**, 2665 (1968).
25. L. J. Boucher, D. E. Bruins, and T. F. Yen, and D. L. Weaver, J. Chem. Comm. **7**, 363 (1969).
26. E. C. Tynan and T. F. Yen, Fuel (London) **43**, 191 (1969).
27. F. E. Dickson and L. Petrakis, J. Phys. Chem. **74**, 2850 (1970).
28. J. H. Rho, A. J. Bauman, T. F. Yen, and J. Bonner, Science **167**, 754 (1970).
29. J. H. Rho, A. J. Bauman, T. F. Yen, and J. Bonner, Proceedings of the Apollo 11 Lunar Science Conference, Vol. 2, Pergamon Press, New York, 1970, pp. 1920-1932.
30. J. P. Dickie, M. N. Haller, and T. F. Yen, J. Colloid & Interface Sci. **29**, 475 (1969).
31. G. B. Vaughan, E. C. Tynan, and T. F. Yen, Chem. Geol. **6(3)**, in print, 1970.
32. T. F. Yen and S. R. Silverman, ACS, Div. Petroleum Chem., Preprints **14(3)**, E22-E39 (1969).

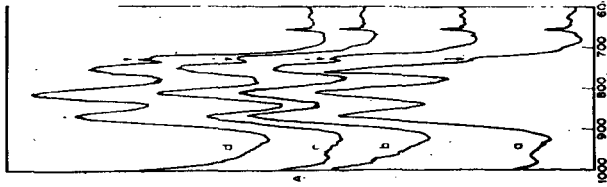
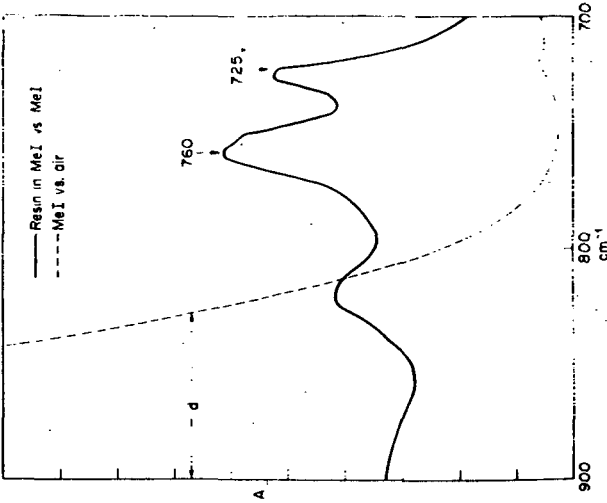


Fig. 1. Typical Bending and Rocking Vibrations of

Some Bitumens:

- a. Asphaltene from Kuwait Visbreaker Tar
- b. Asphaltene from Mara Crude
- c. Resin from Baxterville Crude
- d. Asphaltene from Raudhatain Crude

(Spectra for asphaltic sample in carbon disulfide vs. carbon disulfide, r is methylene rocking, numbers in parentheses are 1, isolated; 2, 2-adjacent; 3, 3-adjacent C-H bending).

Fig. 2. Typical Infrared Differential Spectrum for a West Texas Resin in Methyl Iodide

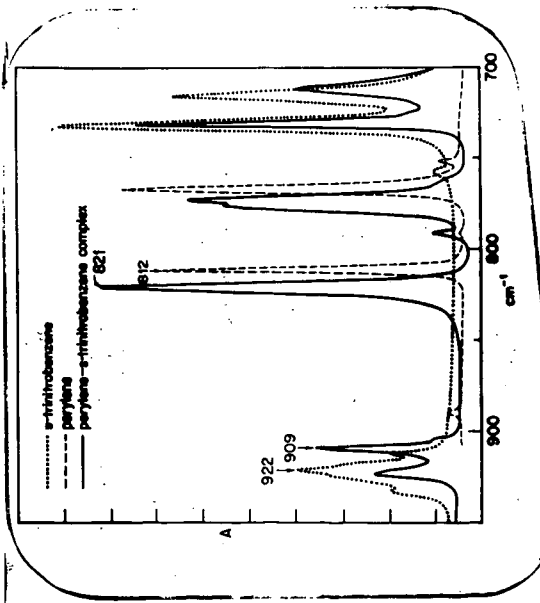


Fig. 3. Infrared Spectra of a Typical Donor-Acceptor Charge-Transfer Complex in the Bending Region (Nujol Mull)

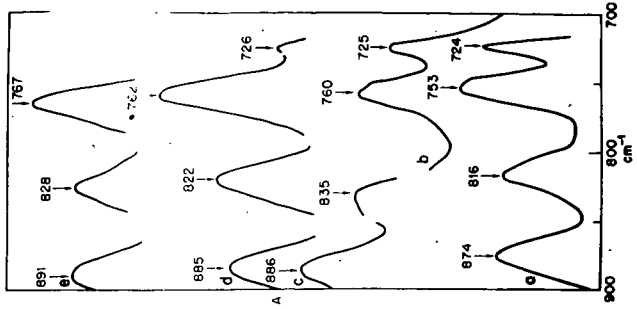


Fig. 4. Differential Infrared Spectra of a Resin Fraction from a West Texas Crude in
 a. Nujol
 b. Methyl Iodide
 c. 5% Tetracyanoethylene in Benzonitrile
 d. 2.5% s-Trinitrobenzene in Nitrobenzene-Carbon Disulfide (1:10)
 e. 2.5% m Dinitrobenzene in Nitrobenzene-Carbon Disulfide (1:10)
 (The discontinued line represents the "dead" region of the media)

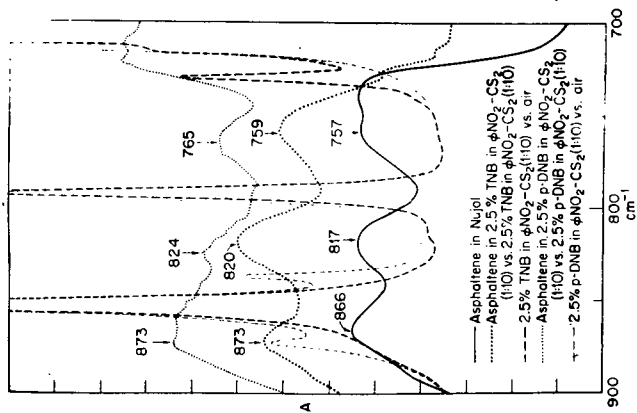


Fig. 5. Differential Infrared Spectra of the Asphaltene Fraction from a Wafra Heavy Residua in Different Complexing Media

Milligram Scale Automatic Preparative GLC of the Steranes
and Triterpanes Isolated from Green River Formation Oil Shale

E. Gelpi, P. C. Wszolek, E. Yang, and A. L. Burlingame

Space Sciences Laboratory
University of California, Berkeley, California 94720

Introduction

To the organic geochemist the study of the cyclic hydrocarbon fraction extractable from the Green River Formation Oil Shale is both a multifaceted challenge and a promising reward: A challenge in that to secure meaningful information from the very complex mixture of isomeric hydrocarbons in the Green River bitumens (1), he must make use of the most efficient and sophisticated separation and identification techniques; and a reward in that the complete structural characterization of such a unique array of alicyclic hydrocarbons will allow, through the concept of "molecular fossils" (2), a better understanding of the ecological setting at the time the sediment was laid down (3). Although much work has been done in this area in the past five years (1, 4-8) only a few of the major constituents in the range C_{27} - C_{31} have been identified. Included in the list are the 5α - and 5β - isomers of the C_{27} , C_{28} and C_{29} tetracyclic steranes (1,4,5,7,8) and a few isomeric pentacyclic triterpanes with empirical formulas, $C_{30}H_{52}$, $C_{30}H_{56}$, $C_{29}H_{50}$, $C_{31}H_{54}$ (4-7). However, most of these identifications are still tentative and as a consequence the stereochemical configurations of the molecules are not known. This is due to the difficulties encountered in resolving the whole mixture, especially each group of isomers into individual components. The most versatile technique in this field has been the combination of the gas chromatograph with the mass spectrometer (1,7), but even in cases where GLC gives the necessary resolution, structural assignment from the MS data alone can be rather ambiguous particularly among the different isomeric forms.

The approach followed in this work (9) rests first of all on the determination of the optimum operating GLC parameters for preparative collection, in the highest purity possible, of any preselected compound. This will allow complete structural characterizations by other spectrometric methods, such as C^{13} NMR or x-ray diffraction.

Experimental

A. Sample description and treatment. The sample used in this work originated at the Colony Mine, 15 miles N.W. of Grand Valley, Colorado. About 17.5 Kg were pulverized in a ball-mill for 10 days and then extracted ultrasonically twice (15-30 minutes each time), with a mixture of benzene-methanol (2:1). The bitumen fraction thus extracted weighed 250 g which represents a recovery of 1.4% of the total.

B. Separation of the acidic fraction. The extract was sonicated and saponified with 1.5 liters of 2M KOH/methanol for 3 hours. The resulting basic solution was extracted with n-heptane (300-450 ml) and then washed with water to remove the acids.

C. Separation of the basic fraction. The heptane fraction was washed with 700 ml of 6N HCl and then again with water to remove the basic components.

D. Column Chromatography. After removal of the acidic and basic fractions the remaining heptane extract was chromatographed on a column of activated Al_2O_3 (37.5 cm high by 4.5 cm i.d.). Heptane, benzene and methanol were used sequentially in order to separate the non-polar aliphatic-alicyclic hydrocarbons, from the aromatic and other polar lipid components. Three cuts of 300 ml each were obtained for the heptane eluate. Cuts No. 2 and 3 were found to be enriched in the aliphatic and alicyclic fractions respectively.

E. Digestion with molecular sieves. Both cuts 2 and 3 (dissolved in benzene) were treated with 5 A molecular sieves (10) for three days under reflux, to separate the straight chain from the branched and cyclic hydrocarbons.

F. Thiourea adduction. The resulting branched-cyclic fraction was adducted with thiourea according to the following procedure (5). The branched-cyclic hydrocarbons were dissolved in 700 ml of chloroform before the addition of a saturated solution of thiourea in 700 ml of methanol. The resulting mixture was heated until it was homo-

genous, cooled, and kept at room temperature for one day. Thiourea adduct needles fell out of solution on cooling, and these were later collected, rinsed with cold chloroform and dissolved in water. The water solution was then extracted three times with heptane. The thiourea adduction was repeated once on the supernatant solution so that the overall treatment yielded a combined adduct fraction enriched in the 5 α -steranes and a non-adduct fraction enriched in the 5 β -steranes and the triterpanes (9).

G. Liquid gel-filtration chromatography. About two gr of the total non-adduct were chromatographed on Sephadex LH:20 to partially separate the 5 β -steranes from the triterpanes. Details of this step have been presented elsewhere (9).

H. Gas-liquid chromatograph. All of the packed columns were prepared with short lengths of 316 stainless steel tubing purchased from the Perkin-Elmer Corp., Norwalk, Connecticut. The columns were packed under vibration and beating (11) and conditioned at 290°C until ready for use. The stationary phases and supports were purchased from: 5% SE-30 (methyl silicone) on 100-120 Varaport 30 and 3% SE-30 on 80/100 Aeropak: Varian Aerograph, Walnut Creek, California; 3% SE-30 on 100/120 Gas Chrom Q: Applied Science, State College, Pa.; OV-101 (dimethylsilicone fluid): Supelco, Inc., Supelco Park, Bellefonte, Pa. All analytical gas chromatographic data were obtained on a Perkin-Elmer Model 900 gas chromatograph equipped with flame ionization detectors. In general, the detector temperature was kept at 370 \pm 10°C. Helium was used as the carrier gas and all data were obtained under isothermal conditions.

I. Preparative GLC. One of the standard Perkin-Elmer Model 900 gas chromatographs available in our laboratory was coupled to the model 900 preparative attachment (Cat. No. 009-8002) for automatic cyclic preparative work. The combined system can be seen in Figure 1, and its principle of operation will be described below.

J. Electrostatic precipitation. The unit Model 850 Prepkromatic electrostatic precipitator was purchased from Nester Faust Mfg. Corp., Newark, Delaware, 18711, and was used without modification.

Results and discussion

1. Analytical GLC

The complexity of the alicyclic hydrocarbon mixtures in the molecular weight range of interest to us is shown in Figure 2. The adduction of the heptane eluates with thiourea, as described above, is very useful in that it segregates almost quantitatively the tetracyclic sterane isomers according to the stereochemical configuration (cis or trans) of the 5, 10 ring fusion. Only the steranes (cholestane, C₂₇; ergostane, C₂₈; sitostane, C₂₉) are labelled in the figure. Other peaks correspond to the triterpanes. Thus the pattern obtained after digestion with molecular sieves and before adduction with thiourea would be the sum of the two GC traces shown in Figure 2A.

Although the GC patterns of the thiourea non-adduct fractions (Figures 2A, B, C) cannot be considered too complex at first glance, the difficulties associated with the isolation and identification of each component can be understood by inspection of the chromatographic trace in Figure 2D. This is the chromatogram of the same mixture on a short capillary column with an efficiency about five times greater (9) than, for instance, that of the packed column giving the separation shown in Figure 2B. Three changes in the GC pattern of Figure 2D are most evident. The peak corresponding to the tetracyclic sterane 5 α -C₂₉ in chromatograms A, B and C (Figure 2) is actually a mixture of two components and the same is true for the two large peaks eluting after the major component.

With these facts in mind, it is evident that prior to attempting any preparative isolation or GC/MS identification of the different components in these mixtures, special attention must be paid to the chromatographic parameters required for maximum separation. This point (optimization of GLC parameters) has been treated in detail in the literature (9), and only a few general ideas will be added here.

Due to their total non-polar character and close structural similarities, the choice of chromatographic methods for these types of separations becomes rather limited. Although we are presently investigating the possibilities of a high pressure

liquid chromatography system, GLC seems to be the most practical and efficient technique. However, the types of columns that can be used are limited to the long and narrow bore analytical columns (high efficiencies) due to the complexity of the mixtures. One is also limited to high operating temperatures by the molecular weight of these compounds, which in turn restrict the choice of stationary phases to only those most thermally stable. Because of the characteristically large elution volumes of these compounds the support size in analytical packed columns must be less than 100 mesh to achieve fast enough flow rates.

In terms of the separation of individual compounds in substantial amounts, their preparative GLC is restricted to small sample sizes if high column efficiencies are to be maintained (9). Recovery yields can be extremely low if standard trapping systems are used, due to the high tendency that these hydrocarbons have to form aerosols.

For the purpose of this work chromatographic resolution becomes an all decisive factor. Since resolution (R) is directly proportional to both the efficiency (N) and the selectivity (α) of the column, it follows that R could be increased by a favorable change in any of the two factors. However, the choice of liquid phases is restricted by high operating temperatures as stated above, so that not much can be done in terms of choosing the proper selectivity factors. This spells out the requirement for the highest possible efficiencies of the chromatographic system. For instance, considering the doublet of peaks eluting between 42 and 43 minutes in Figure 2D, it is possible to calculate the required minimum efficiency to separate them with a given resolution by means of the formula (12): $Nr = 16R^2 (\alpha/\alpha - 1)^2 (k_2 + 1/k_2)^2$.

From the chromatogram in Figure 2D: $R = 0.7$; $\alpha = 1.02$; and $k_2 = 10.9$. (The factor k_2 , known as the retardation ratio (12), is expressed as the ratio of the corrected retention time of peak 2 in a binary mixture to the retention time of the air peak). To double the resolution from 0.7 to 1.4, Nr must then be equal to 96249 theoretical plates. Since the efficiency of the 30 m long capillary column (Figure 2D) can be calculated, also from the GC trace, to be equivalent to 15,000 plates, which sets the height of a theoretical plate at 2 mm, the length required to obtain 96249 plates for an equivalent column would be 193.5 m. Thus, just to double the resolution in this particular case one needs to increase the number of plates and the length about 6.4 times. The magnitude of these numbers, well above those characteristic of large diameter preparative columns, forced us to investigate the potential use of small bore analytical columns for preparative purposes, giving special attention to the effect of sample size on resolution and efficiency. This effect is shown graphically in Figures 3 and 4. As predicted, the sharpest decline of resolution with the increase in sample size (Figure 3) occurs in the 0.1 cm i.d. column, while the 0.45 cm i.d. column is less affected and the 0.20 cm i.d. columns are in an intermediate position. The broken line corresponds to two 3 m x 0.10 cm i.d. columns coupled together and, although higher resolutions can thus be obtained, the slope is not any better than that obtained for each one alone. The parallel loss of resolution and efficiency with sample size is shown in Figure 4. Note the simultaneous change of slope in both parameters at 50 μ g sample size (9).

2. Preparative GLC

Considering the narrow sample size range (1 - 150 g) to which one is limited by the requirements of resolution and efficiency, a repetitive automatic injection and collection unit becomes a necessity, especially if milligram amounts of each substance are to be collected in a reasonable amount of time. For this purpose, one of the two Perkin-Elmer Model 900 gas chromatographs available in the laboratory was fitted with the Model 900 preparative attachment as shown in Figure 1. A schematic diagram of the complete system is given in Figure 5. The carrier gas flows from 1 to 9 through the solenoid and non-return valves 2 and 3. In the injection block a small split takes place. Most of the carrier gas goes into the GC column 10, but a small part (3 - 8 ml/min) flows out through 8, the dosing capillary and into the sample vessel. This constant backflow is regulated by valve 5. Thus, at any given

time the pressure at the head of the column equals the pressure in the sample vessel. Dosing is triggered by the electronic programmer unit which contains the control electronics for automatic cyclic operation and controls solenoid valve 2. When a dosing command is given by the programmer the entire gas flow is diverted through 4 into the sample vessel. In consequence the equilibrium in pressures is momentarily upset so that sample flows from 7 to 9. The quantity of sample that is thus injected into the column is fixed by the total time that the solenoid valve 2 is open, the dimensions of the dosing capillary and the viscosity of the sample. When 2 is closed by the programmer the original column pre-pressure is re-established in 9 and the capillary is flushed free of sample.

At the exit of the column the effluent is split so that from 1 to 10%, or more in some cases, goes to the flame ionization detector and the rest goes on through the distributor assembly to the traps which are opened and closed by solenoid valves placed on their exit sides. This eliminates moving parts in the flow path of the sample before it is collected. The traps are opened and closed according to preset threshold values and according to a pre-selected peak sequence which is controlled by the electronic programmer. One of them (waste trap) is always on as a bypass trap to avoid losing the part of the effluent not directed to the other traps. Both the injection and collection systems have been modified in our laboratory to allow the use of analytical size columns in the preparative mode and to insure maximum recovery of the compounds emerging from the column. This will be described in detail elsewhere. The results obtained with this system are shown in Figure 6. Both chromatograms correspond to those shown in Figure 2A for the thiourea adduct and non-adduct fractions.

The preparative isolation of both the adduct and non-adduct fraction was achieved by taking into account the proper parameters to insure optimum resolution (9), and minimum analysis time in accordance with the considerations discussed above. The operational parameters selected for the collection of the two major peaks in the thiourea adduct (Figure 6, top), 5α -cholestane and 5α -ergostane, are given in Table I. The data in Table I is also representative of other longer runs. In one of them the unit operated continuously in the automatic mode for a total of 116 hours and 20 minutes. The top chromatogram in Figure 6 is taken from one of the actual automatic cycles. From this chromatogram, the operating efficiency of the column under the conditions selected for the run can be calculated as equivalent to 3047 theoretical plates, and the resolution for a mixture of 5α - and 5β -cholestane as 1.79 for sample sizes of 100 μ g/peak. Common threshold values for the opening and closing of the traps were set for the front (F) and rear (R) of each one of the two peaks. Peak 1, collected in trap I, corresponds to 5α -cholestane and peak 2, collected in trap II, corresponds to 5α -ergostane. The shaded areas indicate how much of the peak was directed to the corresponding trap and the length of time for which each trap was opened. The purity of bands collected in this fashion was assayed by re-chromatographing them on a more efficient column ($N = 6789$ theoretical plates). The results are shown in Figure 7. The chromatogram of the total adduct is given in Figure 7A for purposes of comparison with that shown on Figure 2A. Figure 7B shows what was collected in the waste trap. Note the practical disappearance of the two major peaks from the pattern. The band of 5α -cholestane, collected in trap I, is shown in Figure 7C and that of 5α -ergostane collected in trap II is shown in Figure 7D and Figure 7E. Both steranes can be estimated chromatographically at a purity greater than 99%. Quantitative data are given in Table II. The contribution of column bleed to the figures given in Table II has not been deducted; however, it can be estimated to be negligible in traps I and II and less than 10 mg in the waste trap. Assuming a total contribution of 10 mg of column bleed the recovery yield is still 94.3%. It is obvious from these chromatograms any mixing or cross contamination of traps in the distributor assembly is practically negligible with this system.

Similar parameters as those shown in Table I were set up for the collection of the four major multi-component peaks in the non-adduct fraction (Figure 6, bottom). However, in this case the diameter of the column was reduced to half (from 0.45 cm i.d. to 0.20 cm i.d.) to approach the minimum resolution factors required for the

preliminary separations of these substances. The flow rate (56.6 cc/min) selected was a compromise between the optimum for maximum resolution and the fastest allowable for minimum analysis time. However, analysis time was favored over resolution in this case, since it could be calculated that this column would not be able to resolve the multi-component peaks under any conditions.

The split ratio was readjusted by changing the stream splitter so that only 2.1% of the total effluent was directed to the FID. The variable threshold programmer allowed the collection of each band with individually set thresholds as indicated on Figure 6, bottom. The purity of the collected bands was again assayed by GLC on the same column used to check out the bands collected from the adduct fraction. The total GC pattern of the pentacyclic triterpane fraction is shown in Figure 8A. The GLC trace obtained from the material collected in the waste trap shows the relative degree of removal of each of the peaks which were collected in traps I through IV (Figure 8C - F). The peak collected in trap I shows the presence of a minor component underneath its front slope, and furthermore, it is known from the separation on capillary columns (see Figure 2, doublet of peaks at about 35 minutes) to be a 50:50 mixture of two components, one of them corresponding to the 5α - C_{29} sterane in retention time.

The two small peaks following the major compound collected in trap II can be easily explained considering the threshold levels 2R and 3F in Figure 6, bottom. During the time trap II stayed open (2F - 2R) it was a small amount of component 3, which is itself a mixture of at least two components as indicated by the chromatogram in Figure 8E. The same is true for component 4 in trap 4 (Figure 8F). The cross contamination of trap 3 with the components collected in trap 4 is consequence of an accidental error in trap sequencing due to a faulty injection. This is of little importance in this case because it was known that each of these peaks would have to be re-chromatographed on capillary columns of an efficiency and length at least equivalent to those calculated above in order to resolve them completely.

At the time of this writing, less than 10mg of the non-adduct fraction have been run through the system. Full quantitative data will be presented at a later date, together with the results obtained with the use of capillary columns in the preparative system.

Another major problem encountered in this work deals with the tendency that these substances have in forming aerosols, thus decreasing the collection efficiency. Extensive work in this area with labelled cholesterol and other standards showed this to be a significant factor. Many trap configurations, packing materials and coolant systems were tested, unsuccessfully for the most part. The most effective system was determined to be that of electrostatic precipitation. For this purpose a commercial unit was bought from Nester Faust and the standard Perkin-Elmer traps designed for aerosol forming substances were modified to fit the slip over double lead probes. The unit when turned on sets a field of 5000 volts AC at 0.040 amps between the two electrodes. Without the electrostatic precipitator, collection efficiencies of the order of 60% were difficult to achieve, while they went up to about 95% with the use of the precipitator. No change at all was ever observed in any of the GC patterns even when this possibility was checked with standards, which indicates that compound breakdown does not take place with the AC voltage, and that the electrostatic precipitator is safe to use in these separations.

Conclusions

The isolation of relatively large quantities of each one of the steranes and triterpanes from the Green River Shale bitumens with this system will enable us to undertake a full study of their molecular structures. The data obtained so far indicates that with proper consideration of the basic parameters of the chromatographic process it becomes possible not only to separate very complex mixtures, but also to collect each component on an individual basis and in high purities for further study. Thus, it appears that if analytical specifications can be incorporated into a standard preparative system, new ways will be open in the field of natural product analysis toward the isolation of the significant components within any given

mixture. The manufacturers of the existing preparative systems should give some attention to the many chemists handling mixtures that simply cannot be resolved on standard preparative gas chromatographs. These kinds of problems, similar to the one discussed here, will ultimately call for reliable automatic units with injection systems capable of going down to the 1 µg level or less and with efficient trapping systems for collection of submilligram amounts.

Acknowledgments: We thank Mr. G. Johanson and Mr. S. Gaskell for technical assistance. Financial support was provided by the U. S. National Aeronautics and Space Administration Grants NA 9-7889 and NGL 05-003-003.

References:

1. E. J. Gallegos, "Identification of new steranes, terpanes and branched paraffins in Green River Shale by combined capillary gas chromatography and mass spectrometry." Presented ACS meeting, Div. Petrol. Chem. Vol. 15, No. 3, Chicago, Illinois, September 13-18, 1970.
2. M. Calvin, "Chemical evolution", Oxford University Press, New York, 1969.
3. W. H. Bradley, Geol. Soc. Am. Bull., 81, 985 (1970).
4. A. L. Burlingame, P. Haug, T. BeTsky, and M. Calvin, Proc. Nat. Acad. Sci., 54, 1406 (1965).
5. T. J. Murphy, A. McCormick, and G. Eglinton, Science, 151, 1040 (1967).
6. I. R. Hills, E. V. Whitehead, D. E. Anders, J. J. Cummins, and W. E. Robinson, Chem. Communications 752 (1966).
7. W. Henderson, V. Wollrab, and G. Eglinton, "Advances in organic geochemistry", P. A. Schenck and I. Havenaar, eds., Pergamon Press, 1968.
8. P. C. Anderson, P. M. Gardner, E. V. Whitehead, D. E. Anders, and W. E. Robinson, Geochim. Cosmochim. Acta, 38, 1304 (1969).
9. E. Geipi, P. Wszolek, E. Yang and A. L. Burlingame, J. Chrom. Science (in press). Presented at the 6th International Symposium on Advances in Chromatography, Miami Beach, Florida, June 2-5, 1970.
10. C. Fenselau and M. Calvin, Nature, 212, 889 (1966).
11. A. B. Littlewood, "Gas chromatography", Academic Press, New York, 1962.
12. I. Halász and E. Heine, "Progress in gas chromatography", J. H. Purnell, ed., Interscience, New York, 1968.

Table I

Green River Shale Adduct Fraction - Typical Operating Parameters for Automatic Preparative GLC.

Column: 6m x 0.45 cm i.d. 5% OV-1
on 60/80 mesh supelcoport

Carrier gas: He, 163.5 cc/min

Temperatures: Injector 290°C
Column 270°C
Detector 380°C
Distributor 370°C

No. of injections: 42

Total Time/cycle: 59' 22"

Total time (42 cycles): 41 hours 33'

Average volume injected: 17.4 μ l

Range in vol. injected: 7 μ l to 21.3 μ l

Average amount injected: 79.0 μ g (5 α -cholestane)

Max. amount injected: 96.9 μ g (5 α -cholestane)
194 μ g (5 α -ergostane)

Split ratio: 11% to FID

Dosing time: 3 seconds

Trigger levels: See Figure 6.

Table II

Quantitative Estimate of Recovery Yields from Total Adduct Fraction.

Adduct fraction; total: 251.000 mg

Not used: 115.760 mg

Trap I (5 α -cholestane): 10.800 mg

Trap II (5 α -ergostane): 25.561 mg

Waste trap: 70.350 mg

Split to FID 11%: 24.471 mg

Total accounted for: 246.942 mg

Recovery yield: 98.3%

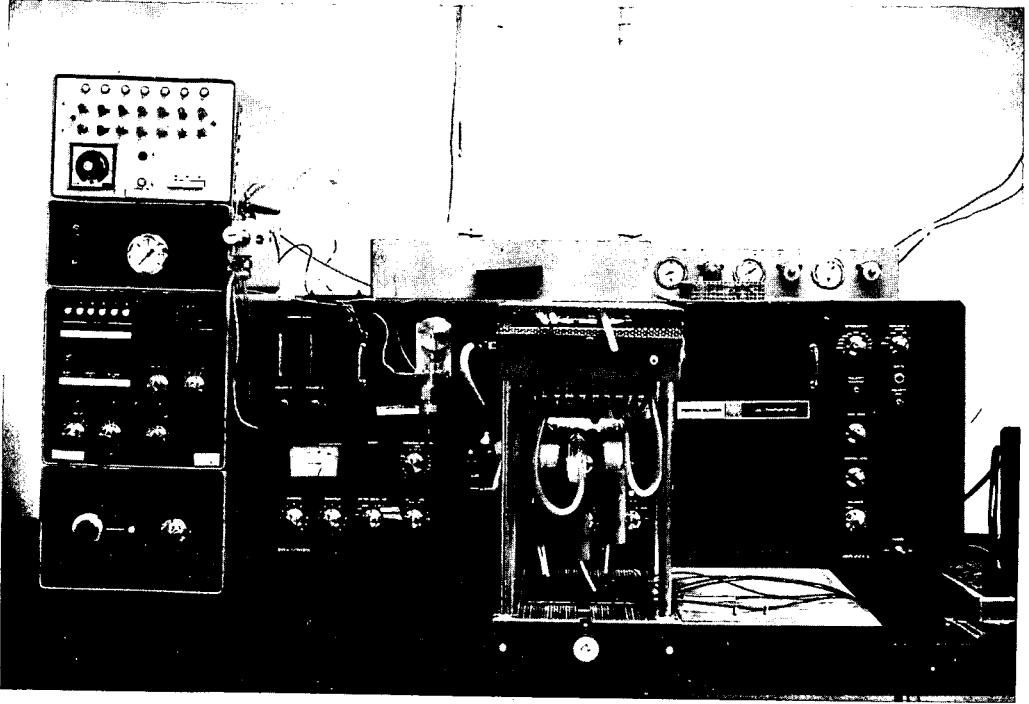
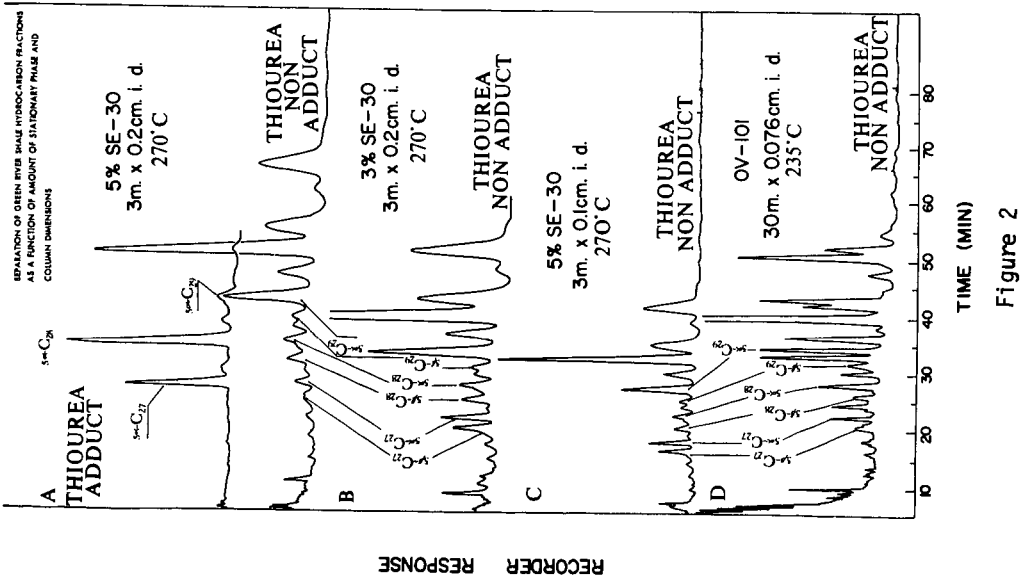


Figure 1



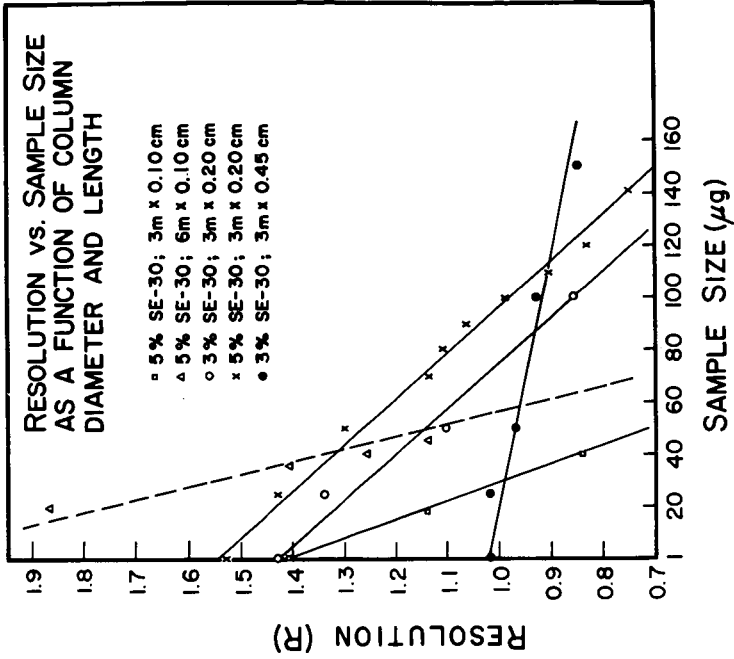


Figure 3

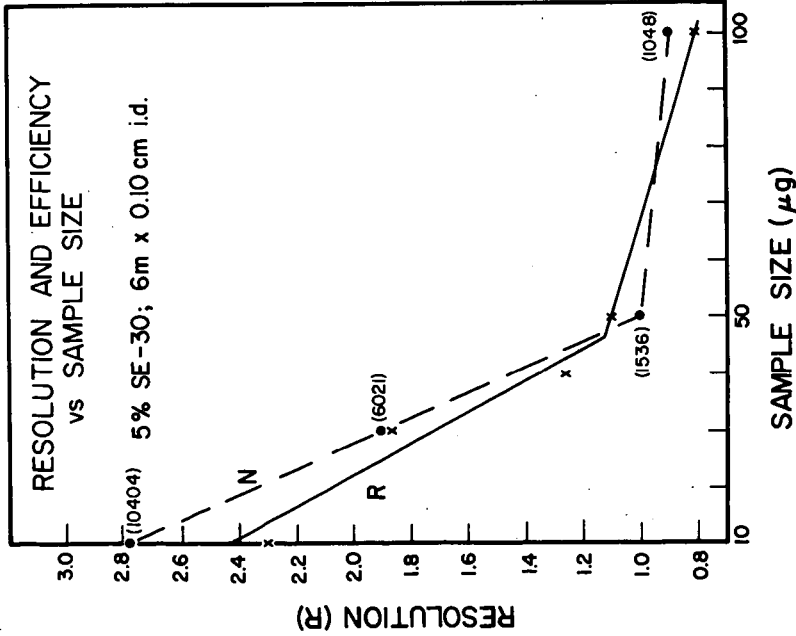


Figure 4

Schematic of Automatic Preparative Accessory

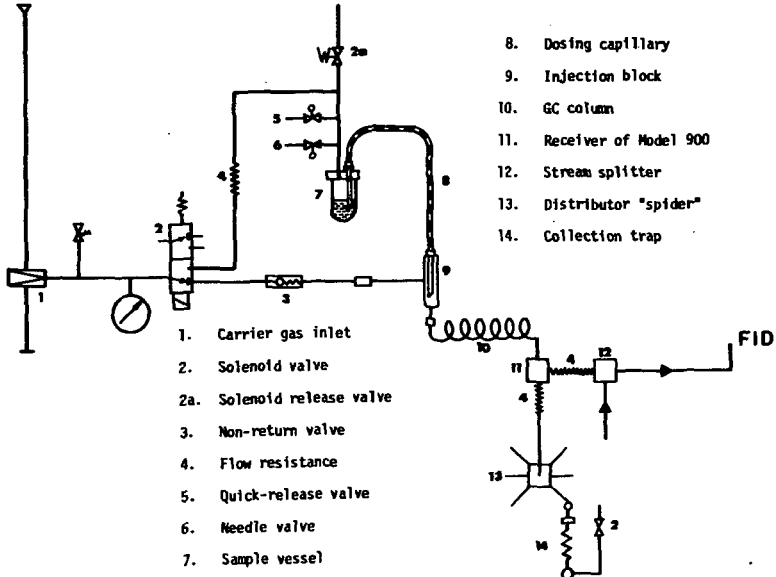


Figure 5

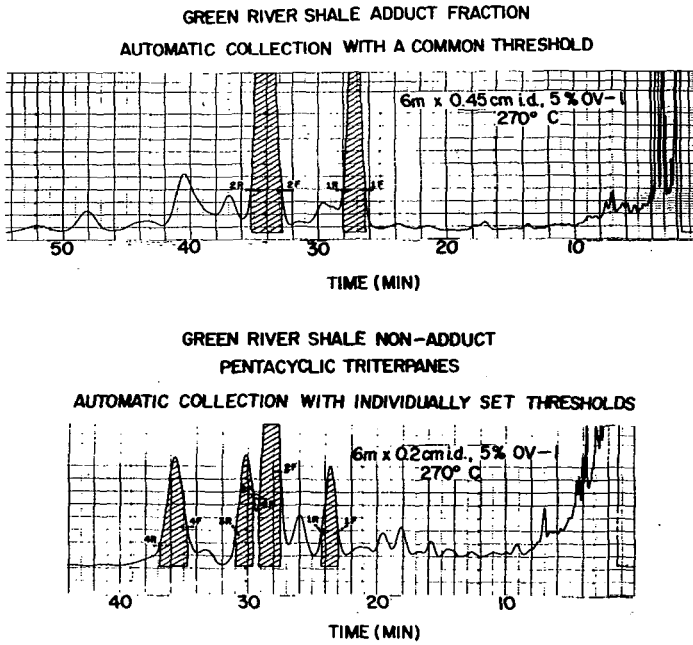


Figure 6

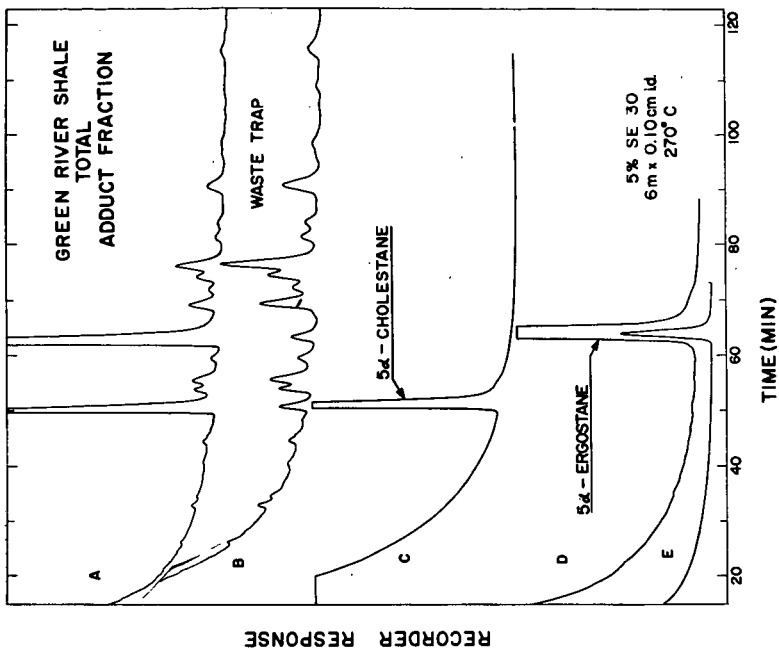


Figure 7

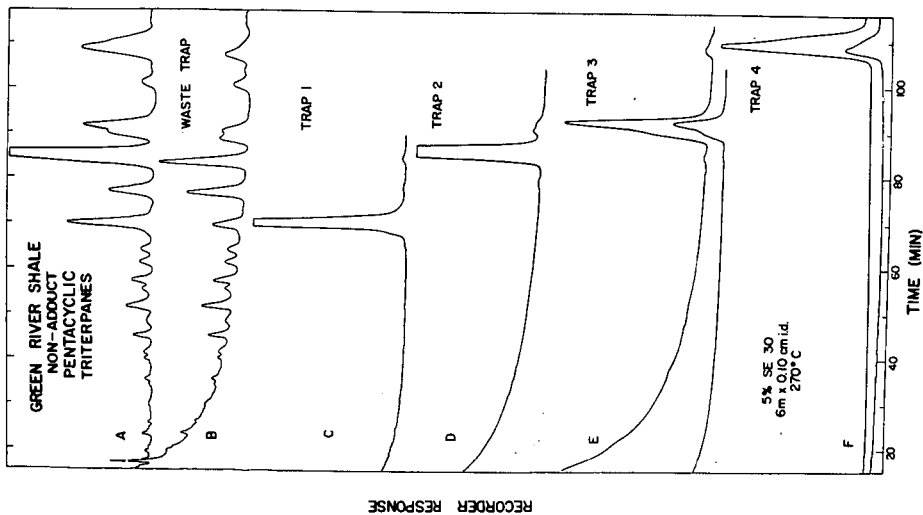


Figure 8

CHARACTERIZATION OF A SHALE OIL PRODUCED BY IN SITU RETORTING

H. B. Jensen, R. E. Poulson, and G. L. Cook

U.S. Department of the Interior, Bureau of Mines
Laramie Energy Research Center, Laramie, Wyoming 82070

INTRODUCTION

In situ or in place retorting has many potential advantages over the more conventional mining/retorting approach. One of the major advantages is that in situ retorting avoids the costly and disfiguring mining and spent-shale disposal steps associated with the mining/retorting approach. Another potential advantage is that it may make it possible to recover oil from formations that are not amenable to the mining/retorting approach. Many investigators have recounted at length the problems of in situ retorting and Burwell, Sterner, and Carpenter¹ have adequately referenced these investigations. Whereas it is not the purpose of this paper to delve into extended discussion of in situ retorting, it may help the reader to have an idea of the conditions under which in situ oils are produced. This paper will, therefore, describe briefly an in situ experiment and a brief description will also be made of each of the retorts that produced the oils with which the in situ oils will be compared.

This paper will describe two crude shale oils that were recovered from successful in situ-combustion retorting experiments.¹ The description will be based primarily on the results of the application of the Bureau of Mines crude shale-oil analysis² to these two crudes. In addition to describing the properties of the two in situ crudes in terms of this analysis, the properties of crude shale oils from aboveground retorts will also be described. Comparison of the oils from the aboveground retorts with each other will be made in order to determine the effect of change of retorting parameters upon oil character. Comparison of the in situ oils with the aboveground-retort oils will allow explanation of the retorting conditions under which the in situ oils were produced. This indirect approach to the problem of describing the conditions under which in situ retorting is accomplished is necessary because of the inaccessibility of the retort zone to visual inspection, either during or after retorting.

DESCRIPTION OF RETORTS

Aboveground Retorts

Two types of aboveground retorts featuring internal combustion for heating purposes will be discussed. The main difference in these two types, as far as this paper is concerned, is in the size of shale that is charged. The gas combustion retort is a type that uses crushed, screened, small-size shale and that accomplishes retorting with short, rapid shale heatup. The 10-ton retort and the 150-ton retort are of the type that uses mine-run shale and that accomplishes retorting with a long, slow shale heatup. Thus gas combustion retorting is done rapidly at relatively high temperatures compared with the retorting done in the type of retorts that use mine-run shale because in gas combustion retorting the shale does not undergo a long, low-temperature period of soaking. Table 1 lists the size of shale and the combustion-zone velocity for the aboveground retorting experiments.

Gas Combustion Retort. --The gas combustion retort is characterized by the use of continuous gravity flow of crushed, screened shale; direct gas-to-solids heat exchange; and heat supply by internal combustion. The retort is a vertical, refractory-lined vessel equipped with shale- and

TABLE 1. - Raw-shale size distribution and velocity of combustion zone

Retort	Source of shale	Wt pct of raw shale				Combustion zone velocity, ft/day
		Raw shale size, inches				
		Less than 4	4 to 10	10 to 20	Greater than 20	
Gas comb. ^{1/}	2/ Colo.	3/ 100	0	0	0	200
10-Ton	2/ Colo.	50	20	15	15	2
10-Ton	2/ Wyo.	35	35	20	5	2
150-Ton	2/ Colo.	40	20	20	20	2

^{1/} Gas combustion.

^{2/} Colo. = Anvil Points, Colorado; Wyo. = Rock Springs, Wyoming.

^{3/} All shale minus 3-inch plus 1/4-inch.

gas-distributing devices. The combustion air and retort products move countercurrently to the shale. Incoming shale serves to cool the products of retorting and is in turn rapidly heated to retorting temperature by the gases. The hot, retorted shale preheats the recycle gas before the recycle gas enters the combustion zone in the retort. In the combustion zone, the heat for retorting is produced by burning some of the organic residue on the shale plus recycle gas. A complete description of the gas combustion retort and its operation is given in a Bureau of Mines publication by Ruark, et al.³

10-Ton Retort. --The 10-ton retort was built and operated to study the retorting characteristics of mine-run shale having pieces as large as 20 inches on each side.⁴ The retort is a batch unit consisting of a cylindrical steel shell 6 feet inside diameter by 12 feet tall. This shell surrounds a tapered refractory lining 6 inches thick at the bottom and 9 inches thick at the top. A 1-inch steel plate that is perforated with 3/8-inch holes is used as a grate.

In practice, the retort is loaded with mine-run shale and the bed of shale is ignited at the top with a natural-gas burner. After ignition the burner is shut down. Subsequently air and recycle gas are fed to the top of the retort to maintain combustion and to accomplish retorting by heating the bed of shale from the top downward with the hot combustion gases. Control of the combustion-zone velocity is accomplished by adjusting air and recycle-gas feed rates.

150-Ton Retort. --In principles of construction and operation the 150-ton retort is similar to the 10-ton retort.⁵ It was built primarily to study the retorting characteristics of ungraded shale containing blocks of shale even larger than would fit into the 10-ton retort. The 150-ton retort is 11-1/2 feet inside diameter by 45 feet high. For the run which produced the 150-ton retort oil described in this report, the mine-run raw shale contained blocks of shale measuring as large as 3 feet x 4 feet x 5 feet and weighing as much as 3-3/4 tons.

In Situ Retort

The two in situ oils were produced during in situ combustion experiments conducted in the Green River oil-shale formation near Rock Springs, Wyoming.¹ One objective of these experiments was to study the engineering problems associated with the establishment, maintenance, and control of a self-sustaining combustion zone in previously fractured oil shale. A second objective was to produce shale oil using such a self-sustaining combustion zone. Both combustion experiments were successful in meeting their objectives. The following description is for the Bureau's first in situ experiment¹ near Rock Springs, Wyoming at a location designated as site 4. The

experimental conditions for the second in situ experiment at a site 7 will not be described because they were similar to those at site 4.

For the site 4 experiment, a 20-foot thick section of oil shale, located from 68 to 88 feet below the surface, was ignited by use of a propane burner in the center well of an expanded, five-spot development pattern. Four wells of the five-spot pattern were located on the corners of a square 25 feet on each side; the fifth well was in the center of the square. After combustion was established, the propane burner was removed and air was injected into the center well. The combustion zone was maintained in the formation for 6 weeks, at which time air injection was terminated and the combustion phase of the experiment was brought to a close. The outlying or observation wells of the expanded five-spot pattern were the wells from which flowed the unused air, the combustion products, and the retort products. Several thousand gallons of shale oil were recovered from the experiment. The oil described in this paper was produced during the last week of the experiment and is considered a representative, "steady-state" oil. Site geology, site preparation, instrumentation, pre-ignition fracturing, ignition, and retorting have been described in detail by Burwell, et al.¹

OIL CHARACTERIZATION PROCEDURES

Bureau of Mines Crude Shale-Oil Analysis. --A complete description of this analysis method has been reported by Stevens, et al.² Basically, the method tests a crude shale oil for the properties listed in table 2. In addition, specific gravity and total nitrogen content are determined on the following distillation fractions: Naphtha (IBP to 400° F), light distillate (400 to 600° F), light gas oil (600 to 800° F), and a distillation residuum (above 800° F). The naphtha and light distillate fractions are further tested for tar acid, tar base, saturate, olefin, and aromatic contents.

TABLE 2. - Properties of crude shale oils

Retort	Source of shale	Oil properties				
		Specific gravity, 60°/60° F	Pour point, °F	Viscosity, 100° F SUS	Nitrogen, wt pct	Sulfur, wt pct
Gas comb.	Colo.	0.942	80	370	1.46	0.77
10-Ton	Colo.	.923	60	112	1.57	.79
10-Ton	Wyo.	.920	50	112	1.27	.59
150-Ton	Colo.	.909	60	98	1.59	.94
In situ-4 ^{1/2}	Wyo.	.885	40	78	1.36	.72
In situ-7 ^{2/2}	Wyo.	.899	30	52	1.84	.78

^{1/} Site 4, Rock Springs, Wyoming, in situ experiment.

^{2/} Site 7, Rock Springs, Wyoming, in situ experiment.

Simulated Distillation. --This analysis method employs a nonpolar, temperature-programmed gas liquid chromatographic system to obtain an estimation of the distillation range of crude oils. The resulting simulated-distillation (sd) data can be used to predict the amount of each distillate in the crude as weight percent of the crude. The sd parameters used to obtain the crude oil compositions reported in this paper are as follows: The column was 0.180 inch inside diameter x 18 inches long; the packing was 5 percent w/w UCW-98 on 70/80 mesh Chromosorb W, acid and base washed; the temperature was programmed to give a normal triacontane emergence time of 30 minutes; and flame-ionization detection was used.

The sd weight percent data were converted to the volume percent data shown in table 3 by using the observed specific gravities of the three, lowest boiling fractions and by using estimated gravities for the highest boiling fraction and for the residuum. These estimations took into account: (1) The relative amounts of heavy gas oil and residuum from sd and (2) the observed specific gravity of the residuum from the above crude shale-oil analysis.

TABLE 3. - Crude oil composition

Retort	Source of shale	Fraction, vol pct of crude ^{1/}				
		Naphtha, IBP to 400° F	Light distillate, 400° to 600° F	Light gas oil, 600° to 800° F	Heavy gas oil, 800° to 1,000° F	Residuum, over 1,000° F
Gas comb.	Colo.	5.6	18.9	25.4	27.5	22.7
10-Ton	Colo.	5.7	26.2	33.3	26.2	8.6
10-Ton	Wyo.	5.0	29.7	36.0	24.4	4.9
150-Ton	Colo.	6.5	30.9	35.6	20.4	6.6
In situ-4	Wyo.	14.9	48.3	24.0	6.2	6.6
In situ-7	Wyo.	11.2	41.5	29.6	12.3	5.4

^{1/} Determined by adjusting simulated-distillation data for specific gravity of the fractions.

RESULTS AND DISCUSSION

Table 1 lists the size of shale and the combustion-zone velocity for the aboveground retorting experiments. The four experiments listed in the table were chosen to demonstrate effect of the following parameters on shale-oil character: (1) Rapid retorting of small-size shale, (2) slow retorting of mine-run shale, (3) slow retorting of mine-run shale with added large blocks, and (4) shale source. Gas-combustion retorting of Colorado shale demonstrates the effect of rapidly retorting crushed and screened small shale. The experiment in which Colorado shale was charged to the 10-ton retort demonstrates the effect of slowly retorting mine-run shale. Wyoming shale charged to the 10-ton retort demonstrates the effect of slowly retorting shale from a different source. The 150-ton retort experiment demonstrates the effect of slowly retorting larger mine-run shale than was retorted in the 10-ton experiments. Table 2 lists some properties of these four oils and also the properties of the two oils produced by the two in situ combustion experiments, and table 3 lists the distillation yields from each of the six crude oils.

The effects of shale size, combustion-zone velocity, and effective retorting temperature are shown by comparing the properties of the oil from the rapid retorting of small shale (gas-combustion retort) with those of oils from the slow retorting of large shale (10-ton and 150-ton retorts). In general the naphtha, light distillate, and light gas oil contents increase and the heavy gas oil and residuum contents decrease as the retorting rate and temperature become lower and the shale larger. If the foregoing parameters are the ones that have a marked influence on the properties of the oils from the aboveground retorts, then the properties of the two in situ oils can be used to demonstrate the relative value of these parameters for in situ retorting. The in situ crude oils have even higher contents of light components (naphtha and light distillate) and lower contents of heavy components (light gas oil, heavy gas oil, and residuum) than do the oils from the slow, low-temperature, aboveground retorting of mine-run shale. Thus the in situ retorting was likely accomplished at lower temperatures, at slower combustion-zone velocities, and on larger or at least a greater proportion of large shale blocks than were used in the aboveground retorting experiments.

The crude-oil composition (table 3) and the crude oil yields for the aboveground oils (column 3, table 4) can be used to calculate the amount of each distillate that is produced from each ton of 30-gallon-per-ton (gpt) oil shale. The calculated data in table 4 (columns 4 through 8) show that for each of the four aboveground experiments the combined quantity of naphtha and light distillate is about the same and amounts to about 6.9 gpt of 30-gpt shale. The quantity of light gas oil also remains constant at about 7 gpt of 30-gpt shale. However, the quantities of heavy gas oil and of residuum are shown to be markedly dependent upon the retorting parameters of shale size, combustion-zone velocity, and retorting temperature. The quantity of heavy gas oil from the gas-combustion experiment is 7.4 gpt, from the two 10-ton experiments it is 5.5 gpt, and from the 150-ton it is 3.7 gpt. The quantity of residuum shows an even greater decrease with change in the retorting parameters. Residue production from the gas combustion retort amounts to 6.1 gpt, whereas from the 10-ton and 150-ton retorts it is only 1.3 gpt. The diminution of heavy oils from those retorts which utilize large blocks of shale without an accompanying increase in light oils indicates that little secondary cracking takes place in any of the large-shale, slow-retorting systems. Indeed it appears that there is some sort of distillation being carried out in which the heavy components are deposited on cold raw shale to be consumed later by the combustion zone when it passes through the area of deposition. Any secondary cracking of this heavy material should yield an increased quantity of the light oils, unless the cracking is such that gas and coke are the only products. If this is so, the net result is the same as burning the heavy components without cracking because the gases would be burned with the recycle gas and the coke would be burned when the combustion zone traverses the area of deposition.

TABLE 4. - Distillate yields for aboveground retorts

Retort	Source of shale	Yield, gpt of 30-gpt raw shale					
		Crude oil ^{1/}	Naphtha	Light distillate	Light gas oil	Heavy gas oil	Residuum
Gas comb.	Colo.	27.0	1.5	5.1	6.9	7.4	6.1
10-Ton	Colo.	20.5	1.2	5.4	6.8	5.4	1.7
10-Ton	Wyo.	22.9	1.1	6.8	8.2	5.6	1.1
150-Ton	Colo.	18.0	1.2	5.5	6.4	3.7	1.2

^{1/} Obtained from the oil recoveries for each experiment.

If it is postulated that in situ retorting produces the same quantity of naphtha plus light distillate from each ton of shale averaging 30 gpt as did the aboveground retorts, namely 6.9, then the compositional data listed in table 3 for the two in situ oils can be used to calculate approximate quantities of each of the fractions. These quantities will add together to give total oil recovery in terms of gpt of 30-gpt shale and thus give an estimation of oil yields for each of the two experiments. Table 5 gives the results of these calculations and indicates that the experiment on site 4 had a yield of 10.9 gpt of 30-gpt shale and the experiment on site 7 had a yield of 13.1 gpt of 30-gpt shale. These calculate to Fischer assay recoveries of 36 percent and 44 percent respectively from the shale in the retorted zone.

The objective of the two experiments in the 10-ton retort was to demonstrate the effect of shale source on oil properties. The crude oil properties (table 3), the crude oil composition (table 4), and the distillate yields (table 5) show very little difference in properties of the oils from the two 10-ton experiments each using shale from a different source. Hence the differences in properties among oils from the three aboveground retorts and from the two in situ experiments can logically be said to be due to retorting parameters rather than shale source.

TABLE 5. - Calculated distillate yields for in situ experiments

Experimental site	Yield, gpt of 30-gpt raw shale				Crude oil	Yield, vol pct of Fischer assay
	Naphtha plus light distillate	Light gas oil	Heavy gas oil	Residuum		
In situ-4	6.9	2.6	0.7	0.7	10.9	36
In situ-7	6.9	3.9	1.6	.7	13.1	44

The Bureau of Mines crude shale-oil analysis tests the naphtha and light distillate fractions for saturate, olefin, and aromatic contents. Table 6 and table 7 list this analysis for these fractions from all of the six crude oils. The concentration of aromatics remains constant for each fraction. It was previously shown that for aboveground retorting the quantity of naphtha and light distillate in gpt of 30-gpt shale also was fairly constant. Therefore the quantity of aromatics is independent of the retorting parameters, and the combined quantity of saturates and olefins is also independent of the retorting parameters. However, for aboveground retorting the ratio of saturate quantity to olefin quantity is shown to be dependent upon the parameters of shale size, combustion-zone velocity, and retorting temperature. As the shale size becomes larger and combustion-zone velocity and retorting temperature become smaller, the ratio of saturates to olefins becomes larger. If this increase in saturates in the aboveground experiments is due to the slow retorting of large blocks of shale, then the in situ oils demonstrate that the in situ retorting was accomplished on larger shale and at slower rates than was the aboveground retorting.

TABLE 6. - Hydrocarbon-type analysis of neutral naphtha

Retort	Source of shale	Hydrocarbon type, vol pct		
		Saturates	Olefins	Aromatics
Gas comb.	Colo.	30	50	20
10-Ton	Colo.	34	44	22
10-Ton	Wyo.	37	42	21
150-Ton	Colo.	41	37	22
In situ-4	Wyo.	61	16	23
In situ-7	Wyo.	57	16	27

TABLE 7. - Hydrocarbon-type analysis of neutral light distillate

Retort	Source of shale	Hydrocarbon type, vol pct		
		Saturates	Olefins	Aromatics
Gas comb.	Colo.	31	41	28
10-Ton	Colo.	38	37	25
10-Ton	Wyo.	36	35	29
150-Ton	Colo.	49	28	23
In situ-4	Wyo.	55	15	30
In situ-7	Wyo.	50	22	28

Hill⁶ and Dougan⁷ have reported the characteristics of a noncombustion in situ shale oil that was produced by injection of hot natural gas at controlled temperature. In most respects the character of their crude oil is similar to that of our combustion in situ oils. Table 8 lists the distillate yields from their noncombustion in situ oil, the yields from our two combustion in situ oils, and the yields from gas-combustion oil. Their combined naphtha and light distillate fractions account for 80 percent of their in situ crude. Our two in situ oils have 60 percent from the site 4 experiment and 50 percent from the site 7 experiment. The amount of gas-combustion crude that is accounted for by these two light fractions is 25 percent. The decrease in heavy gas oil and residuum contents of their crude compared to gas-combustion crude is greater than the decrease noted when our in situ heavy gas oil and residuum contents are compared to gas combustion.

TABLE 8. - Comparison of distillate yields from noncombustion in situ retorting, combustion in situ retorting, and gas combustion retorting

Retorting method	Fraction, vol pct of crude				Residuum
	Naphtha	Light distillate	Light gas oil	Heavy gas oil	
Hill, noncombustion in situ	40	40	15	4	1
BuMines, combustion in situ-4	14	46	25	7	8
BuMines, combustion in situ-7	10	40	30	13	7
BuMines, gas combustion	6	19	25	27	23

Table 9 lists the hydrocarbon-type analyses for the light distillates from each of these same crude oils. There is a greater difference noted when the saturate/olefin ratio for gas-combustion oil is compared to that ratio for the Hill's oil than when that ratio is compared for gas-combustion oil and our in situ oils. The distillate yield and hydrocarbon-type data from Hill's in situ crude indicate that the absence of oxygen in the retort gas may be partly responsible for the high naphtha and high saturate contents. Also responsible, as shown by our work, are the parameters involving shale size, retorting (combustion-zone) rate, and effective retorting temperature.

TABLE 9. - Comparison of light-distillate hydrocarbon-type compositions from noncombustion in situ retorting, combustion in situ retorting, and gas combustion retorting

Retorting method	Hydrocarbon type, vol pct		
	Saturates	Olefins	Aromatics
Hill, noncombustion in situ	64	5	31
BuMines, combustion in situ-4	55	15	30
BuMines, combustion in situ-7	52	22	28
BuMines, gas combustion	31	41	28

The concentration of aromatics in Hill's light distillate and of all of the light distillates studied in this work have a limited spread (tables 7 and 9), suggesting that the production of aromatics in this boiling range is independent of shale size, retorting rate, effective retorting temperature, and retort-gas composition.

One respect in which Hill's low-temperature oil does vary from our in situ oils is in the nitrogen content. Hill's crude had a nitrogen content of 0.8 percent, whereas the average for the six oils

in this study was 1.5 percent, or nearly twice as much. Hill gives the following explanation for his low nitrogen value:

"In the high temperature processes all of the kerogen undergoes decomposition. The nitrogen atoms become an integral part of the polymer and the thermal decomposition of this polymer gives products containing this nitrogen well distributed among the final product molecules.

Based on the experimental results we have concluded that the nitrogen in the kerogen is present in molecules of very high molecular weight which tend to remain in the shale at the decomposition temperatures below 800°F."

If the big difference in the two in situ retorting systems is the presence of air or the absence of methane, then it seems that nitrogen concentration in the crude oil is dependent more upon the retort-gas-composition parameter than on the other retorting parameters. It is either the presence of the methane or absence of oxygen that reduces the incorporation of nitrogen in the resulting shale oil.

Qualitatively speaking with respect to distillate yield and distillate composition, we can say that Hill's noncombustion in situ oil is similar to our combustion in situ oils. Quantitatively speaking we can say that the retorting parameters that control the character of the combustion in situ oils are the same parameters that largely control the character of the noncombustion in situ oil. These parameters are shale size, combustion-zone velocity, and effective retorting temperature.

SUMMARY

Differences in properties are noted when crude oils produced by rapidly retorting small-size (less than 3 inch) oil shale in aboveground retorts are compared with crude oils produced by slowly retorting large-size, mine-run shale in aboveground retorts. Significant extensions of these differences are noted when the latter oils are compared to in situ oils. For example, the specific gravity decreases from 0.94 to 0.92 to 0.89; the pour point decreases from 80° F to 60° F to 40° F; and the 100° F viscosity decreases from 400 SUS to 100 SUS to 65 SUS. Compositional changes are also noted; for example, the content of light distillate in the crude oil increases from 20 percent to 30 percent to 45 percent, while the residuum decreases from 20 percent to 7 percent to 6 percent. Another change is noted in the hydrocarbon-type distributions in the naphthas and light distillates. For example, the concentration of saturates in the light distillate increases from 30 to 40 to 50 volume percent while the olefins decrease from 40 to 30 to 20. The concentration of the aromatics in all of the light distillates is constant at about 30 volume percent.

When these compositional data are considered together with the oil yields from the aboveground retorts, the quantities of naphtha, of light distillate, of light gas oil, and of heavy gas oil each remain about the same. Expressed as gallons of each fraction per ton of 30-gpt shale, the average for each fraction is 1, 6, 6, and 7 respectively. However, the quantity of residuum from the small shale is considerably greater than from the mine-run shale. These figures are 6 and 1 respectively. Thus most of the decrease seen in recovery of oil from the aboveground retorting of mine-run shale compared with small shale is in the recovery of the residuum fraction. Because no increase in light materials accompanies the decrease in residuum, it is obvious that the loss of residuum is because the residuum is burned in those experiments that utilize large, mine-run oil shale.

The constancy of quantity of light products from the aboveground retorts can be used to estimate the oil recovery of the in situ process. For the two combustion in situ experiments, these recoveries were estimated to be 10.9 gpt and 13.1 gpt of 30-gpt shale.

Differences in characteristics between combustion in situ oil and the noncombustion in situ oil described by Hill and coworkers, such as olefin and nitrogen contents, could be due to the presence or absence of an oxidative atmosphere during retorting. Those oil characteristics that are the same for both combustion in situ oil and noncombustion in situ oil and that are different for these two in situ oils compared to oil produced by rapidly retorting small raw shale are due to the retorting parameters of shale size, combustion-zone velocity, and effective retorting temperature. These latter characteristics include distillate contents of the crude and hydrocarbon-type distribution within distillates.

ACKNOWLEDGMENTS

The work upon which this report is based was done under a cooperative agreement between the Bureau of Mines, U.S. Department of the Interior, and the University of Wyoming.

REFERENCES

1. Burwell, E. L., T. E. Sterner, and H. C. Carpenter. Shale Oil Recovery by In Situ Retorting. Accepted for publication in the December 1970 issue of the *Journal of Petroleum Technology*.
2. Stevens, R. F., G. U. Dinneen, and J. S. Ball. Analysis of Crude Shale Oil. BuMines Rept. of Inv. 4898 (1952).
3. Ruark, J. R., H. W. Sohns, and H. C. Carpenter. Gas Combustion Retorting of Oil Shale Under Anvil Points Lease Agreement: Stage 1. BuMines Rept. of Inv. 7303 (1969).
4. Carpenter, H. C., and H. W. Sohns. Application of Aboveground Retorting Variables to In Situ Oil Shale Processing. *Colo. School of Mines Quarterly*, v. 63, No. 4, 71 (1968).
5. Harak, A. E., A. Long, Jr., H. C. Carpenter. Preliminary Design and Operation of a 150-Ton Oil Shale Retort. Presented at the 6th Oil Shale Symposium, Denver, Colorado, February 1970. (To be published as a symposium issue in *Colorado School of Mines Quarterly*.)
6. Hill, George Richard, and Paul Dougan. The Characteristics of a Low Temperature In Situ Shale Oil. *Colo. School of Mines Quarterly*, v. 62, No. 3, 75 (1967).
7. Dougan, P. M., G. R. Hill, F. S. Reynolds, and P. J. Root. The Feasibility of In Situ Retorting of Oil Shale in the Piceance Creek Basin of Northwestern Colorado. Presented at U.N. Symposium on the Development and Utilization of Oil Shale Resources, Tallin, Estonia, SSR, August 1968.

INORGANIC SOLVENT PROCESS FOR SO₂ POLLUTION CONTROL

Allan Sass and H. F. Bauer

Garrett Research and Development Company, Inc.
1855 Carrion Road, La Verne, California 91750

ABSTRACT

An organic salt mixture has been developed that has a high absorbing capacity for sulfur dioxide. Upon testing in flue gas atmospheres it appears to be very effective in the comparatively complete removal of SO₂ from stack gases, with reasonable loading efficiencies and contacting characteristics. The inorganic salts are a fluid with a very low viscosity at the normal stack gas temperatures of from 250 to 450 F. The vapor pressure of this melt is in the neighborhood of 10⁵ mm, and thus vapor pressure losses would be minimal. The salts are also apparently unaffected by fly ash, and can be easily separated from a fly ash slurry. The SO₂ can be regenerated from the absorbed melt in a conventional manner. It appears that this solvent could provide an improved and lower cost SO₂ scrubbing system than others currently being tested.

INFRARED AND RAMAN SPECTRA OF INTRACTABLE CARBONACEOUS
SUBSTANCES--REASSIGNMENTS IN COAL SPECTRA

R. A. Friedel and J. A. Queiser

Pittsburgh Energy Research Center, Bureau of Mines
U.S. Department of the Interior, Pittsburgh, Pa. 15213

G. L. Carlson

Carnegie-Mellon University, Pittsburgh, Pa.

INTRODUCTION

Infrared and Raman investigations of intractable carbonaceous materials such as carbon blacks, coal chars, activated carbons, and graphite, have not been possible in the past. Friedel and Hofer have succeeded in obtaining an infrared transmission spectrum of one of the most difficult of these, a coal-based activated carbon (Fig. 1),^{1/} by the use of appropriate sample preparation and instrumental techniques. Extensive and efficient grinding were found to be important. There are other carbonaceous materials, both more and less tractable than activated carbon; the literature contains infrared spectra of formidable materials such as pyrolytic chars,^{2,3,4,5/} carbon blacks,^{6,7/} and coal chars.^{2,8,9/} Coals should also be mentioned here though they are easier to work with; it is possible to obtain good transmission spectra of coals with absorption intensities up to 80 percent.^{5,9,10,11/} The attenuated total reflectance method (ATR) is also suitable for obtaining infrared spectra of coals; J. S. Mattson in recent unpublished work has obtained a spectrum of Pittsburgh coal by the ATR method (private communication). Also, Mattson et al. have published spectra of sorbates on activated carbon using the ATR method.^{12,13/}

Raman spectra of carbonaceous materials have been very difficult to obtain because of the lack, until recently, of appropriate laser light sources. Tuinstra and Koenig have now reported Raman spectra of graphite and various carbons.^{14/} We have obtained Raman spectra of coals and other carbonaceous materials that are reported in this article. In nearly all spectroscopic studies of organic or inorganic materials it is desirable to obtain laser-Raman spectra along with infrared spectra. The two methods are completely complementary and can provide considerable structural information when used together.

Infrared transmission measurements on KBr pellets of various carbonaceous materials have produced good spectra. Accordingly attempts were made to obtain spectra of the most difficult carbonaceous substance--graphite. The infrared absorption of graphite was first studied by Cannon^{15/} who investigated a thin mineral oil mull of graphite. No spectral bands were observed; absorption was essentially the same throughout the 5,000-650 cm^{-1} infrared range. No spectral information was obtainable from such data.

Another unsuccessful attempt was made to obtain absorption spectra of graphite in the infrared (Friedel, unpublished work). Samples were prepared by rubbing powdered graphite on soft polyethylene which retained the graphite as a film; no specific infrared absorption was found. However, absorption and reflectance bands were found in the ultraviolet region with films of graphite on soft polyethylene.^{16/}

Infrared studies of polycrystalline graphite have been carried out by Foster and Howarth who determined spectra of refractive and absorption indices from 1 to 10 microns by a reflection method.¹⁷ One weak absorption peak was observed at $\sim 1300 \text{ cm}^{-1}$, superimposed on a broad band extending from 1 to 10 microns. Coals were also investigated; the spectra obtained were diffuse and not as informative as the conventional absorption spectra of coals.

EXPERIMENTAL

For the present investigation of absorption spectra of carbon black, activated carbons and ground graphite in the $4,000\text{-}250 \text{ cm}^{-1}$ infrared, we applied the sample preparation technique that was successful with activated carbons, namely, very extensive and efficient grinding.¹ Partial spectra were obtained after grinding for 24 hours but for better development of the spectrum many more hours of grinding were required. As noted elsewhere it was necessary to utilize a very small sample, as a large sample softens the blow of the ball bearings used for grinding in a small steel capsule.¹ It is obvious that much more extensive grinding would be required for graphite because of its good lubricating characteristics. Grinding for 96 hours developed a reasonably good infrared spectrum (Fig. 2). The advantageous effect of grinding is illustrated in Figure 3 by the improvement in resolution.

The difficulty of grinding carbonaceous materials increases in this order: Coals, low-temperature chars, carbon blacks (Fig. 4), activated carbons (Fig. 4), carborundum, and graphite. Spectral resolution in all cases improved with grinding; without extensive grinding, scattering difficulties were formidable and only poor resolution conditions could be used.

Perkin-Elmer instruments, PE-21 and PE-521 were used to obtain infrared spectra. Transmission spectra of KBr pellets of the carbonaceous materials were recorded.

Laser-Raman spectra were obtained on a Cary 81 instrument. Coal spectra were obtained on both powders and highly polished solid pieces; analyses of the coals are given in Table 1. Powdered samples of carbon blacks and activated carbons were studied. Graphite was studied both in the form of a ground powder and as a solid piece of Union Carbide highly oriented pyrolytic graphite. A list of materials studied is given in Table 1.

Lasers used: (1) Spectra-Physics, 141 Argon-ion; power delivered to the sample is 40 milliwatts. (2) Spectra-Physics, 125 He-Ne; power delivered to the sample is 35 milliwatts.

DISCUSSION OF RESULTS

1. Graphite and Carbons

The extensive grinding applied to graphite reduces the sample to minute particle sizes on which useful infrared transmission measurements were obtainable. The process works also for various carbon blacks, activated carbons, and carborundum. The frequencies found for ground graphite are essentially the same as those found for the various carbons. By the criterion of X-ray diffraction patterns, it is apparent that the materials measured are not crystalline graphites. Under extensive grinding graphite loses the characteristic X-ray diffraction peaks¹⁸. Nevertheless the infrared spectra obtained on ground graphite provide information concerning the molecular structures involved. Although graphite is altered by the grinding, the disappearance of crystallinity does not mean that the carbon-carbon bondings in the original graphite are altered. The grinding operation does not introduce sufficient energy into the system to break signifi-

cant numbers of carbon-carbon bonds nor to produce reactions that would change the graphitic structure. Therefore it is considered that the infrared spectrum of graphite after extensive grinding is indeed characteristic of the unsaturated molecular structure of graphite (Fig. 2). Two broad infrared bands were observed at 1565 and 1382 cm^{-1} after 72 hours of grinding. With continued grinding to 120 hours the two bands become stronger and sharper, as shown in Figure 3, and the frequencies shift slightly to 1587 and 1362 cm^{-1} (Table 2). In addition to these two absorption bands of graphite there is a weak absorption band at 830 cm^{-1} and another, possibly a combination band, at 2200 cm^{-1} .

These infrared frequencies are very similar to our laser-Raman results and to those reported by Tuinstra and Koenig.^{14/} The results indicate for ground graphite one intense scattering band at 1575 cm^{-1} and a weaker band at 1355 cm^{-1} . Tuinstra and Koenig assigned these frequencies to the E_{2g} and the A_{1g} modes respectively of crystalline graphite with D_{6h}^{2d} crystal symmetry. The two infrared bands that we find at 1587 and 1362 cm^{-1} compare reasonably well with the Raman bands. Further, the infrared maximum of the strongest band shifts from 1565 to 1587 as particle sizes decrease with grinding. Tuinstra and Koenig found that a closely similar shift occurred in the Raman spectra with decreasing particle sizes. The infrared bands were obtained on ground graphite for which X-ray measurements indicate that the typical fine structure of crystalline graphite has disappeared. And yet, the frequencies observed are practically the same as those of the Raman bands. It appears that the observed infrared and Raman spectra are not related to the crystallinity of graphite. Perhaps vibrations of the "aromatic" structure of graphite, crystalline or non-crystalline, are responsible for the observed spectra.

The weak infrared bands found at 830 and 2200 cm^{-1} are not reported for the Raman spectra. It is likely that the 2200 band is a combination band resulting from the 830 and the 1362 cm^{-1} bands which total 2212 cm^{-1} . This value is reasonably close to the observed 2200 cm^{-1} . The 830 cm^{-1} band could be due to an aromatic impurity in graphite. However, this would then remove the possibility of assigning the 2200 cm^{-1} band as a combination. The Raman spectrum of ground graphite may have a line at 830 cm^{-1} , corresponding to the infrared absorption at 830 cm^{-1} ; there is interfering absorption at 800 cm^{-1} due to a glass prism used in the Raman optical system of the Cary 81 instrument at Carnegie-Mellon University.

2. New Assignments in Coal Spectra

The application of infrared and Raman spectra to the study of intractable carbonaceous material has produced information valuable to researchers involved in studies of the structure of coal. Spectral frequencies are principally assignable to functional groups but some of the important spectral features, not assignable to functional groups, have been involved in considerable conjecture concerning proper assignments. There has been much disagreement in the case of the 1600 cm^{-1} infrared band, the most intense band in coal spectra. After the initial work of Cannon and Sutherland^{10/} the 1600 cm^{-1} infrared band was usually assigned to aromatic structures, thought to be mainly 1-, 2-, and 3-ring compounds. Brown^{8/} and Friedel^{9/} independently proposed that the band is assignable to conjugated, chelated carbonyl structures; derivatives of acetylacetone are known to have very strong and broad bands near 1600 cm^{-1} .^{19/} Friedel and Durie, and their coworkers, ^{20,21/} and Fujii, et al.,^{22/} have made further studies of the 1600 cm^{-1} band using chemical methods along with infrared to substantiate the conjugated chelated C=O structure. Oxygen-18 labeled chars were studied in an unsuccessful effort to prove that oxygen atoms were part of the structure involved in the 1600 cm^{-1} band.^{20,21/}

Table 1.- Coal analyses; graphites and carbons

<u>Coals</u>	<u>C</u>	<u>H</u>	<u>O</u>	<u>N</u>	<u>S</u> (wt.percents)
Lignite (see Table 3)	74.2	4.5	19.4	1.3	0.6
Subbituminous	78.7	5.5	13.3	1.6	0.9
hvBb	80.5	5.5	8.7	1.9	3.4
hvAb (Ohio)	82.4	5.4	8.5	1.3	2.4
hvAb (Pennsylvania)	83.1	5.6	8.7	1.3	1.3
lvb	90.0	4.5	3.4	1.5	0.6
Anthracite	94.2	2.7	1.7	0.8	0.6

Graphite and carbon samples investigated

Pyrolytic graphite, highly oriented piece (Union Carbide & Carbon)

Graphite powder (Ultra Carbon)

Activated carbon, coal-base (CAL Carbon)

Activated carbon, cocoanut-base (UCC carbon)

Carbon black from coal (Bureau of Mines)

Channel black (Micronex)

Table 2.- Infrared and Raman frequencies of graphite (in cm^{-1})

Raman	1582	1360		
Infrared	1587	1362	830 (w)	2200 (w)

Aromatics and/or chelated carbonyls have seemed for some time to be the most likely possibilities to produce the 1600 cm^{-1} band. However, all possible structures have not been investigated. Structures that were seldom considered are included in the group of intractable carbonaceous materials--graphite, carbons, and activated carbons. The infrared and Raman spectra of these have not been available until recently. For coals, in addition to infrared results, the authors have obtained Raman results on seven coals that show two broad lines in each sample in the $1575\text{-}1620$ and $1350\text{-}1400\text{ cm}^{-1}$ regions. Other weak lines have also been found (Table 3).

The Raman spectra of carbons and graphite obtained by Tuinstra and Koenig^{14/} have the characteristic Raman lines at $1575\text{-}1590$ and 1355 cm^{-1} ; they also found that a single crystal of graphite gave only one Raman line at $1575\text{-}1590\text{ cm}^{-1}$. The present authors have found a single Raman line at 1582 cm^{-1} for a highly oriented pyrolytic graphite. We have succeeded in obtaining good infrared spectra for graphite and carbons; practically the same frequencies appear in both infrared and Raman spectra.

It has long been necessary to find an assignment for spectral absorption that exists in the important CH bending region, $1540\text{-}1370\text{ cm}^{-1}$; it has been known since 1959 that completely deuterated chars still show broad relatively intense absorption in this region, even though CH groups are not present.^{23/} Spectra of graphitic structures have their frequencies in the proper region and may be the proper explanation for this unknown absorption. Intensities are important factors in the assignment of infrared bands and Raman lines. The intensity of the infrared band at 1600 cm^{-1} in the spectrum of ground graphite is high, even with the low resolution required for making the measurements. Actually the maximum absorbance of the $\sim 1600\text{ cm}^{-1}$ band is about the same as the 1600 cm^{-1} band in coals. Area intensity is very great, so there is plenty of absorption intensity in the region of the 1600 cm^{-1} band to justify assignment to graphitic structures.

Raman spectra have been run on a variety of coals, both powders and highly polished pieces. It seems reasonable to expect that the Raman and infrared spectra of complex materials like coals should have about the same number of spectral frequencies. We observe nearly 20 bands and band shoulders in infrared spectra but only two broad lines in Raman spectra of coals. Perhaps the small number of Raman lines is due to laser degradation of the samples by the beam. We are not yet certain how drastically combustible materials such as coals are affected by the intense irradiation from a laser beam. We find no evidence of combustion of the coal; no tar or smoke is produced. However, degradation of the samples does occur, as indicated by a spot that appears on the polished surface of each coal specimen as a result of the irradiation. The Raman spectra we observe might be spectra of carbonized coal rather than of coal.

The bands at about 1600 cm^{-1} in infrared and Raman spectra of graphite, carbons and coals are not surprising. The 1600 cm^{-1} band has been known from infrared spectra of coals for a long time. However, the 1360 cm^{-1} band appears to be anomalous at first glance. There is no corresponding band in the infrared spectrum of coals. The peak of the band is at 1360 , but the overall width of the band is very great--much greater than the width of the 1600 cm^{-1} band. In fact the combination of the 1600 and 1360 bands extends from 1800 to 900 cm^{-1} . Figure 5 demonstrates the close comparison of absorption band intensity and band shape in the spectra of coal and ground graphite. The frequency range covered by the two combined bands, 1600 and 1360 cm^{-1} , is almost identically the same as the range found in coal spectra, namely $1800\text{-}900\text{ cm}^{-1}$. Also the low-frequency branch of the band tails off gradually from 1360 to 900 cm^{-1} ; the high-frequency portion of this broad band system drops off precipitously from 1800 to 1600 cm^{-1} . Identically the same thing is observed in coal spectra, with the exception that superimposed

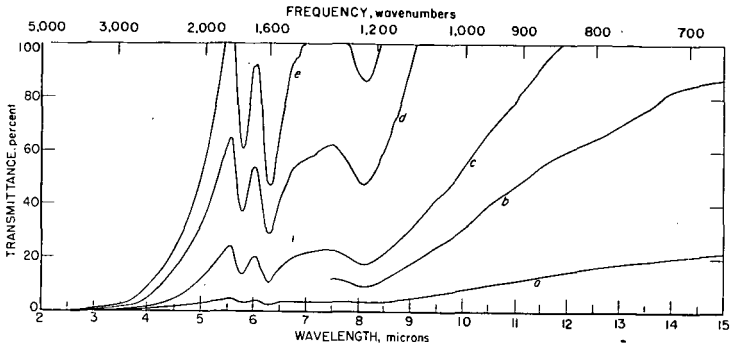


Figure 1

L-11089

Figure 1.- Infrared spectra of Pittsburgh activated carbon, type CAL. Spectrum a: KBr pellet, 0.5 wt % carbon in 200 mg of KBr; spectra b, c, d, e: scale expansions of spectrum a, at 3X, 5.5X, 14X, and 21X, respectively.

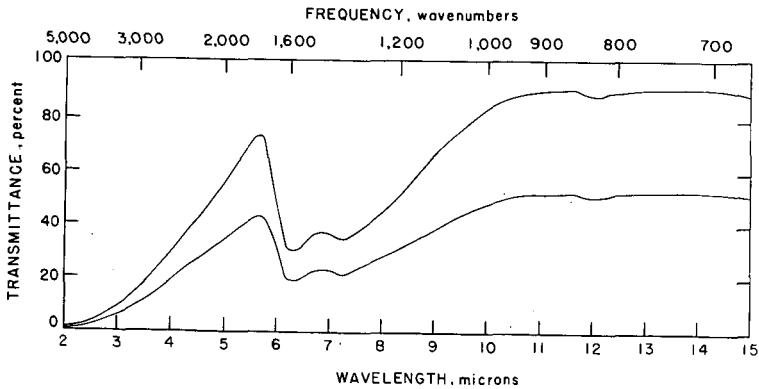


Figure 2

L-11856

Figure 2.- Infrared spectra of graphite after grinding for 96 hours. Bottom curve, as is; top curve is scale-expanded.

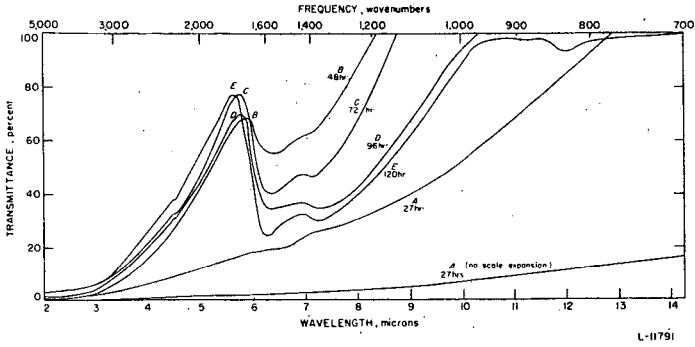


Figure 3

Figure 3.- Infrared spectral intensities of ground graphite increase with efficient grinding. Aliquots were removed from the sample after grinding for the times indicated. Spectra B, C, D, and E are scale-expanded.

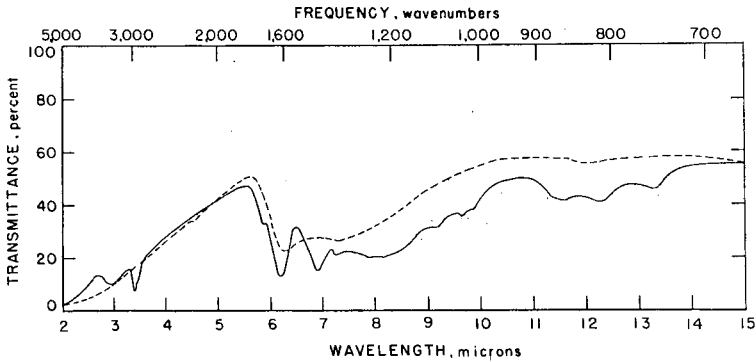
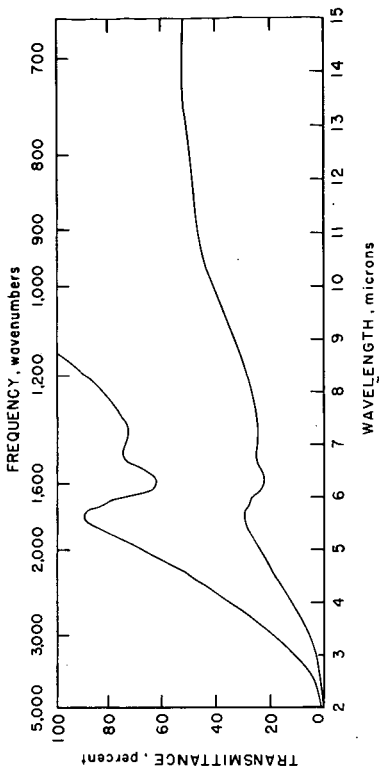


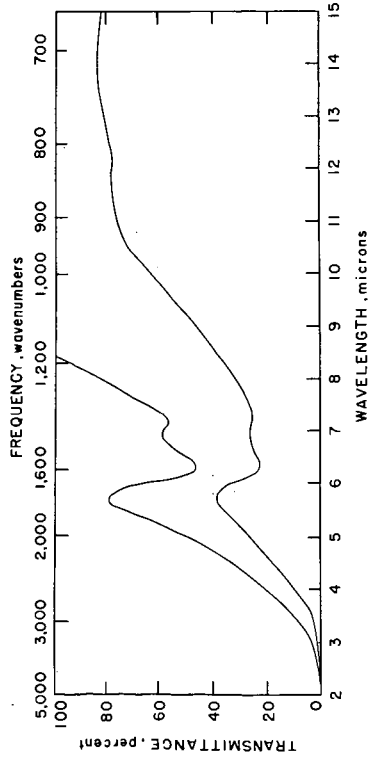
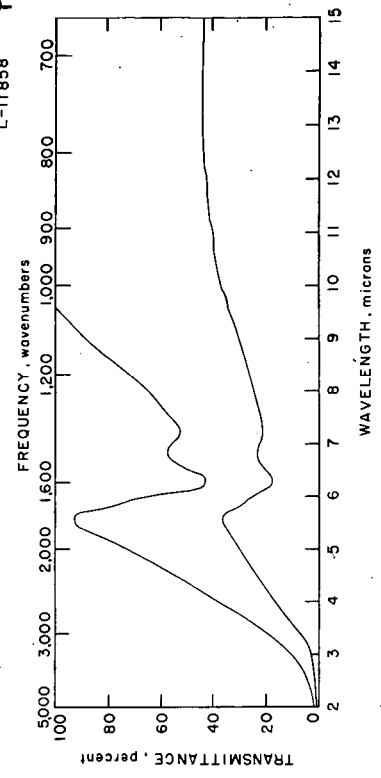
Figure 5

L-11860

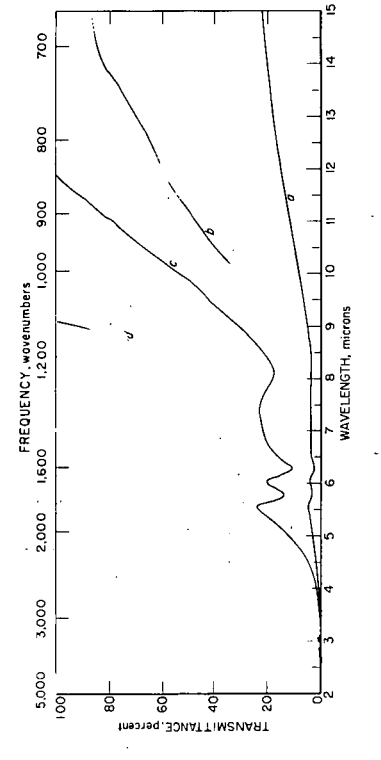
Figure 5.- Infrared spectra indicate the close similarity of the intense absorption regions from 1800 to 900 cm^{-1} for Pittsburgh coal ———, and ground graphite - - - -.



-130-



L-11857



L-11859

Figure 4. Infrared spectra: (a) Channel black; (b) carbon black from coal; (c) activated carbon from coal (CAL carbon); (d) activated carbon from coccoanut (UCC carbon). In each case the top curve(s) are scale-expanded.

Table 3.- Raman spectra of coals, graphite, and carbons (in cm⁻¹)

Coals:

Lignite (74.2% C) Baukol-Noonan Strip Mine Noonan Bed, Divide Co., N. Dak.	1600 (s,br) ^{a/}	1350 (w,br)	1200 (w)	705 (w)
Subbituminous (78.7% C) Rock Springs No. 7 Bed, Clark Mine Sweetwater Co., Wyo.	1620 (s,br)	1380 (br)		720 (w)
hvBb (80.5% C) No. 6 Bed, Atkinson Mine, Hopkins Co., Ky.	1605 (s)	1390 (m)		
hvAb (82.4% C) Pittsburgh No. 8 Bed, Piney Fork No. 1 Mine, Jefferson Co., Ohio	1610 (m)	1380 (m)		
hvAb (83.1% C) Pittsburgh Bed, Bruceston Mine, Allegheny Co., Pa.	1607 (s)	1382 (m)		
lvb (90.0% C) Pocahontas No. 3 Bed, Buckeye No. 3 Mine, Wyoming Co., W. Va.	1609 (s)	1355 (s)		
Anthracite (94.2% C) St. Nicholas Breaker, Reading Coal Co., Reading, Pa.	2960 (s,br)	1610 (s,shp)	1340 (m)	1200 (br)

Table 3.- Raman spectra of coals, graphite, and carbons (in cm^{-1})
(cont'd)

<u>Graphites and Carbons</u>	
Graphite, pyrolytic, highly oriented (UCC)	1582 (s,shp)
Graphite powder (UC)	1580 (w) (very w)*
CAL activated carbon	1600 (m) 1340 (m)
Channel black (Micronex)	1600 (s) 1340 (w) 1180 (m)
Graphite, single crystal ^{b/}	1575 (s,shp)
Graphite, polycrystalline ^{b/}	1575-1592 (s,shp) 1355 (m)
Activated charcoal ^{b/}	1575 (m) 1355 (m)

^{a/} s = strong; m = moderate; w = weak; br = broad; shp = sharp;
h = high; l = low; v = volatile; b = bituminous; A, B = classifications of hvb coals.
^{b/} Reference 14.
* A very weak line may be present at about 1360 cm^{-1} .

on this broad band system in coal spectra are CH bands at 1460 and 1375 cm^{-1} and broad absorption usually attributed to phenolic structures at 1250 cm^{-1} . The absorption due to phenoxy groups at 1250 cm^{-1} , presumably phenols, is probably very weak, and the major absorption is likely due to the graphitic structure. The overall structure of this wide band system, 1800-900 cm^{-1} , has always been a mystery. The broad, intense infrared band at $\sim 1360 \text{ cm}^{-1}$ has been attributed completely to the obvious bands at 1460, 1375, and 1250 cm^{-1} . The broad structure centering on 1250 cm^{-1} has usually in the past been assigned to phenolic structures, but this assignment never made particular sense because there are not tremendous concentrations of phenols in coals. It makes more sense to assign a small amount of this 1800-900 cm^{-1} absorption to phenolic and CH structures and the major portion of the absorption to the graphitic structures.

In studies of infrared spectra of coals an anomaly involving the intensities of aliphatic CH stretching and bending frequencies has remained unsolved until now. The aliphatic CH stretching frequency in spectra of organic substances nearly always produces a more intense band than the CH bending frequencies; in coal spectra, however, the intensities are reversed. We can now see that the bending frequencies have greater apparent intensity because of intense broad absorption produced in this spectral region by "graphitic" components.

Specifically, we are assigning the 1800-900 cm^{-1} absorption mainly to graphitic structures. Aromatics cannot be excluded, and small amounts are known to be present, but these cannot account for the broad 1800-900 cm^{-1} absorption nearly as well as highly absorbing graphitic structures.

Aliphatic structures such as quaternary carbon atoms in diamond-type structures need to be considered. The presence in coals and carbons of diamond-like structures was proposed in 1959.²⁴ The presence or absence of such structures has remained debatable; the new spectral data presented herein provide some information on this point. The infrared measurements on diamonds indicate that two kinds of spectra exist: (1) Type I diamonds have infrared absorption in two spectral regions, 4000 to 1800 cm^{-1} and 1400 to 1000 cm^{-1} ; (2) Type II diamonds have only the one absorption region, 4000 to 1800 cm^{-1} ; it is significant that Type II diamonds have essentially no absorption at frequencies from 1800 to at least 400 cm^{-1} .²⁵ Type II diamonds are in fact used as transparent cell windows for special infrared cells. The most intense absorption band observed for diamonds, 1290 cm^{-1} , has a very small absorption coefficient, 0.0039 liter / gm cm. The corresponding coefficient for the 1600 cm^{-1} band in coal spectra is 0.49 liter/gm cm. Thus, if the carbon atoms of coal were all in diamond structures, these structures could account for no more than $.0039/.49 \times 100$ or 0.8 percent of the observed absorption. The remaining absorption, 99.2 percent, would have to come from some other source. This evidence supports our assignment of the intense absorption in the spectra of coals and carbons at 1600 and 1360 cm^{-1} to strongly absorbing graphitic structures.

By this assignment spectroscopists have nearly gone full circle in two decades from assigning the 1600 cm^{-1} band to aromatic structures, then to conjugated chelated carbonyls, and lastly, to a graphitic structure. The assignment of the long unknown source of the absorption from 1800 to 900 cm^{-1} is very important. This spectral region was the principal remaining unknown absorption in coal spectra. The presence of a graphitic type, non-crystalline structure is a most important contribution to the study of coal structure. Graphitic structures will almost certainly remain behind after thermal reactions liberate volatile materials; it is obvious that graphitic structures, crystalline or amorphous, will not be volatile nor extractable.

It is quite possible that the components emitted from coal under coking conditions or other thermal conditions may be materials that were trapped in the molecular sieve structure of coal. Anderson at the U.S. Bureau of Mines first demonstrated that coals are molecular sieves.^{26/} Vahrman has recently stated that from his work on exhaustive extraction he believes the extractable organic components of coals are released from molecular sieve structures.^{27/} Molecular sieve structures may constitute the residues that remain behind after extraction or carbonization. Apparently no studies have been made on carbonaceous residues to ascertain whether or not they also possess properties of molecular sieves.

SUMMARY

Infrared and Raman spectra of the intractable carbonaceous materials are difficult to obtain. For coals, carbon blacks, and chars prepared at low temperatures infrared spectra have been obtained with relative ease. Activated carbons are difficult to grind down to small particle sizes, and only recently have good infrared transmission spectra been obtained. More difficult materials have now been successfully studied by the transmission infrared method--most notably ground graphite, high-temperature carbons, high-temperature chars, and carborundum. After long grinding graphite loses its crystallinity but the molecular structure of the carbon matrix apparently remains unchanged; broad, intense infrared bands are observed at about 1590 and 1360 cm^{-1} for ground graphite and for some activated carbons.

The frequencies of the two broad infrared bands are in excellent agreement with the frequencies of the two laser-Raman lines found for various carbons: ~1600 and 1360 cm^{-1} . The laser-Raman spectra are the same for coals, carbons, and graphites. However, the similarity of these laser-Raman spectra indicate in the case of coal that we may be observing the spectrum of carbonized coal rather than of coal. Coal may burn or carbonize in the laser beam.

In the light of these new spectral results, reassignment of some bands in the infrared spectra of coals has become necessary. Graphite-like structures (non-crystalline) are believed to be responsible for the broad 1600 cm^{-1} band in coals, and the broader 1360 cm^{-1} band, which appear to fit closely the broad band contour from 1800 to 900 cm^{-1} in the infrared spectra of coals. The intensities of the 1600 and 1360 cm^{-1} bands in ground graphite are more than sufficient to account for the band intensities observed in the spectra of coals and chars. Diamond-like structures such as quaternary carbon atoms do not appear to be involved.

ACKNOWLEDGMENTS

We are grateful to Dr. L. J. E. Hofer, Mellon Institute, and Dr. L. S. Singer, Union Carbide Parma Laboratories, for samples of carbons and graphites.

REFERENCES

1. R. A. Friedel and L. J. E. Hofer, *J. Phys. Chem.*, 74, 2921 (1970).
2. R. A. Friedel and M. G. Pelipetz, *J. Opt. Soc. Am.* 43, 1051 (1953).
3. R. A. Friedel, *Proc. 4th Carbon Conf.*, ed., S. Mrozowski, Pergamon Press, New York, 1960, pp. 321-336.
4. R.A. Friedel, R. A. Durie, and Y. Shewchyk, *Carbon* 5, 559 (1968).
5. J. K. Brown, *J. Chem. Soc.* 1955, 744.
6. V. A. Garten and D. E. Weiss, *Australian J. Chem.* 10, 295 (1957).
7. V. A. Garten and D. E. Weiss, *Proc. 3rd Carbon Conf.*, ed., S. Mrozowski, Pergamon Press, New York, 1959, p. 295.
8. J. K. Brown, *J. Chem. Soc.* 1955, 752.
9. R. A. Friedel and J. A. Queiser, *Anal. Chem.* 28, 22 (1956).
10. C. G. Cannon and G.B.B.M. Sutherland, *Trans. Faraday Soc.* 41, 279 (1945).
11. R. A. Friedel, *Brennstoff-Chemie* 44, 23 (1963).
12. J. S. Mattson, H. B. Mark, Jr., M. D. Malbin, W. J. Weber, and J. C. Crittenden, *J. Colloid. & Interface Science* 31, 116, 131 (1969).
13. J. S. Mattson and H. B. Mark, Jr., *Anal. Chem.* 41, 355 (1969).
14. F. Tuinstra and J. L. Koenig, *J. Chem. Phys.* 53, 1126 (1970).
15. C. G. Cannon, *Nature* 171, 308 (1953).
16. R. A. Friedel and H. L. Retcofsky, *Proc. 5th Carbon Conf., Vol. II*, ed., S. Mrozowski, Pergamon Press, London, 1963, p. 165.
17. P. J. Foster and C. R. Howarth, *Carbon* 6, 719 (1968).
18. P. L. Walker, Jr., and S. B. Seeley, *Proc. 3rd Carbon Conf.*, ed., S. Mrozowski, Pergamon Press, New York, 1959, p. 481.
19. R. A. Friedel, *Applied Infrared Spectroscopy*, ed., D. N. Kendall, Reinhold Pub. Co., New York, 1966, pp. 319, 321.
20. R. A. Friedel, R. A. Durie, and Y. Shewchyk, *Carbon* 5, 559 (1967).
21. R. A. Durie, Y. Shewchyk, and R. A. Friedel, *Spectrochim. Acta* 24A, 1543 (1968).
22. S. Fujii, *Fuel* 42, 17, 341 (1963).

23. R. A. Friedel, *Applied Optics* 2, 1109 (1963).
24. R. A. Friedel, *Science* 130, 220 (1959).
25. E. R. Lippincott, L. S. Whatley, and H. C. Duecker, *Applied Infrared Spectroscopy*, ed., D. N. Kendall, Reinhold Co., New York, 1966, pp. 437-438.
26. R. B. Anderson, L.J.E. Hofer, and J. Bayer, *Fuel* 41, 559 (1962).
27. J. A. Spence and M. Vahrman, *Fuel* 49, 395 (1970).

A STUDY OF CATALYSIS OF COAL GASIFICATION
AT ELEVATED PRESSURES

W. P. Haynes and H. Neilson
U.S. Bureau of Mines
4800 Forbes Avenue, Pittsburgh, Pa. 15213

J. H. Field
The Benfield Corporation
666 Washington Road, Pittsburgh, Pa. 15228

ABSTRACT

Bench-scale tests were conducted to determine the effect of additives and catalysts upon the steam-gasification of coal at high pressure. Gasification was conducted in 0.6" diameter fixed beds at 300 psi and 750 to 950 C. Over 20 chemical compounds and additives were evaluated at 850 C in standard gasification tests. Data are presented which show that nearly all of the additives tested increased the overall rate of carbon gasification significantly, with alkali metal compounds resulting in the largest increases (over 60%). Generally, the increase in hydrogen production greatly exceeded the increase in carbon gasification, indicating that the tested additives promoted the water gas shift reaction. The additives also increased methane production by up to 20 percent. Additional experiments are discussed concerning the effectiveness of Raney Nickel as a catalyst when it is admixed with the coal, when it is sprayed on a metal surface and then inserted in the coal bed, and when used at temperatures of up to 950 C. The effect of other parameters is also considered, such as the degree of gasification and the recycle of additives. Results of the overall investigations thus far suggest that the gasification step of the Bureau of Mines Synthane process can be improved significantly by means of suitable catalysts.

A KINETIC STUDY OF THE HYDROGENATION
OF BITUMINOUS COAL

by Wendell H. Wiser, Mahmoud El-Feky and George R. Hill

Abstract

The catalytic hydrogenation of several coals from the western United States has been investigated in the temperature range 350° to 500°C utilizing hydrogen pressures up to 3500 psi. Yields of liquids plus gases up to 82 percent have been obtained utilizing ammonium molybdate catalyst. The reaction is observed to be second order over most of the time range at lower temperatures, with activation enthalpy of 39 kcal per mole and entropy of activation of -17 entropy units. A first order reaction was observed at lower temperatures at times greater than about three hours, with activation enthalpy of 9 kcal per mole and entropy of activation of -56 entropy units. Possible mechanisms are discussed.